

PATHWAYS FOR ECOLOGICAL CHANGE IN CANADIAN
HIGH ARCTIC WETLANDS UNDER RAPID TWENTIETH
CENTURY WARMING

Thomas George Sim

Submitted in accordance with the requirements for the degree of Master of Science by
Research

The University of Leeds

School of Geography

September 2018

DECLARATION

The candidate confirms that the work submitted is his own and that appropriate credit has been given where reference has been made to the work of others.

This copy has been supplied on the understanding that it is copyright material and that no quotation from the thesis may be published without proper acknowledgement.

The right of Thomas George Sim to be identified as Author of this work has been asserted by Thomas George Sim in accordance with the Copyright, Designs and Patents Act 1988.

ACKNOWLEDGEMENTS

I would like to thank the generous support and advice of my supervisors Graeme Swindles, Paul Morris and Jennifer Galloway. I thank Mariusz Gałka for completion of the plant macrofossil analysis and for his continued advice throughout the project.

For the Banks Island sample collection, I thank Jennifer Galloway, Rod Smith of Geological Survey Canada, Andrew Durbano, and René Gysler of Great Slave Helicopters. Sample collection occurred during a Geological Survey of Canada Geo-Mapping for Energy and Minerals Program (GEM Western Arctic) field program. For the Elu Inlet sample collection, I thank Jennifer Galloway, Thomas Hadlari, Attima Hadlari, Elisabeth Jansen-Hadlari, Francis Emingak, Braden Gregory, and Nawaf Nasser. Funding for field logistics was provided by a Polar Knowledge Canada/Savoir polaire Canada Grant #1516-149 to Jennifer Galloway and Timothy Patterson and the Geological Survey of Canada Environmental Geoscience Program. I acknowledge the generous support of Natural Resources Canada/Geological Survey of Canada in funding the radiocarbon dating and thank the André E. Lalonde AMS Laboratory, University of Ottawa, for the rapid analysis.

I would like to thank David Ashley, Dave Wilson and Rachel Gasior for their help and advice in the laboratory analysis of my samples at the University of Leeds and the School of Earth and Environment Instrument Workshop for building my custom volumetric peat cutter. For the helpful discussion and comments regarding the identification and classification of Vaginicolidae I thank Matt Amesbury, Anatoly Bobrov, Louis Beyens, Dan Charman, Clément Duckert, Diego Fontaneto, Anush Kosakyan, Mariusz Lamentowicz, Michelle McKeown, Edward Mitchell, Thomas Roland, Ferry Siemensma and Dave Wilkinson. I thank Donal Mullan for his advice on using re-analysis climate data and the contributors to the Climate Explorer site for the re-analysis and station data used in this thesis. I am grateful to Environment Canada for the extended temperature records for the Sachs Harbour station. I acknowledge receiving isostatic uplift data from <http://grace.jpl.nasa.gov>. I also thank Konrad Gajewski for his advice on interpretation of past temperature reconstructions and for direction to pollen temperature reconstruction datafiles.

Finally, I would like to thank my girlfriend Kristen, my family and my friends for their encouragement and support.

ABSTRACT

The response of Arctic wetland ecosystems and their associated organic carbon stores to future warming is uncertain. For the first time in the Canadian High Arctic I use a multi-proxy palaeoecological approach to test how organic-rich wetlands have responded to pronounced warming since the mid-twentieth century. This approach enables ecological analysis on a timescale beyond that of contemporary studies. An ice-wedge polygon mire was a dual-state system with the raised centre mound showing no response to recent warming, but ~AD 2000 the surrounding trough exhibited a shift to wetter conditions and a transition from sedge and herb-dominated to brown moss-dominated vegetation. The accumulation of this vegetation layer may have the effect of insulating ice-wedges and provide a negative ecological feedback to permafrost degradation, mitigating potential carbon losses. In a valley fen, an increase in growing degree days above 0°C (GDD₀) since ~AD 1950 is linked to greater inundation from increased snow and ice melt early in the growing season, coupled with increased drying towards the end of the growing season from elevated evapotranspiration. This may have initiated a pathway to wetland desiccation – although wetland persistence is likely to be determined by future Arctic precipitation patterns. In a coastal fen, greater GDD₀ combined with isostatic uplift induced shrubification ~AD 1950 and led to rapid carbon accumulation. After this, increasing bird grazing pressures from ~AD 2000 may have affected vegetation and carbon accumulation. My results illustrate a variety of pathways for change in High Arctic wetlands in response to rapid warming. The results of this study suggest that predictions of the future extent and carbon accumulation rates of northern peatlands should consider the marked, yet complex response of High Arctic wetlands to warming alongside external non-climatic factors such as increased bird grazing pressures.

TABLE OF CONTENTS

Declaration.....	i
Acknowledgements.....	ii
Abstract.....	iii
Table of Contents.....	iv
List of Figures and Tables.....	vi
Abbreviations.....	xiii
1. Literature review.....	1
1.1 Overview.....	1
1.2 Permafrost wetlands and peatlands.....	2
1.2.1 Definitions, formation and extent.....	2
1.2.2 Carbon stocks.....	5
1.2.3 Carbon dynamics and climate change.....	6
1.3 Considering a palaeoenvironmental approach.....	11
1.3.1 Carbon accumulation estimates.....	11
1.3.2 Contemporary vs. palaeoenvironmental approach.....	12
1.3.3 Testate amoebae.....	12
1.4 Aim and objectives.....	14
2. Methodology.....	15
2.1 Study sites.....	15
2.2 Growing degree day calculation and calibration.....	17
2.3 Palaeoenvironmental analysis.....	21
2.3.1 Age with depth.....	21
2.3.2 Peat physical properties.....	21
2.3.3 Plant macrofossils.....	22
2.3.4 Testate amoebae.....	23
2.3.5 Statistical analysis.....	26
3. Results.....	27
3.1 Growing degree days.....	27
3.2 Palaeoenvironmental results.....	28
3.2.1 Polygon Mire raised centre.....	28
3.2.2 Polygon Mire trough.....	36
3.2.3 Valley Fen.....	44

3.2.4 Coastal Fen A.....	52
3.2.5 Coastal Fen B.....	60
3.2.6 Palaeoenvironmental summary.....	68
4. Discussion.....	69
4.1 Twentieth century improvement in western Arctic growing season quality	69
4.2 Polygon Mire – autogenic and allogenic ecosystem processes with increased thaw ...	70
4.3 Valley Fen – increasing extremes in growing season hydrology.....	73
4.4 Coastal Fen – warming and grazing induced ecosystem state shifts.....	75
5. Conclusion.....	80
References	82
Appendix	99

LIST OF FIGURES AND TABLES

Figure 1. A) Permafrost zonation and distribution in Canada. B) Mean annual near surface temperature across Canada. C) Peatland distribution, class and extent coverage in Canada	3
Figure 2. Relative estimated soil carbon storage for global peatland regions.	6
Figure 3. Factors affecting wetland carbon accumulation in terms of external drivers, location characteristics, ecosystem processes and carbon dynamics.	7
Figure 4. Five-stage model for the response of permafrost peatlands to increasing temperature (Swindles, et al., 2015a)	11
Figure 5. Upper panel: map showing the location of wetland sites where peat monoliths were sampled for palaeoenvironmental analysis, nearby weather stations (presented in Figure 32), pollen lake cores used for Holocene temperature reconstruction of the western Arctic region (Gajewski, 2015; presented in Figure 32). Boundaries between permafrost zones and the northern extent of the tree line are also shown (Brown et al., 2002). Lower panel shows photographs taken from each site.....	15
Figure 6. Aerial imagery of site locations. A-C sourced from ESRI via ArcGIS and D-F sourced from Planet Lab.....	17
Figure 7. Re-analysis climate data interpolated for each site compared to corresponding monitoring data of nearby weather stations.....	19
Figure 8. Calibration of Coastal Fen re-analysis monthly temperature with Cambridge Bay measurements and resultant annual GDD ₀ from calibrated re-analysis monthly temperature .	20
Figure 9. Sketches of <i>Platycola truncata</i> (de Fromentel 1874) alongside photographs of subfossil lorica (70–100 µm) from my samples	23
Table 1. Summary of the hydrological indicator classification of testate amoeba taxon	25
Figure 10. Growing degree days above 0°C for each wetland site 1851–2011 calculated from monthly temperature re-analysis data (Compo et al., 2011)	27
Table 2. Radiocarbon ¹⁴ C dating summary table from the Polygon Mire raised centre monolith, including individual date calibration plots. † = Suess effect.	28
Figure 11. Age-depth model for the Polygon Mire raised centre monolith. The model was constructed using a cubic spline between dates.	29
Figure 12. Physical properties summary stratigraphic diagram for the Polygon Mire raised centre monolith.	31
Figure 13. Relative abundance (%) of testate amoebae for the Polygon Mire raised centre monolith.....	33
Figure 14. Abundance (%) of plant macrofossils for the Polygon Mire raised centre monolith.	35
Figure 15. Age-depth model for the Polygon Mire trough monolith. The model was constructed using linear interpolation between dates.....	36
Table 3. Radiocarbon ¹⁴ C dating summary table from the Polygon Mire trough monolith, including individual date calibration plots. † = Suess effect.	37
Figure 16. Physical properties summary stratigraphic diagram for the Polygon Mire trough monolith.....	39
Figure 17. Relative abundance (%) of testate amoebae for the Polygon Mire trough monolith	41

Figure 18. Abundance (%) of plant macrofossils for the Polygon Mire trough monolith.	43
Table 4. Radiocarbon ¹⁴ C dating summary table from the Valley Fen monolith, including individual date calibration plots. ‡ = Suess effect.	44
Figure 19. Age-depth model for the Valley Fen monolith. The model was constructed using a polynomial regression (2nd order smoothing) between dates.	45
Figure 20. Physical properties summary stratigraphic diagram for the Valley Fen monolith.	47
Figure 21. Relative abundance (%) of testate amoebae for the Valley Fen monolith.....	49
Figure 22. Abundance (%) of plant macrofossils for the Valley Fen monolith.	51
Table 5. Radiocarbon ¹⁴ C dating summary table from the Coastal Fen A monolith, including individual date calibration plots. ‡ = Suess effect.	52
Figure 23. Age-depth model for the Coastal Fen A monolith. The model was constructed using a cubic spline between dates	53
Figure 24. Physical properties summary stratigraphic diagram for the Coastal Fen A monolith.....	55
Figure 25. Relative abundance (%) of testate amoebae for the Coastal Fen A monolith.	57
Figure 26. Abundance (%) of plant macrofossils for the Coastal Fen A monolith.....	59
Table 6. Radiocarbon ¹⁴ C dating summary table from the Coastal Fen B monolith, including individual date calibration plots. ‡ = Suess effect.	60
Figure 27. Age-depth model for the Coastal Fen B monolith. The model was constructed using a cubic spline between dates	61
Figure 28. Physical properties summary stratigraphic diagram for the Coastal Fen B monolith.....	63
Figure 29. Relative abundance (%) of testate amoebae for the Coastal Fen B monolith.	65
Figure 30. Abundance (%) of plant macrofossils for the Coastal Fen B monolith.	67
Figure 31. Summary stratigraphic diagram of palaeoenvironmental variables from the Polygon Mire raised centre (A), Polygon Mire trough (B), the Valley Fen (C) and Coastal Fen (D and E).	68
Figure 32. Climatic data showing recent warming for my sites in the western Canadian Arctic study region. A) Historical temperature data from nearby weather stations, B) GDD ₀ = Growing degree days above 0°C for each wetland site 1851–2011 calculated from monthly temperature re-analysis data (Compo et al., 2011). C) Mean July temperature for the western Arctic during the Holocene reconstructed from pollen analysis.....	69
Figure 33. Site photo taken mid-July 2016 at the Polygon Mire site (74.46 °N, 121.04 °E) showing slumping of raised polygon centres into adjacent troughs.	72
Figure 34. Site photo taken mid-July 2016 at the Valley Fen site (74.05 °N, 118.43 °E) showing snow patches on the hilltops of the surrounding catchment.....	74
Figure 35. Site photos taken mid-August 2017 at the Coastal Fen site (68.65 °N, 105.45 °E). A) Large bare patch including some dead vegetation, with the early stages of moss recolonization in the top right. B) Moss recolonization towards edge of the disturbed area. C) Clear avian footprints in a bare patch. D) Avian excrement and a feather observed on site.....	77
Figure A1. Available precipitation data for my study sites in the western Canadian Arctic study region: 1) Mould Bay, 2) Sachs Harbour and 3) Cambridge Bay. A) Annual precipitation trends. B)	

Average monthly precipitation. Source: Climate explorer site and Environment Canada.....99

ABBREVIATIONS

Abbreviation	
GDD₀	Growing degree day above 0°C
CO₂	Carbon dioxide
CH₄	Methane
PAR	Photosynthetically active radiation
GHG	Greenhouse gas
NPP	Net primary productivity
AMOC	At Most One Change
pMC	Percentage modern carbon
V_t	Volume of peat
M_w	Wet mass
M_d	Dry mass
ρ	Bulk density
M_a	Ash mass
OM	Organic matter
ρ_{om}	Organic matter bulk density
LORCA	Long-term apparent rate of carbon accumulation
θ	Hydrological indicator classification
U/WT	Unclear/wide-tolerance
SDI	Shannon's diversity index
NMDS	Non-metric multidimensional scaling
CONISS	Constrained incremental sum of squares
QMBS	Queen Maud Gulf Migratory Bird Sanctuary

1. LITERATURE REVIEW

1.1 OVERVIEW

Northern wetland ecosystems – in particular peatlands - store large amounts of organic carbon (Tarnocai et al., 2009) and their response to warming remains a key area of research (Belyea, 2009; Morris et al., 2015; Waddington et al., 2015). More specifically, thawing permafrost may expose carbon that has remained inert for millennia because of frozen soil conditions, to decomposition and subsequent emission as carbon dioxide (CO₂) (aerobic) and methane (CH₄) (anaerobic) – potentially initiating positive climate warming feedbacks (Gorham, 1991; Dorrepaal et al., 2009; Froking et al., 2011; Olefeldt et al., 2013; Schuur et al., 2015). However with warming at high latitudes, increased plant productivity may also increase carbon accumulation in peatlands (e.g. Klein et al., 2013; Swindles, et al., 2015a) and facilitate the northern expansion of peatlands (Charman et al., 2015; Gallego-Sala et al., 2018) to potentially mitigate some of the carbon losses elsewhere.

Greater understanding of carbon dynamics and feedbacks in permafrost wetlands and peatlands in response to climate forcing is essential to ensure successful incorporation into Earth system models of climate change (Chaudhary et al., 2017) and to best advise management practices (McLaughlin & Webster, 2013). Palaeoenvironmental investigations into the carbon accumulation, hydrological and ecological response of permafrost peatlands to climate over recent decades and centuries will help address a gap in current knowledge of peatland response to climatic forcing (Yu, 2012; Loisel et al., 2014; Swindles, et al., 2015a).

1.2 PERMAFROST WETLANDS AND PEATLANDS

1.2.1 DEFINITIONS, FORMATION AND EXTENT

Wetlands and peatlands have no universal classification and are defined differently by many agencies, organisations and scientists. Here I discuss a number of these definitions in the context of northern-latitude Boreal, Subarctic and Arctic regions. Wetlands are a broader classification than peatlands and are defined by Joosten & Clarke, (2002, p.24) as:

“...an area that is inundated or saturated by water at a frequency and for a duration sufficient to support a prevalence of vegetation typically adapted for life in saturated soil conditions.”

Wetlands can therefore include a range of habitats globally across different biomes including bogs, fens, swamps, marshes, and temporary or permanent shallow lakes (Keddy, 2010). Peatlands are a type of wetland topped with a surface layer of organic matter (or peat) and are defined by Wieder et al., (2006, p.1) as:

“...terrestrial environments where over the long term, on an areal basis, net primary production exceeds organic matter decomposition, leading to the substantial accumulation of a deposit rich in incompletely decomposed organic matter, or peat.”

Other definitions of peatlands are more specific and can require: the presence of peat forming vegetation (Paavilainen & Päivänen, 1995) or a minimum depth of peat e.g. 30 cm (Hånell, 1991), 40 cm (Zoltai & Pollett, 1983; National Wetlands Working Group, 1997), or 45 cm (Hammond, 1981). Peat can be defined as material of a certain organic matter content at dry mass e.g. $\geq 30\%$ (Joosten & Clarke, 2002) or $\geq 50\%$ (Burton & Hodgson, 1987). Northern peatlands can be broadly subcategorised into bogs and fens. Bogs are ombrotrophic with precipitation providing all their nutrients and water supply, while fens receive additional moisture and potentially nutrient input from groundwater and catchment runoff alongside precipitation (Rydin & Jeglum, 2006). Fens can be minerotrophic (rich fen) or more ombrotrophic (poor-fen). Bogs are associated with low pH and nutrient poor conditions, while fens typically have a higher pH and can be more nutrient rich - this can influence soil and vegetation characteristics (Rydin & Jeglum, 2006). Permafrost is ground (rock or soil) that remains at or below a temperature of 0°C for two consecutive years (French, 2017). Therefore, permafrost peatlands or permafrost wetlands occur in the cold regions of the world.

Pan-Arctic peatlands are believed to have begun developing ~16.5 Ka BP following widespread deglaciation, with the majority initiating between 12–8 Ka BP (MacDonald et al., 2006), linked to enhanced plant productivity from warming growing seasons (Morris et al., 2018). Permafrost distribution is linked to ground temperatures (Figure 1A and 1B) that generally correlates with climatic conditions. Aggradation of permafrost has been observed around ~5–3 Ka BP, corresponding to a general climatic cooling in the neoglacial e.g. northern Alberta (Zoltai, 1993) and southern Northwest Territories (Pelletier et al., 2017). Peatland initiation can occur through primary mire formation, paludification and terrestrialisation. Primary mire formation occurs when peat forms directly on wet newly exposed mineral soil or bare ground after coastal uplift or deglaciation (Ruppel et al., 2013). Paludification occurs through successional processes on vegetated, flat and wet mineral soils and terrestrialisation occurs via the gradual filling of shallow water bodies with inorganic and organic debris (Lavoie et al., 2005; Kuhry & Turunen, 2006).

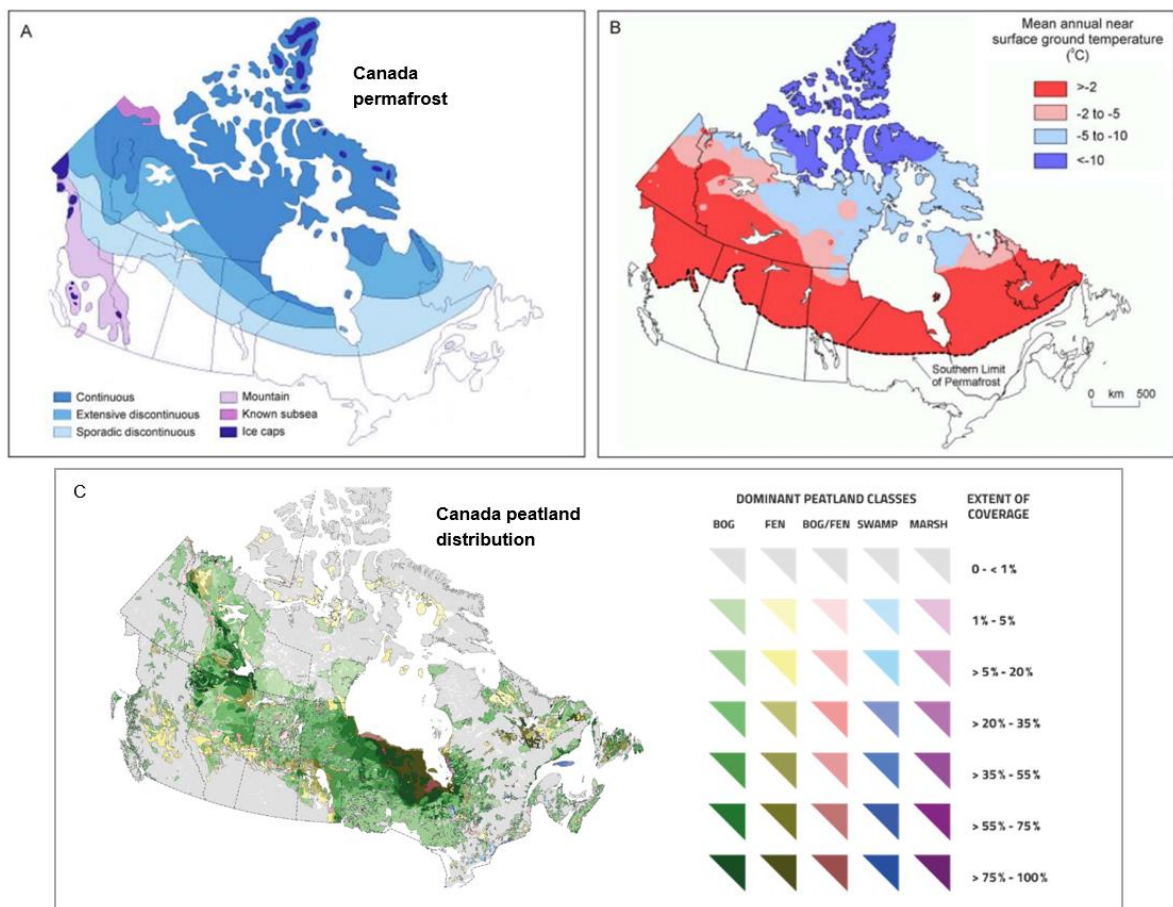


Figure 1. A) Permafrost zonation and distribution in Canada. Continuous (≥ 90 –100%), extensive discontinuous (≥ 50 –90%), sporadic discontinuous (≥ 10 –50%). B) Mean annual near surface ground temperature. Sourced from Heginbottom et al. (1995). C) Peatland distribution, class and extent coverage in Canada – sourced from Tarnocai et al. (2011).

The widely used diplotelmic (two layered) model in peatlands differentiates the permanently saturated zone (catotelm) and the near surface layer (actotelm), with the catotelm said to experience levels of decomposition orders of magnitude lower than in the actotelm (Ingram, 1978). However, the simplicity of this diplotelmic hypothesis has been questioned, and in reality is much more complex (Holden & Burt, 2003, Belyea & Baird, 2006; Rydin & Jeglum, 2006; Morris et al., 2011). Ultimately peatlands are initiated when, under conditions of adequate moisture, the production of organic matter persistently exceeds decomposition (Charman, 2002). Typically, peatlands initially form as fens and can undergo a transition to a bog as peat accumulates and raises the water table above the influence of groundwater (Keddy, 2010). In northern latitudes *Sphagnum* is a key peat-forming genus in ombrotrophic peatlands, favouring the water-saturated and anaerobic conditions that create an environment where accumulation of organic matter is higher than decomposition (Joosten & Clarke, 2002; Limpens et al., 2008). Brown mosses are an important group of peat-forming taxa in more minerotrophic peatlands (Vitt et al., 1995), although peatlands can also be dominated by sedge or trees (Zoltai & Martikainen, 1996; Ott & Chimner, 2016;).

The coincidence of underlying permafrost and peat creates palsas, peat plateaus and polygon mires with a shallow and often seasonal active layer where most of ecological, hydrological and biogeochemical activity takes place (Zoltai & Tarnocai, 1975; Kane et al., 1991; Vardy et al., 2000; Arlen-Pouliot & Bhiry, 2005). The presence of permafrost can reduce drainage and improve water retention in the seasonal active layer and therefore increasing moisture availability during the growing season to facilitate the formation of wetlands (Woo & Winter, 1993). Palsas are typically found in the discontinuous permafrost and are formed of permanently frozen peat mounds with a core of peat and mineral soil (Seppälä, 1982) up to 150 m across and 12 m in height (Lagarec, 1982). Peat plateaus are flat areas of peat elevated above the peatland surface with permafrost ranging from extensive to patchy that may or may not encompass the underlying mineral soil (van Everdingen, 2005). Ice-wedge patterned ground is an abundant feature in the continuous permafrost where cold winter temperatures result in cracking from thermal contraction (Lachenbruch, 1962; Mackay, 1974). Polygon mires occur when peat formation is coincident with ice-wedge ground, a process more common in peaty rather than mineral soil (Kokelj et al., 2014). In the Arctic, wetlands typically fall into three classifications: polygon wetlands, on ground affected by ice-wedge formations; patchy wetlands, on previously-

glaciated terrain with favourable topographic depressions; and coastal wetlands, in zones of isostatic uplift (Glenn & Woo, 1997; Woo & Young, 2006).

Over 80% of estimated peatland extent is found in the northern hemisphere in temperate-cold climates and on predominately flat topography, mainly in the Boreal and Subarctic regions of Canada, Russia and the USA (Kuhry & Turunen, 2006; Tarnocai, 2006; Limpens et al., 2008). In Canada, peatlands cover ~13% of the terrestrial landscape and are mainly distributed in the Boreal (64%) and Subarctic (33%) zones, with little extent in the Arctic (3%) (Tarnocai et al., 2011). Here Tarnocai et al. (2011) define peatlands as wetlands with at least 40 cm of peat. The distribution of northern peatlands and permafrost demonstrates a large degree of overlap across the pan-Arctic and in Canada specifically, where over one third of peatlands are perennially frozen (Figure 1A and 1C). Around one quarter of northern peatlands occur in areas of continuous permafrost (90–100% extent) and ~40% occur in discontinuous (50–90% extent), sporadic (10–50% extent) or isolated (< 10% extent) areas of permafrost (Laurence et al., 2007). In the Arctic, as the growing season cools and shortens - limiting plant primary production and therefore organic matter input - peatlands with a substantial organic matter surface layer become rarer. Although, wetlands in general remain relatively common, occupying ~8% of the pan-Arctic non-glaciated land area (Walker et al., 2005).

1.2.2 CARBON STOCKS

During the Holocene northern peatlands have typically acted as net sinks of CO₂ and sources of CH₄ (Smith et al., 2004; MacDonald et al., 2006) to the extent they have had a net cooling effect on the entire planet (Frolking et al., 2011). The imbalance between net primary productivity (NPP), decomposition and erosion experienced in peatlands can result in substantial carbon accumulation over decades, centuries and millennia (Gorham, 1991; Charman et al., 2013). Consequently, despite covering < 3% of the terrestrial surface of the earth, peatlands store a large amount of global terrestrial soil carbon that has accumulated over the Holocene (Limpens et al., 2008). Northern peatlands are estimated to contain the majority of global peatland carbon (Figure 2) at around 500 ± 100 Pg C (Yu et al., 2010; Yu, 2012), of which 147 Pg C is thought to be stored in Canadian peatlands (Tarnocai, 2006). Meanwhile, permafrost peatlands of the pan-Arctic region are estimated to contain ~277 Pg C (Tarnocai et al., 2009). In the context of the global carbon cycle, permafrost peatlands equate to 14% of all terrestrial soil carbon, which is equivalent to more than a third of the entire atmospheric carbon store (Houghton, 2007;

Tarnocai et al., 2009). The stability of these carbon stocks is potentially vulnerable to twenty-first century climate change.

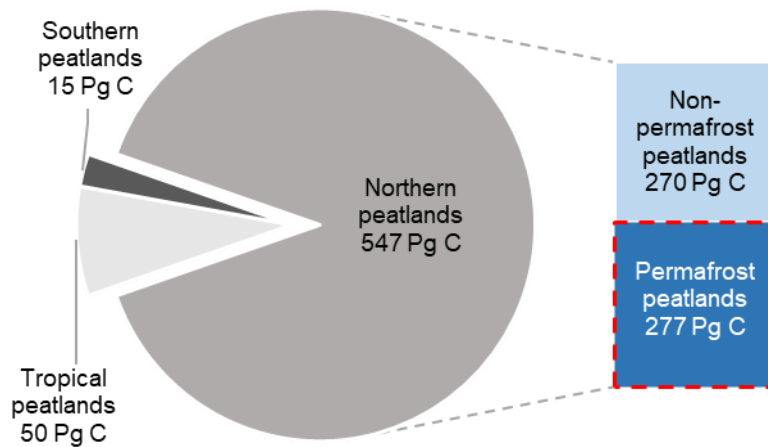


Figure 2. Relative estimated soil carbon storage for global peatland regions. Northern peatlands = $>30^{\circ}\text{N}$, tropical peatlands = 30°N to 30°S , southern peatlands = $>30^{\circ}\text{S}$. Created using global peatland region soil carbon estimates (Yu et al., 2010) and permafrost peatland soil carbon estimates (Tarnocai et al., 2009).

1.2.3 CARBON DYNAMICS AND CLIMATE CHANGE

The global climate is widely accepted to be experiencing a warming phase driven by a combination of both natural processes and anthropogenic emissions of greenhouse gases (GHGs) (Bindoff et al., 2013). Over the twenty-first century global mean surface temperature is likely to increase by $0.3\text{--}4.8^{\circ}\text{C}$ relative to 1986–2005 levels, depending on the GHG emissions scenario (Collins et al., 2013). In the Arctic, average temperatures observed over the past few decades are substantially higher than any over the last 2 Ka (Kaufman et al., 2009). Climate warming over the last century has been greatest in the Arctic and will continue in the twenty-first century at a rate far above the global average, alongside likely increases in Arctic precipitation by the mid-twenty-first century (Christensen et al., 2013). Warming is expected to be greatest in the Arctic because of the polar amplification phenomenon, primarily attributed to changes in albedo from melting snow and sea ice (Serreze, et al., 2009, Screen & Simmonds, 2010). Other mechanisms contributing to polar amplification in the Arctic are thought to be changes in atmospheric and oceanic circulation; and water vapour and cloud cover (Serreze & Barry, 2011; Collins et al., 2013).

The response of both global wetlands and permafrost peatlands in particular to this potential rapid climate warming remains uncertain and highly debated in the literature. Earth system models (Chaudhary et al., 2017) and management practices (McLaughlin & Webster, 2013)

would both benefit from improved understanding of peatland carbon dynamics in response to climate change. The complex factors influencing a net warming or net cooling effect from peatland systems in the context of twenty-first century climate warming and understanding of these factors alongside associated feedbacks will be summarised in the following sections and evaluated to identify research gaps.

1.2.3.1 CARBON ACCUMULATION

Climate can have direct implications upon plant productivity and organic matter decomposition, and indirectly through influences on hydrology and vegetation that in turn impact productivity, decomposition, erosion and wildfire frequency – collectively influencing carbon accumulation (Yu et al., 2009; Frohling et al., 2011; Olefeldt & Roulet, 2012). On a millennial timescale growing degree days above 0°C (GDD₀) and photosynthetically active radiation (PAR) in the presence of adequate moisture have been correlated with increased carbon accumulation in mid to high-latitude peatlands (Charman et al., 2013). The balance between uptake and loss is what determines carbon accumulation, however there are a combination of factors and interacting processes that determines this (Figure 3).

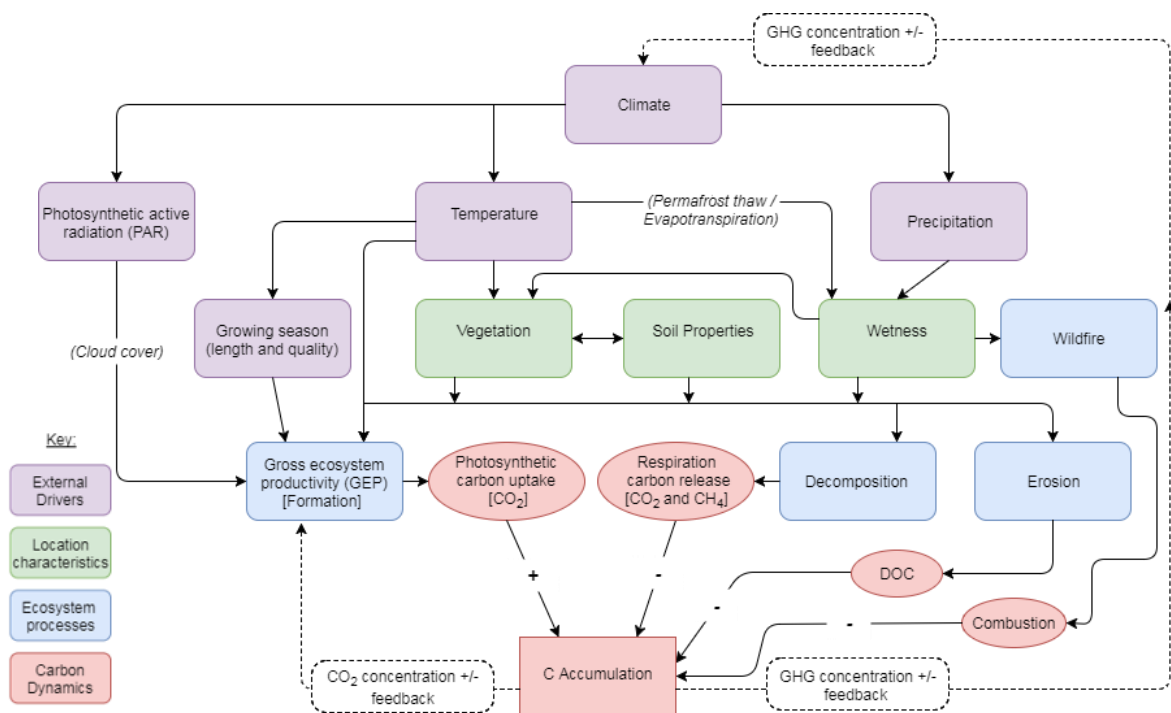


Figure 3. Factors affecting wetland carbon accumulation in terms of external drivers, location characteristics, ecosystem processes and carbon dynamics. Factors are not mutually exclusive from each other, summary diagram only.

In continuous permafrost regions a shorter and colder growing season can slow carbon accumulation by reducing plant productivity, but this is partially compensated by reduced decomposition under colder temperatures (Charman et al., 2013; Chaudhary et al., 2017). On the other hand in tropical peatlands, under much warmer conditions enhanced microbial decomposition counters increased primary productivity, resulting in comparatively lower carbon accumulation than in northern peatlands (Gallego-Sala et al., 2018). Where plant productivity is in equal to or less than microbial decomposition, carbon accumulation and peat formation does not occur – as can be the case in some Arctic wetlands that lack a surface layer of organic matter or peat. Carbon accumulation rates of northern peatlands have been observed to be most restricted in regions of continuous permafrost, becoming less restricted in discontinuous permafrost and unaffected in sporadic permafrost (Robinson et al., 2003), although the relationship between permafrost and carbon accumulation is not simple. Aggradation of permafrost causes uplift in peatlands and can lead to drier conditions that increases aerobic acrotelm decomposition (Sannel & Kuhry, 2008; Loisel et al., 2014). However, colder conditions in deeper peat can inhibit decomposition (Pelletier et al., 2017). Soil temperature exhibits control upon permafrost distribution at a macroscale (Figure 1A and 1B), although local factors and complex feedbacks influence this distribution - mainly in zones of discontinuous permafrost (Beilman et al., 2001). Despite lower carbon accumulation, the large carbon store exhibited by permafrost peatlands becomes significant when considered in the context of interaction and feedback with the global climate system.

1.2.3.2 CARBON DYNAMICS WITH CLIMATE CHANGE

Recent warming at high latitudes has caused permafrost peatlands to experience increases in soil temperature, potential evapotranspiration and growing season length (Riordan et al., 2006). A warming climate has been linked to active layer thickening (Åkerman & Johansson, 2008; Burn & Kokelj, 2009), increased number and size of arctic lakes present in permafrost (Smith et al., 2007) and permafrost disappearance (Christensen et al., 2004). Permafrost thaw and surface collapse in peatlands can result in thermokarst formation and a shallower water table (Zoltai, 1993; Vitt et al., 1994; Johansson et al., 2006). If thawing continues to influence watershed drainage then thermokarsts have been observed to dry, yet this is more common in lakes (Smith et al., 2005). In some areas, a warming and drying climate may increase wildfire frequency, having the potential to both release large amounts of carbon and accelerate permafrost thaw (Zoltai, 1993; Frolking et al., 2011; Turetsky et al., 2015). Similarly, permafrost thaw may increase

erosion and losses of dissolved organic carbon (Olefeldt and Roulet, 2012). In terms of ecology, warming has been associated with increased NPP alongside greater shrub cover and density (Myers-Smith et al., 2011). Specifically in Arctic wetlands, warming has been linked with increased above and below ground plant biomass (Hill & Henry, 2011), and increased melt and evaporation have increased extremes in seasonal hydrological conditions (Woo and Young, 2003; 2006; 2014).

Climate is a key control upon ecosystem processes that ultimately determine carbon accumulation (Figure 3) - therefore a changing climate is likely to impact carbon accumulation. Permafrost thaw could expose vast quantities of previously inert organic carbon to decomposition leading to the gradual and prolonged release of CO₂ and CH₄ to the atmosphere that may accelerate climate change (Dorrepaal et al., 2009; Schuur et al., 2015). Excessive drying of peatlands could lead to increased aerobic decomposition (CO₂) and wetting to increased anaerobic decomposition (CH₄) (Gorham, 1991). However, NPP is likely to increase alongside greater plant productivity with longer and warmer growing seasons, which in northern peatlands is suggested to be more important than microbial decomposition for carbon accumulation (Charman et al., 2013). Furthermore, since the Last Glacial Maximum warming growing seasons have been a key driver of peatland initiation around the world (Morris et al., 2018). With warming, peatland productivity may increase and the climatic envelope for peatland formation may migrate northwards facilitating new peat accumulation that may partially compensate for carbon losses elsewhere (Charman et al., 2015; Gallego-Sala et al., 2018). However there is likely to be a point with warming (estimated to be ~AD 2100), where on a global scale stimulation of microbial decomposition nullifies the increased carbon input from elevated plant productivity - therefore curbing carbon accumulation rates in peatlands (Gallego-Sala et al., 2018).

Increased carbon accumulation at high latitudes in the twentieth alongside warming is evidenced by palaeoenvironmental records from peatlands in Subarctic Sweden (Swindles, et al., 2015a) and Alaska (Klein et al., 2013) and moss banks on the Antarctic Peninsula (Loisel, et al., 2017). This increased peatland carbon accumulation is conditional on the presence of adequate moisture to hinder decomposition of organic carbon and stimulate growth of peat-forming vegetation (Oechel, et al., 1998; Chivers et al., 2009; Charman et al., 2013). However, future hydrological response, vegetation shifts and degradation of permafrost have been identified as

key areas of uncertainty in the prediction of permafrost carbon dynamics (Lawrence et al., 2015; Abbott et al., 2016).

1.2.3.3 NON-LINEAR RESPONSE

Potential feedback mechanisms between peatlands and climate include: fire regimes, methane emissions, nitrogen deposition, growing season length and temperature, photosynthetic active radiation and permafrost thaw (Dorrepaal et al., 2009; Frolking et al., 2011; Charman et al., 2013). However, hydrological processes, organic matter dynamics and energy exchanges control stabilising factors in peatlands and therefore peatlands respond in a non-linear fashion (Belyea, 2009; Swindles et al., 2012). Temperature appears to have a larger influence upon carbon dynamics than precipitation, with autogenic mechanisms between peat accumulation, decomposition, drainage and hydrology buffering gradual changes in precipitation, particularly at millennial timescales (Morris et al., 2015). Beilman and Robinson (2003) found that larger permafrost peatland areas did not respond directly to warming, perhaps because a surface layer of peat - particularly when dry, such as in ombrotrophic bogs - can insulate the underlying permafrost against warming temperatures in the atmosphere and land, therefore thicker peat layers will slow permafrost thaw (Yi et al., 2007; Lawrence et al., 2008). Long periods of stability in peatland systems can be interspersed by abrupt changes regardless of forcing and these changes may be disproportionately large in comparison to the environmental forcing (Belyea, 2009). The non-linear response of carbon accumulation and hydrology in permafrost peatlands to increasing temperature is exemplified in a conceptual model proposed by Swindles, et al. (2015a). Phase 4 in the conceptual model (Figure 4) overleaf exemplifies the point at which autogenic factors (e.g. dome collapse) disconnect peatland hydrology from climate forcing (Swindles et al., 2012; 2015a; Morris et al., 2015). While water table depth and carbon dynamics are closely linked, peatlands are extremely complex systems (Belyea and Baird, 2006) and require a greater understanding of the range and complexity of feedbacks across hydrology, plant ecology, soil biochemistry and micro-meteorology (Waddington et al., 2015).

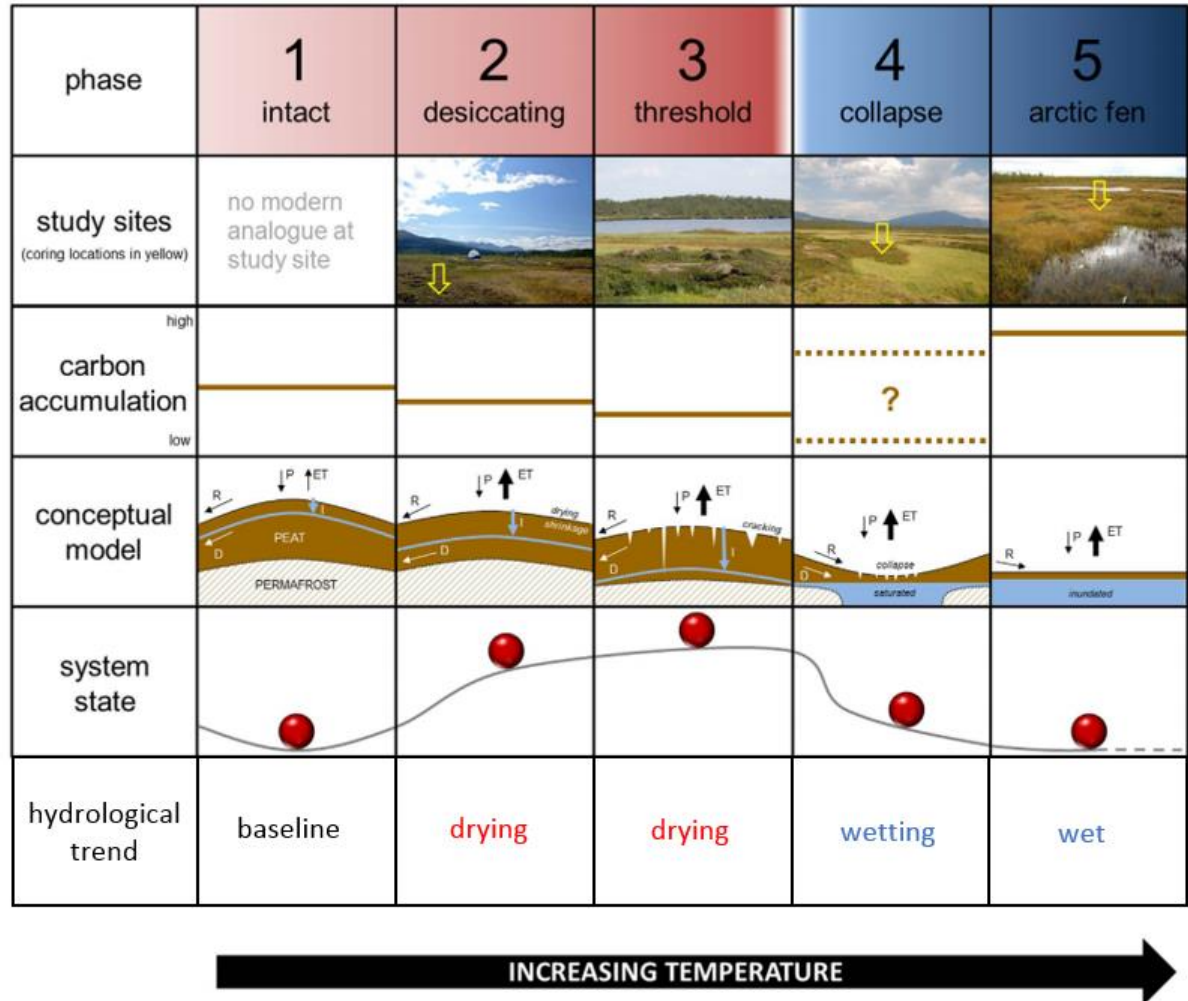


Figure 4. Five-stage model (columns = stages) for the response of permafrost peatlands to increasing temperature (Swindles, et al., 2015a). R = runoff, D = shallow drainage, P = precipitation, ET = evapotranspiration, I = infiltration.

1.3 CONSIDERING A PALAEOENVIRONMENTAL APPROACH

1.3.1 CARBON ACCUMULATION ESTIMATES

Estimates of carbon accumulation rates in Northern peatlands (e.g. Tolonen & Turunen, 1996; MacDonald et al., 2006) suffer from a lack of data from remote regions and often rely entirely on basal age dates to calculate long-term carbon accumulation that will not account for losses to fire and erosion and assumes a linear age-depth model (Yu, 2012; Loisel et al., 2014;). Yu et al., (2009) addressed this to some extent by compiling data from peatlands ($n=33$) with multiple down profile dates, while highlighting an underrepresentation at higher latitudes and at decadal

and centennial timescales. Ovenden (1990) found that carbon accumulation rates generally echo the influence of climate, but unexpectedly found higher accumulation rates in peatlands on Canadian Arctic islands – perhaps because of unrepresentative sampling. Many higher latitude peatlands have experienced an interruption or reduction in peat accumulation – particularly in permafrost peatlands - over the past few thousand years in Canada (Vardy et al., 2000) and Siberia (Beilman et al., 2009). Therefore, it is of interest to further increase understanding carbon dynamics at higher latitudes through a high-temporal resolution palaeoecological approach.

1.3.2 CONTEMPORARY VS. PALAEOENVIRONMENTAL APPROACH

Contemporary field monitoring of permafrost peatlands such as carbon flux to the atmosphere, water table and temperature (Liblik et al., 1997; Burgess et al., 2000), only provides a partial record of their response to warming because they are limited temporally to the last two or three decades since the 1990s (Johansson et al., 2006). Contemporary studies show differing responses of peatland carbon balance to permafrost thaw between peatland types, thaw stage and locations. Helbig et al. (2017) suggest that Boreal forest peatlands will become a net source of carbon, whereas Turetsky et al. (2007) concluded that degradation following permafrost thaw in Boreal peatlands was likely to represent a small net carbon sink on a long-term timescale, but that CH₄ emissions would have a net warming effect for 70 years. Contemporary monitoring has predicted Subarctic peatlands to become net sources of carbon with permafrost thaw (Johansson et al., 2006), yet drained thermokarst lakes have been predicted to provide a net carbon sink (Jones et al., 2012). These findings exemplify the complexity introduced by location specific factors and perhaps highlight that, while contemporary monitoring is essential to build understanding of peatlands dynamics, there are limitations in considering carbon dynamics over shorter timescales where the influence of system feedbacks and lag times may not be apparent (Swindles et al., 2015a; 2016). Therefore, a palaeoecological approach presents the opportunity to develop baseline conditions over a greater temporal timescale to aid a better understanding of the response of permafrost peatlands to recent climate change.

1.3.3 TESTATE AMOEBAE

Testate amoebae are single-celled protists that are routinely used as palaeoenvironmental indicators because of the rapid response they demonstrate to hydrological conditions and the resistance they show to decomposition (Charman et al., 2000; Booth et al., 2010). Contemporary sampling of testate amoeba species abundances from surficial peat alongside water table depth

measurements are used to calculate statistical transfer functions to enable quantitative interpretation of past hydrology from subfossil assemblages. Testate amoeba transfer functions have been developed for a number of regions and peatland types e.g. ombrotrophic peatlands in north-eastern Canada and Maine, United States (Amesbury et al., 2013), *Sphagnum*-dominated peatlands of North America (Booth, 2008), European ombrotrophic peatlands (Charman et al., 2007), minerotrophic (poor fen) and ombrotrophic Boreal and Subarctic peatlands in north-eastern Canada (Lamarre et al., 2013), Subarctic permafrost peatlands in Northern Europe (Swindles, et al., 2015b) and peatlands on the Alaskan North Slope in the continuous permafrost zone (Taylor, et al., 2019).

Protists are typically limited to top few centimetres of a soil profile (Coleman et al., 2017) and therefore in palaeoenvironmental reconstruction subfossils are assumed to be in-situ and representative of the environmental conditions at the time of deposition. The vertical distribution of testate amoebae in peatlands are understood to be limited by moisture, light, temperature, food supply and mineral availability for test building (Charman et al., 2000; Mieczan, 2010; Roe et al., 2017). However, Roe et al. (2017) highlight the complexity of vertical distribution of testate amoeba in surficial peat and *Sphagnum* stems and suggest further investigation in to the influence of testate amoeba encystment (dormant stage) for palaeoenvironmental reconstructions. Similarly in minerotrophic peatlands, pH (Lamarre et al., 2013) and nutrient status (Payne, 2011) can reduce the predictive power of testate amoebae as palaeo-hydrological indicators, requiring more cautious interpretation.

Interpreting climatic influence, even from sites of minimal anthropogenic modification (excluding climate change) requires caution (Morris et al., 2015). Testate amoebae and plant macrofossils prove a snapshot into the hydrological and vegetation conditions under which a layer of peat has formed (Amesbury et al., 2011). Quantifying bulk density, organic matter content and carbon content can provide an insight into carbon dynamics over time (Chambers et al., 2011). Therefore, a multiproxy approach encompassing all these methodologies offers the most comprehensive representation of past conditions. The first application of testate amoebae in Subarctic Canadian permafrost peatlands by Lamarre et al. (2012), emphasised the need for a multi-proxy approach to characterise the strength of allogenic and autogenic processes in peatlands – yet spatial application remains limited.

Ecosystem-scale simulation models of peatland development suggest that a combination of high pass (ecohydrological feedbacks) for precipitation and low pass (secondary decomposition) filters for both temperature and precipitation makes large magnitude events at decadal to centennial timescales the most detectable in palaeoenvironmental investigation (Morris et al., 2015). Furthermore, during the instrumental period of the last 100–150 years (Hansen et al., 2010) there is a lack of high resolution palaeoecological data regarding the response of permafrost peatlands to climate change, with exception of Swindles et al., (2015a) focusing on the Abisko region in Sweden. The close link between hydrology and permafrost carbon dynamics (Gorham, 1991; Moore & Roulet, 1993; Hodgkins et al., 2014; Lawrence et al., 2015; Swindles, et al., 2015a) makes testate amoebae an extremely useful environmental proxy to better understand and therefore predict responses of peatlands to climate change (Swindles, et al., 2015b).

1.4 AIM AND OBJECTIVES

The aim of this thesis is to determine the response of wetlands in the Canadian High Arctic to twentieth century warming. I identify the following specific objectives:

- 1) Build up a comprehensive picture of twentieth century climate change from instrumental and re-analysis data.
- 2) Use a palaeoenvironmental approach to test the ecological response to twentieth century warming of the main Arctic wetland types: (i) a Polygon Mire; (ii) a Valley Fen (patchy wetland); and (iii) a Coastal Fen.

2. METHODOLOGY

2.1 STUDY SITES

The study region is in the continuous permafrost zone of the western Canadian Arctic tundra, between the latitudes of around 68.5°N and 74.5°N (Figure 5; Figure 6).

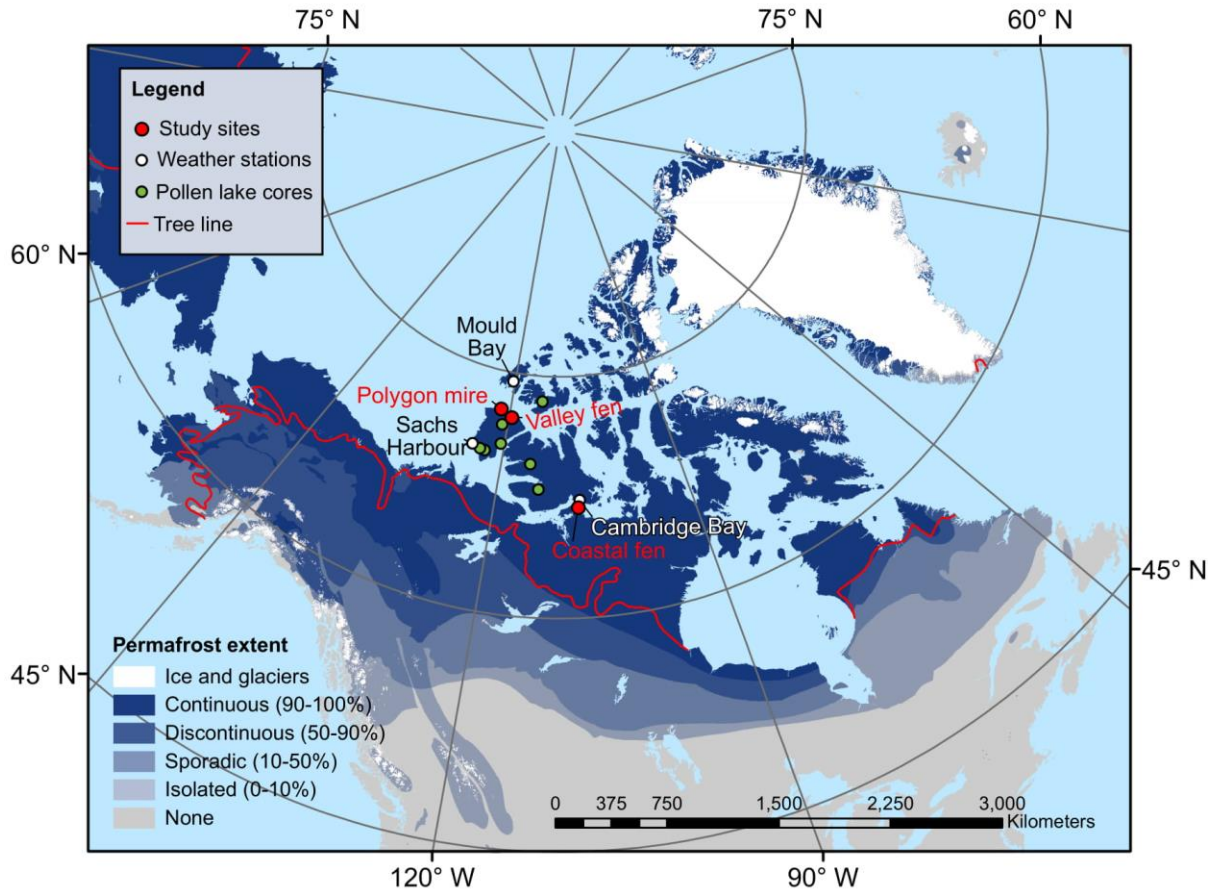


Figure 5. Upper panel shows a map of wetland site locations where peat monoliths were sampled for palaeoenvironmental analysis, nearby weather stations (presented in Figure 32), pollen lake cores used for Holocene temperature reconstruction of the western Arctic region (Gajewski, 2015; presented in Figure 32). Boundaries between permafrost zones and the northern extent of the tree line are also shown (Brown et al., 2002). Lower panel shows photographs taken from each site.

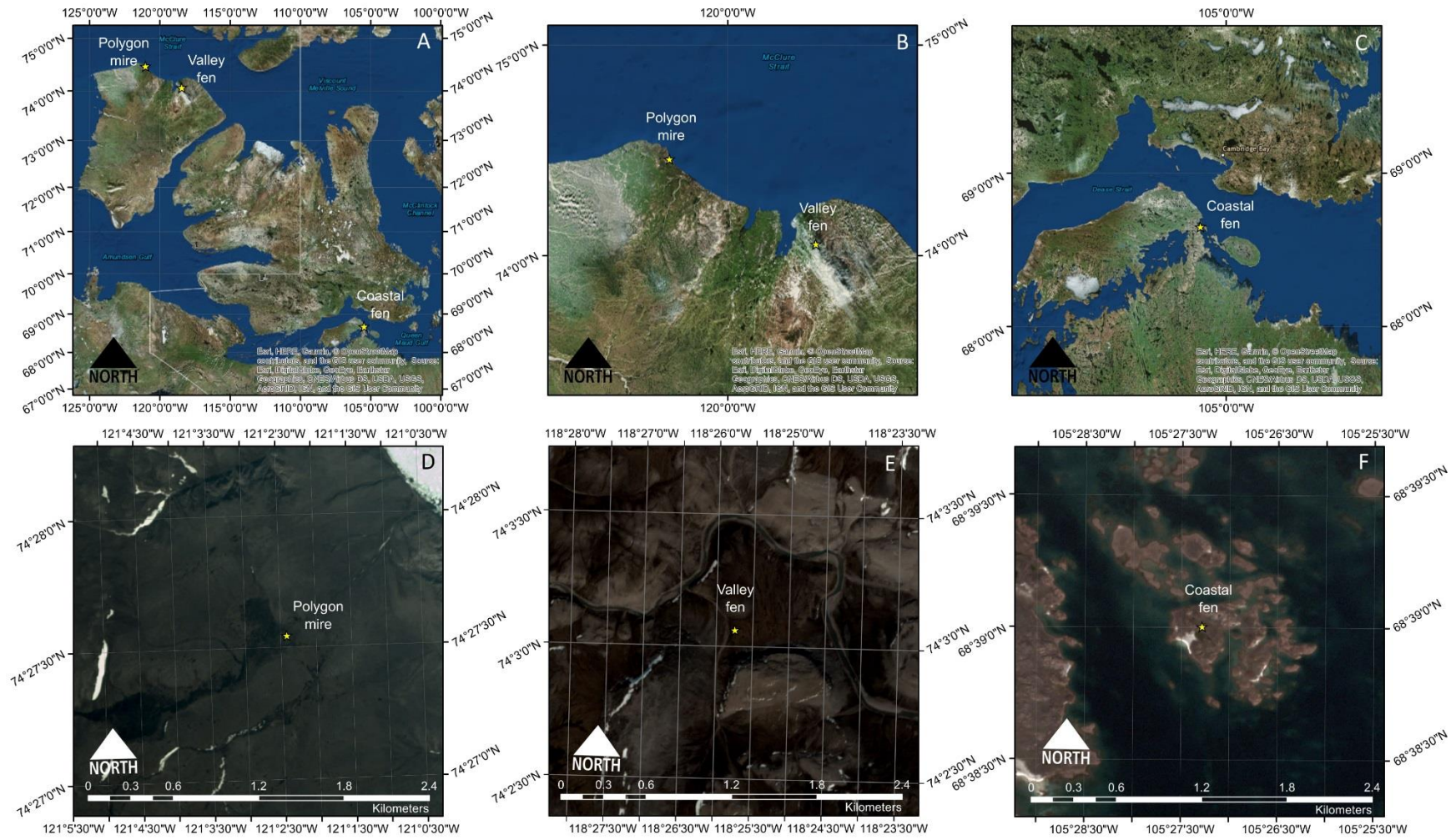


Figure 6. Aerial imagery of site locations. A-C sourced from ESRI via ArcGIS and D-F sourced from Planet Lab.

I selected sites to be representative of the main wetland types in the Canadian High Arctic. I study two wetlands on northern Banks Island, Northwest Territories: a Polygon Mire (74.459°N, 121.04°E) and a Valley Fen (74.05°N, 118.429°E). The Polygon Mire is a broadly flat expanse with distinctive microtopography consisting of more sparsely vegetated raised centre mounds and surrounding vegetated troughs. This distinctive microtopography was captured by extracting a monolith from each of these areas. The Valley Fen is a wet sedge meadow with a large moss fraction situated in a topographic depression. My third site is a Coastal Fen (68.65°N, 105.455°E) located on an island approximately 50 km south of Cambridge Bay, Nunavut, where two monoliths were sampled to serve as replicate palaeo-records. The site was characterised by large patches devoid of vegetation, areas of moss-cover and sedge-cover towards the wetland edge.

The average annual temperature for my wetland sites is typically below -10°C with a short summer growing season from July to August or early September. Precipitation is relatively low and consistent between weather stations proximal to my sites with around half annual precipitation falling in the summer (Figure A1). Average annual precipitation at Mould Bay is 116.3 mm; at Sachs Harbour is 142.9 mm; and at Cambridge Bay is 148.9 mm (Figure A1).

2.2 GROWING DEGREE DAY CALCULATION AND CALIBRATION

Monthly temperature and annual growing degree days above 0°C (GDD₀) estimates from climate re-analysis (Compo et al., 2011) for each site were validated against records from the nearest weather stations (Figure 7). Annual GDD₀ were calculated from monthly temperature values using the following equation:

$$GDD_0 = T_0 * D$$

Where T_0 is monthly temperature values above 0°C and D is days is respective calendar months.

Mould Bay (76.23°N, 119.35°W, 2 m above sea level) was the nearest weather station for the northern Banks Island sites, situated around 180 km north northeast of the Polygon Mire and around 225 km north northwest of the Valley Fen. For the Mould Bay weather station complete monthly temperature records were available for the periods AD 1949–1992 and AD 1994–1996. The Polygon Mire re-analysis data demonstrated a strong relationship with monthly temperature ($r^2 = 0.9718$; Figure 7.1a) and annual GDD₀ ($r^2 = 0.8206$; $p < 0.001$; Figure 7.1b) from Mould Bay. A timeseries of annual GDD₀ from the Polygon Mire re-analysis dataset and the Mould Bay record show comparative magnitudes, with re-analysis long-term average GDD₀ as a

proportion of the measured GDD_0 at 0.84 (Figure 7.1c). Similarly, the Valley Fen re-analysis data showed a strong relationship with monthly temperature ($r^2 = 0.9768$; Figure 7.2a) and annual GDD_0 ($r^2 = 0.8261$; $p < 0.001$; Figure 7.2b) from Mould Bay. A timeseries of annual GDD_0 shows the Valley Fen re-analysis dataset to have consistently more GDD_0 than the Mould Bay record, with re-analysis average GDD_0 as a proportion of measured $GDD_0 = 1.43$ (Figure 7.2c). I attributed the higher GDD_0 values for the Valley Fen to the more southern latitude compared to Mould Bay combined with a more sheltered position from the Beaufort Sea than the Polygon Mire.

The Cambridge Bay weather station (69.1°N, 105.12°W, 27 m above sea level) around 50 km north northeast of the Coastal Fen site was used for validation of the re-analysis data. Complete monthly temperature records were available for the periods AD 1940–1941, AD 1949–2003 and AD 2007–2010. I expected very similar records because of the proximity of the weather station to the site. The Coastal Fen re-analysis data demonstrated a strong relationship with monthly temperature ($r^2 = 0.9746$; Figure 7.3a) and moderate relationship with annual GDD_0 ($r^2 = 0.4918$; $p < 0.001$; Figure 7.3b) from Cambridge Bay. However, a small overestimation in re-analysis monthly temperature (Figure 7.3a) resulted in a large overestimation in annual GDD_0 , by a magnitude of over two (Figures 7.3b and 7.3c). Consequently, I calibrated the re-analysis monthly temperature estimates for the Coastal Fen site with the Cambridge Bay record. To do this I used the strong relationship between re-analysis (Coastal Fen) and measured (Cambridge Bay) monthly temperatures ($r^2 = 0.9746$; $p < 0.001$; $n = 732$; Figure 8.A), represented in this linear regression model:

$$M_{temp} = 0.9221R_{temp} - 4.0703$$

Where M_{temp} is measured monthly temperature (°C) and R_{temp} is re-analysis monthly temperature (°C).

This linear regression model equation was applied to the Coastal Fen re-analysis monthly temperature dataset (Figure 8.B) which was subsequently used to calculate annual GDD_0 (Figure 8.C). The calibrated re-analysis annual GDD_0 dataset demonstrates a moderately strong relationship ($r^2 = 0.45$; $p < 0.001$; Figure 8.C) with measured values and now of a comparable magnitude (calibrated re-analysis average GDD_0 as a proportion of measured = 1.14; Figure 8.D).

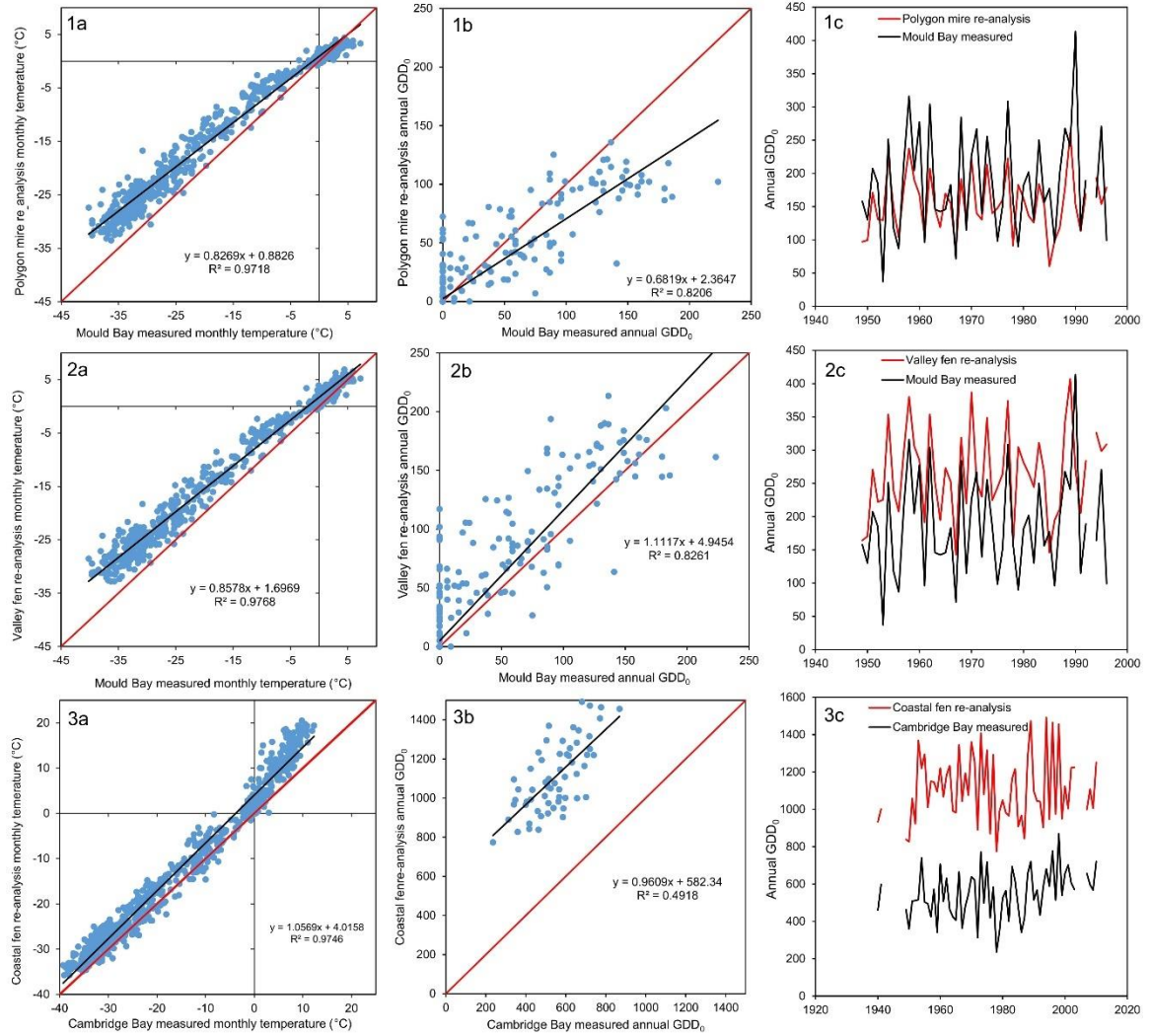


Figure 7. Re-analysis climate data (a = temperature; b and c = GDD₀) interpolated for each site (1 = Polygon Mire; 2 = Valley Fen; 3 = Coastal Fen) compared to corresponding monitoring data of nearby weather stations. In the A and B panels the red line represents a one to one relationship and the black line represents the linear trend-line of the data.

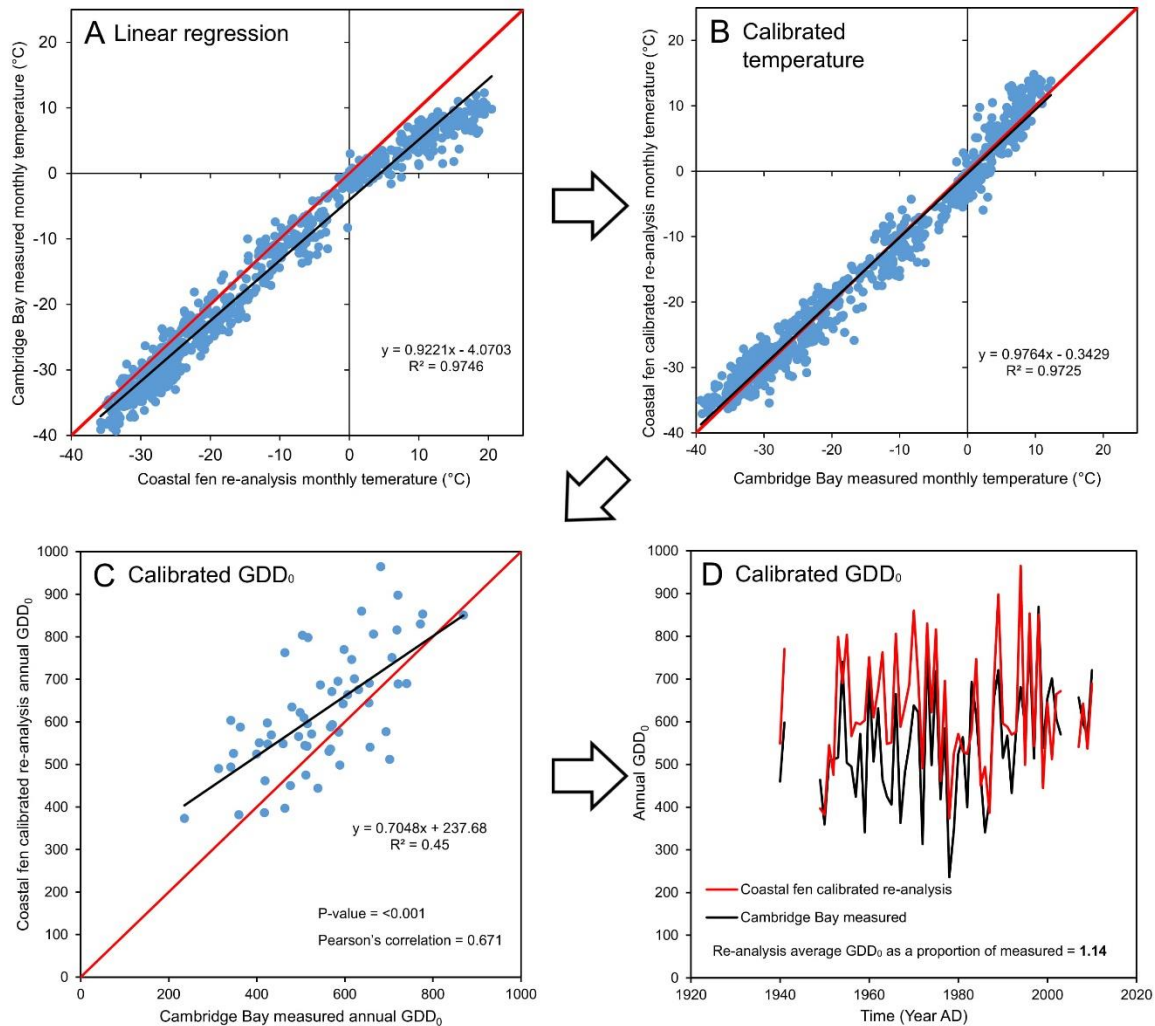


Figure 8. Calibration of Coastal Fen re-analysis monthly temperature with Cambridge Bay measurements and resultant annual GDD₀ from calibrated re-analysis monthly temperature. In the A, B and C and panels the red line represents a one to one relationship and the black line represents the linear trend-line of the data.

The original re-analysis annual GDD₀ for the Polygon Mire and Valley Fen sites, and the calibrated re-analysis annual GDD₀ for the Coastal Fen site were used in my analysis. Change-point analysis (Killick & Eckley, 2014) was conducted in R version 3.4.3 (R Core Team, 2018) on annual GDD₀ timeseries data for each of the three sites. The change-point was calculated using the function for a change in mean and variance (cpt.meanvar) under the default settings, including an At Most One Change (AMOC) approach to determine the singular main change in the data.

2.3 PALAEOENVIRONMENTAL ANALYSIS

Peat monoliths were dug to the base of the active layer at each site, sealed in plastic wrap and stored at 4°C prior to palaeoenvironmental analysis. The Banks Island samples were collected in July 2016, while the Elu Inlet samples near Cambridge Bay were collected in August 2017. In the laboratory at Leeds a central core was cut from these monoliths and sliced at 1 cm intervals with a band saw while frozen for fibrous samples and with a long-serrated knife for the more consolidated samples. At all stages of peat sub-sampling, tools were cleaned after every use with deionised water to avoid contamination (De Vleeschouwer et al., 2010).

2.3.1 AGE-DEPTH MODELS

A combination of above ground plant macrofossil remains and bulk peat samples (where above-ground macrofossils were not present) were extracted from each core and submitted to the A. E. Lalonde AMS Laboratory for ^{14}C radiocarbon dating. Pre-1950 dates were calibrated in R version 3.4.3 (R Core Team, 2018) with Clam version 2.2 (Blaauw, 2010) using the IntCal13 (Reimer et al., 2013) calibration curve. Negative (post-bomb era) radiocarbon ages were calculated by first converting the fraction of modern carbon ($F^{14}\text{C}$; Reimer et al., 2004) into percentage modern carbon (pMC) normalized to 100%. The pMC values were then converted into an equivalent ^{14}C age before being calibrated using the Hua et al. (2013) northern hemisphere zone 1 calibration curve. Where possible, cubic spline or polynomial regression age-depth models were applied to avoid unrealistic abrupt changes in peat accumulation, however where this induced age reversals in the chronology linear interpolation was applied.

2.3.2 PEAT PHYSICAL PROPERTIES

Loss-on-ignition analysis was carried out following Chambers et al. (2011). A volume of 4 cm⁻³ material was extracted from each 1 cm slice with a custom cutter, again the more fibrous peat was cut while frozen to avoid compression and to improve the consistency of bulk density estimates (Vardy et al., 2000). This known total volume of peat (V_t) was placed in labelled crucibles of known weight. Each crucible and sample were weighed to determine wet mass (M_w). Samples were dried overnight at 105°C, placed in a desiccator until cooled and then reweighed to determine dry mass (M_d).

Bulk density (ρ ; g/cm³) was calculated by the following:

$$\rho = \frac{M_d}{V_t}$$

Where M_d = dry mass (g) and V_t = volume (cm³). These dry samples were placed in a furnace at 550°C overnight to combust all organic matter, cooled to room temperature in a desiccator and the remaining ash was weighed (M_a).

Organic matter content (OM; %) was calculated by the following:

$$OM = 100 \left(\frac{M_d - M_a}{M_d} \right)$$

Where M_d = dry mass (g) and M_a = ash mass (g). Organic matter bulk density (ρ_{om} ; g/cm³) was calculated using the following equation:

$$\rho_{OM} = \rho \left(\frac{M_d - M_a}{M_d} \right)$$

Where ρ = bulk density of dry peat (g cm⁻³), M_d = dry mass (g) and M_a = ash mass (g). The long-term apparent rate of carbon accumulation (LORCA; g m⁻² yr⁻¹) was calculated - assuming the carbon content of organic matter was 50% - from the following:

$$LORCA = r(0.5\rho)$$

Where r = net rate of height addition (mm yr⁻¹), ρ = bulk density of dry peat (g cm⁻³).

2.3.3 PLANT MACROFOSSILS

Plant macrofossils were analysed contiguously at 1 cm intervals by Mariusz Gałka. Samples of 4 cm³ were washed and sieved under a warm-water spray using a 0.2 mm mesh sieve. Initially, the entire sample was examined with a stereomicroscope to obtain volume percentages of individual subfossils of vascular plants and mosses. The subfossil carpological remains and vegetative fragments (leaves, rootlets, epidermis) were identified using identification keys (Hadenäs, 2003; Smith, 2004; Flora of North America Editorial Committee, 2007; Mauquoy & van Geel, 2007). See Gałka, et al., (2017a) for a more detailed methodology for plant macrofossil analysis in peatlands.

2.3.4 TESTATE AMOEBAE

A modified version of the method outlined by Booth et al. (2010) was followed to extract testate amoeba. Samples were boiled in water for around 10 minutes and mixed with a glass rod. This solution was passed through a 300 μm sieve and back-sieved through a 15 μm mesh. Sub-samples were left to settle before slides were made up for microscopy. A minimum of 50 testate amoeba sub-fossils were counted per sub-sample using a high-power light microscope at a magnification of 200–400. A count of 50 was deemed representative considering the lower diversity in testate amoeba taxa observed at high latitudes (Beyens & Chardez, 1995). Testate amoeba and ciliates were identified using a range of reference material (Kralik, 1961; Bick, 1972; Corliss, 1979; Charman et al., 2000; Microworld, 2018).

In this study, the ciliate family Vaginicolidae have been incorporated as an additional hydrological indicators because of: high abundance levels across study sites and unambiguous aquatic hydrological preferences (Kralik, 1961; Bick, 1972; Corliss, 1979). The Vaginicolidae classification in this case primarily consists of the species *Platycola truncata* (de Fromentel, 1874; Figure 9), however a broader taxonomic classification to family level has been applied for accuracy.

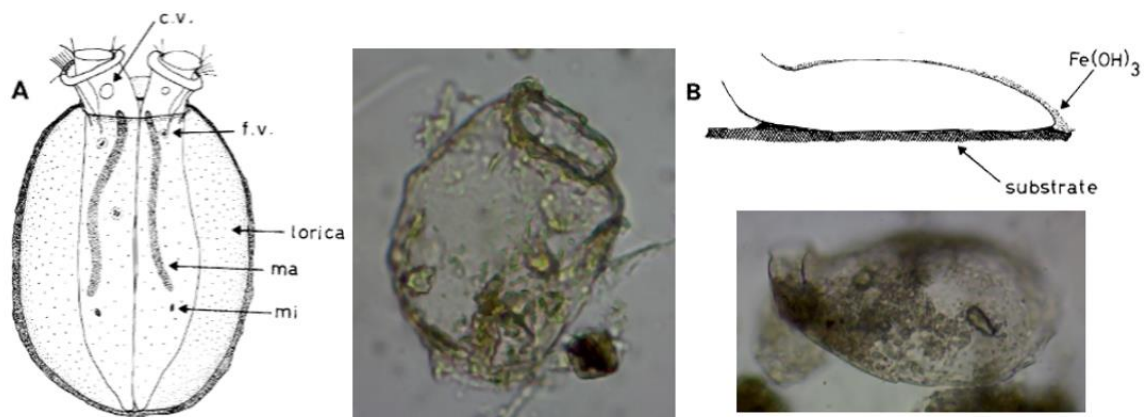


Figure 9. Sketches of *Platycola truncata* (de Fromentel 1874) sourced from (Bick, 1972), typically 65–145 μm (Kralik, 1961). Alongside are photographs of subfossil lorica (70–100 μm) from my samples. A) Ventral view, c.v. = contractile vacuole, f.v. = frontoventrals, lorica = organism casing, ma = macronucleus, mi = micronucleus. B) Lorica longitudinal section.

Including the ciliate family Vaginicolidae alongside testate amoeba is comparable to the inclusion of the rotifer *Habrotricha angusticollis* (Warner & Chengalath, 1991), that has previously been included in reconstruction of past hydrology alongside testate amoeba in peatlands across the northern hemisphere (e.g. Warner & Chengalath, 1991; Booth, 2008; Qin et al., 2013). *P.*

truncata attaches to bare substrate or vegetation (Kralik, 1961; Bick, 1972) and therefore subfossils are assumed to be in situ and indicative of hydrological conditions at the time of deposition in the peat.

In the absence of contemporary ecological data, testate amoebae were grouped into categories of hydrological preference based on a detailed literature review (Table 1). The hydrological indicator classification (θ) was determined by consulting the literature on the optimal hydrological conditions of each testate amoeba taxon or grouping. From each study the taxa were classified into the category wet, intermediate, dry or variable. The θ value (wet = -1, unclear/wide-tolerance = 0, dry = 1) was assigned when $\geq 75\%$ of the references agreed on the classification, however if optimum hydrological conditions of a particular taxon or type were at all ambiguous then a classification of 'unclear/wide-tolerance' was assigned e.g. *Centropyxis aerophila* type and *Diffflugia* "small" type. The literature cited is largely composed of transfer function development studies for the reconstruction of past wetland conditions, however these are typically not specific to permafrost regions. Transfer functions that are specific to permafrost regions include Lamarre et al., (2013), Swindles et al. (2015b) and Taylor et al. (2019). Contemporary ecology resources were used to assess the favoured hydrology conditions of the ciliate family Vaginicolidae (Bick, 1972; Corliss, 1979).

Table 1. Summary of the hydrological indicator classification (wet, unclear/wide-tolerance [U/WT], dry) of testate amoeba taxon. The following references are represented in the table below by the corresponding superscript numbers: Amesbury et al. 2013¹(*), Beyens et al., 1990² (+), Bick, 1972³, Bobrov et al., 1999⁴(*), Booth, 2008⁵(*), Charman et al., 2007⁶(*), Charman et al., 2000⁷(*), Corliss, 1979⁸, Lamarre et al., 2013⁹(*+), Lamentowicz et al., 2008¹⁰(*), Mitchell et al., 1999¹¹(*), Smith, 1992¹², Swindles et al., 2015¹³(*+), Warner & Charman, 1994¹⁴ and Taylor et al., (2019)¹⁵(*+). Key: * = study with transfer function, + = Arctic or Subarctic study.

Classification	Hydrological indicator classification (θ)	Wet	Intermediate	Dry	Variable
<i>Arcella discoides</i> type	Wet	2, 4, 5, 6, 7, 9, 13, 14,	10		7
<i>Arcella hemisphaerica</i>	Wet	5, 10, 14, 15	13		
<i>Centropyxis aculeata</i> type	Wet	1, 2, 6, 7, 9, 10, 11, 12, 13, 14, 15	4, 5		
<i>Centropyxis gasparella</i>	Wet	2			
<i>Coniococassis pontigulasiformis</i>	Wet	2			
<i>Diffugia globulosa</i>	Wet	1, 2, 5, 7, 9, 10, 13, 15			
<i>Diffugia oblonga</i> type		4, 5, 6, 7, 10, 13, 14			
<i>D. bacillifera</i>	Wet	2, 4, 6, 7, 9, 13			
<i>D. bryophila</i>		2, 4			
<i>D. lithophila</i>		1			
<i>Netzelia</i> sp.	Wet	10, 15			
<i>Paraquadrula irregularis</i>	Wet	2, 12			
Vaginicolidae	Wet	3, 8			
<i>Arcella catinus</i> type	U/WT		1, 5, 13, 15	6, 9, 10	2
<i>A. arenaria</i>	U/WT		4		
<i>Centropyxis aerophila</i> type					
<i>C. cassis</i>	U/WT	7	9, 13	4, 6	1, 5
<i>C. platystoma</i>		1, 6, 10, 11, 15	5		
<i>C. sylvatica</i>				4, 15	
<i>C. aerophila</i>				4, 10, 15	2, 12
<i>C. constricta</i>			2	4, 15	
<i>Centropyxis plagiostoma</i> type	U/WT				
<i>Cyclopyxis arcelloides</i> type	U/WT	11, 9	6, 10, 15	4, 5	1
<i>Diffugia</i> "small" spp.					
<i>D. pulex</i>	U/WT	1, 12	6, 9	7, 13	
<i>D. lucida</i>		1, 5, 6, 7, 9, 12	2, 13		
<i>D. pristis</i> type		1, 7	6, 9		
<i>Euglypha compressa</i>	U/WT	6, 7	4, 11, 13	1	
<i>Euglypha degraded</i>	U/WT				
<i>Euglypha laevis</i>	U/WT	2	11		
<i>Euglypha rotunda</i>	U/WT	9	2, 5, 6, 7, 14	1, 15	
<i>Euglypha strigosa</i>	U/WT		1, 5, 6, 10	11, 14, 15	2, 7, 9
<i>Euglypha tuberculata</i>	U/WT	9	5, 6, 7, 10, 14	1, 15	
<i>Heleopera petricola</i>	U/WT	1, 2, 6, 9	4, 5, 10, 11, 14		7
<i>Nebela tinctoria</i> type	U/WT		4, 9, 10, 13	6, 15	2, 5, 7
<i>Phryganella acropodia</i>	U/WT	1, 4, 5, 9, 13	15	2, 11, 14	
<i>Assulina muscorum</i>	Dry		5	1, 6, 7, 9, 10, 13, 14, 15	12
<i>Corythion-Trinema</i> type				1, 6, 7, 9	5
<i>T. lineare</i>	Dry	15	2	1, 4, 7, 10	
<i>C. dubium</i>				2, 4, 11, 13, 14, 15	12

2.3.5 STATISTICAL ANALYSIS

Shannon's Diversity Index (SDI) was calculated from the testate amoeba percentage abundance data and non-metric multidimensional scaling (NMDS) was performed in Past version 3.19 (Hammer et al., 2001). SDI was calculated using a percentiles bootstrap (9999 permutations) to investigate diversity and evenness with depth. NMDS was completed using Bray-Curtis dissimilarity index to provide a trend in the testate amoeba abundance data with depth to complement the interpretation of testate amoeba hydrological indicator abundances. Constrained hierarchical clustering was performed in R version 3.4.3 (R Core Team, 2018) with the packages *vegan* (Oksanen et al., 2017) and *rioja* (Juggins, 2018) using the Bray-Curtis dissimilarity index and constrained incremental sum of squares cluster analysis (CONISS; Grimm, 1987). This clustering was completed on both testate amoeba and plant macrofossil data for each site and provides comparable quantitatively defined stratigraphic zones. Stratigraphic diagrams of abundance values were plotted for all individual testate amoeba and plant macrofossil records using the C2 software package version 1.7.7 (Juggins, 2007).

3. RESULTS

3.1 GROWING DEGREE DAYS

Re-analysis data demonstrates that there is a pronounced increase in GDD_0 across all three wetland sites during the twentieth century, with changepoints in the data detected 1931–1940 (Figure 10). Following respective changepoints, mean GDD_0 at the Polygon Mire increased from 49 ± 50 to 152 ± 46 GDD_0 (changepoint: 1940) and at the Valley Fen, from 105 ± 76 to 260 ± 6 GDD_0 (changepoint: 1936) (error terms indicate standard deviation). At the Coastal Fen after the 1931 changepoint mean GDD_0 increased from 400 ± 132 to 605 ± 68.3 GDD_0 . These increases in GDD_0 have occurred from lengthening and slight warming of the growing season.

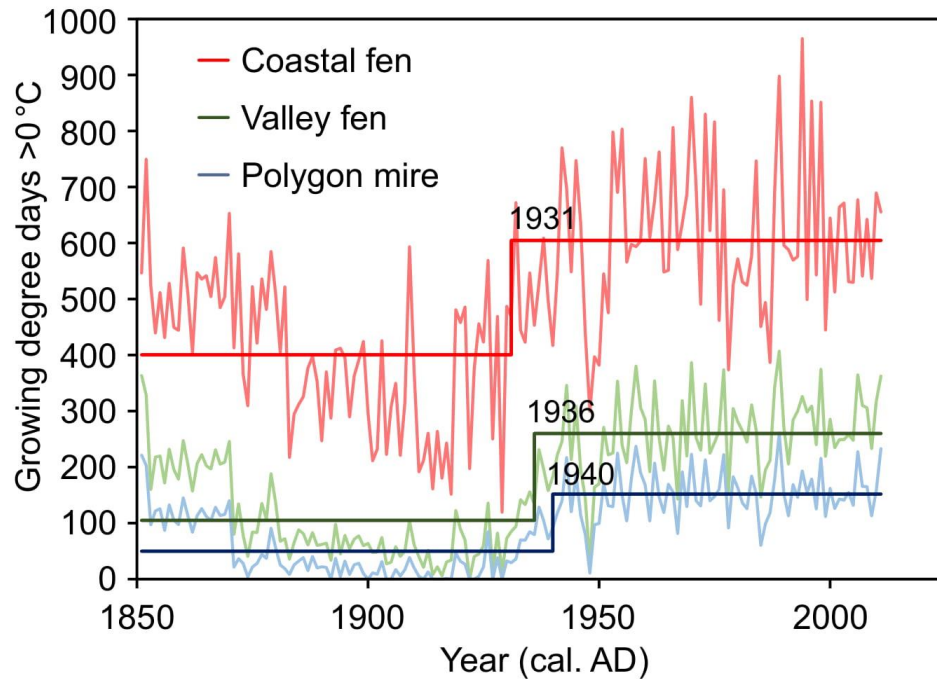


Figure 10. Growing degree days above 0°C for each wetland site 1851–2011 calculated from monthly temperature re-analysis data (Compo et al., 2011), stepped lines indicate the main changepoint in the mean and variance of the data for each site.

3.2 PALAEOENVIRONMENTAL RESULTS

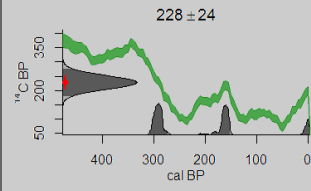
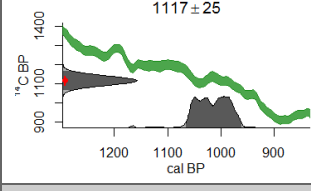
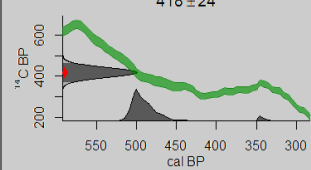
Here I present the palaeoenvironmental results from each of the five monoliths (across the three wetland sites) in turn, before a summary stratigraphic diagram at the end of the results section (Figure 31). This includes age-depth models, physical properties, testate amoebae and plant macrofossils.

3.2.1 POLYGON MIRE RAISED CENTRE

3.2.1.1 AGE-DEPTH MODEL

The Polygon Mire raised centre monolith has three radiocarbon dates with calibrated mean ^{14}C dates ranging from 1117–228 BP (Table 2). The monolith demonstrated an age reversal with the lower two dates in the chronology. The lowest date (6–7 cm, 492 BP) was excluded from the cubic spline age-depth model (Figure 11). Cryoturbation in shallow permafrost soils can lead to downwards stratigraphic mixing of organic matter and an accumulation at the permafrost table, i.e. the base of the active layer (Bockheim & Tarnocai, 1998). Consequently, in this and subsequent age reversals unless otherwise stated I have assumed the younger basal date has been contaminated with younger material. Therefore, the age-depth model suggests the top 4–5 cm of material has accumulated since AD 935 (1015 BP).

Table 2. Radiocarbon ^{14}C dating summary table from the Polygon Mire raised centre monolith, including individual date calibration plots. ‡ = Suess effect.

Site/ Depth (cm)	Lab ID	Material	^{14}C age	±	Calibration range (years BP or AD)	Calibrated median age (years BP or AD)	Calibration plots	Age- depth model
<i>Polygon Mire raised centre 2-3</i>	UOC- 6181	Bulk peat	228 BP	24	309-270 cal. BP (48.2%) 187-149 cal. BP (38.3%) 12calBP- >Modern (8.9%) ‡	199 BP OR AD 1751		Yes
<i>Polygon Mire raised centre 4-5</i>	UOC- 6180	Bulk peat	1117 BP	25	1071-959 cal. BP (95.4%)	1015 BP OR AD 935		Yes
<i>Polygon Mire raised centre 6-7</i>	UOC- 6179	Bulk peat	418 BP	24	519-453 cal. BP (90.8%) 349-335 cal. BP (4.6%)	492 BP OR AD 1458		No

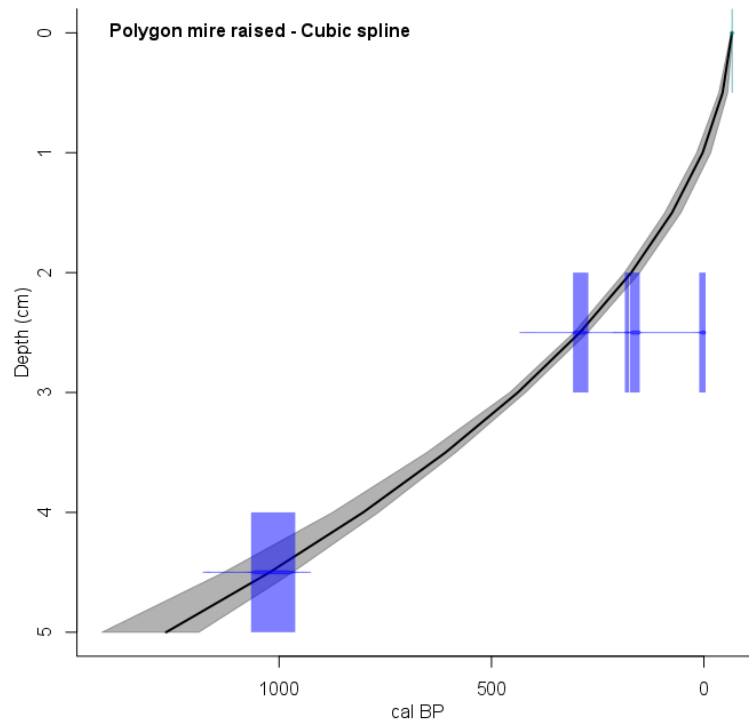


Figure 11. Age-depth model for the Polygon Mire raised centre monolith. The model was constructed using a cubic spline between dates. Black line = best age-depth model, grey = 95% confidence interval of age-depth model, blue = calibrated distributions of ¹⁴C dates.

3.2.1.2 PHYSICAL PROPERTIES

In the Polygon Mire raised centre monolith (11 cm; Figure 12) the material was light-brown in appearance and fibrous in texture. The record shows little change over time with the bulk density remaining relatively high ($0.36 \pm 0.1 \text{ g cm}^{-3}$), moisture content moderate ($49.4 \pm 5.6\%$) and relatively low organic matter content ($29.8 \pm 9.4\%$). The bulk density of organic matter is stable until \sim AD 1700 ($0.09 \pm 0.01 \text{ g cm}^{-3}$), where there is a slight increase ($0.15 \pm 0.002 \text{ g cm}^{-3}$). Modelled carbon accumulation is very low prior to \sim AD 1900 ($2.8 \pm 2.3 \text{ g m}^{-2} \text{ yr}^{-1}$) before showing recent increase to $31.4 \text{ g m}^{-2} \text{ yr}^{-1}$.

Polygon Mire raised centre

Physical properties
analysis: T. Sim

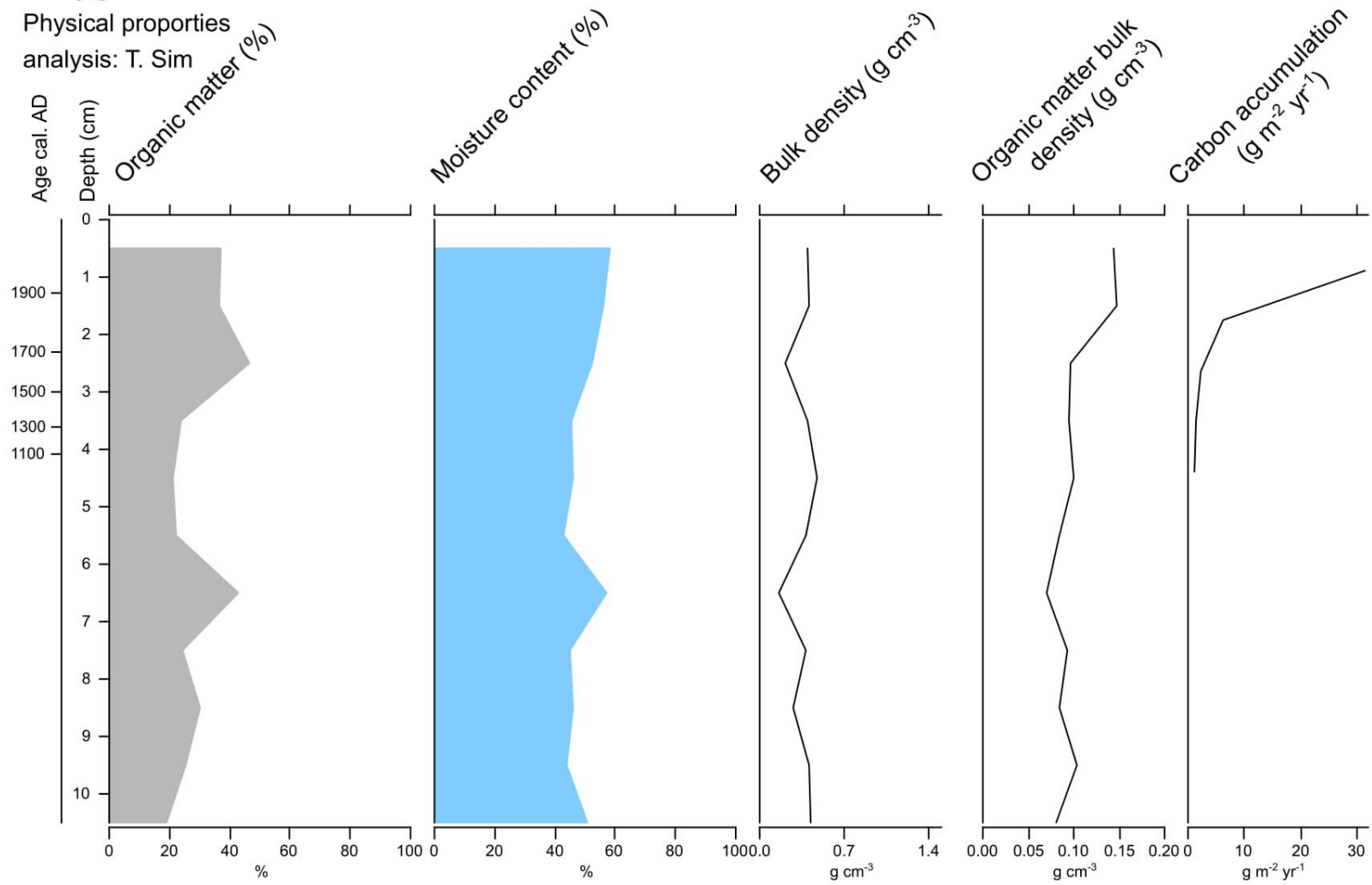


Figure 12. Physical properties summary stratigraphic diagram for the Polygon Mire raised centre monolith.

3.2.1.3 TESTATE AMOEBAE

The testate amoeba record from the Polygon Mire raised centre (Figure 13) suggests a gradual drying up the core with a reduction in wet taxon (max: 42%, min: 2%). *Centropyxis aerophila* type is the dominant taxon throughout the core, increasing gradually from the base of the monolith (max: 84.3%, min: 44%). Vaginicolidae – a wet indicator – gradually decreases up the monolith (max: 30%, min: 0%). Another wet indicator, *Diffflugia oblonga* type demonstrates low relative abundance throughout the record, except for zone 2 (~AD 950–1350) where relative abundance increased to 22–24%. In zone 1 (0–3 cm) the dry indicator *Assulina muscorum* appears in low abundance (0–3.9%).

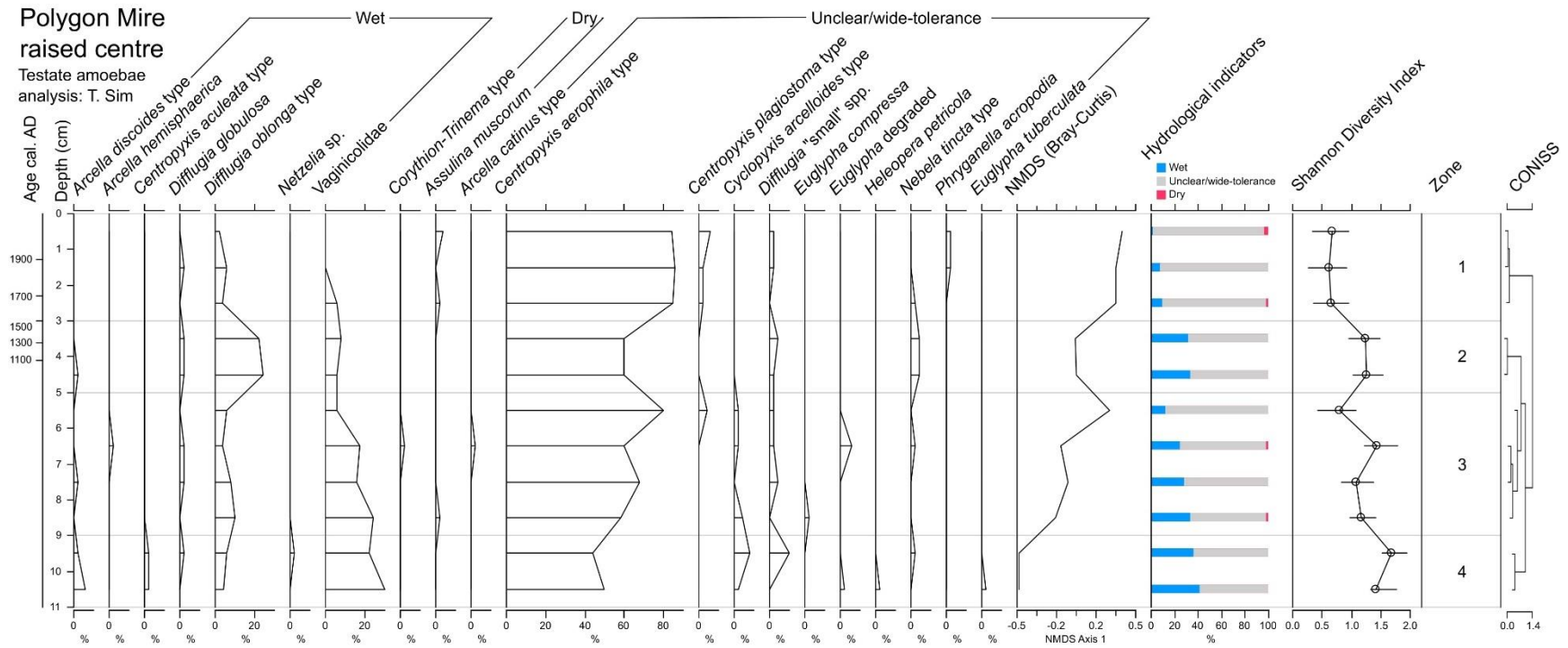


Figure 13. Relative abundance (%) of testate amoebae for the Polygon Mire raised centre monolith. Hydrological indicator values classified in Table 1.

3.2.1.4 PLANT MACROFOSSILS

The monolith from the raised centre of the Polygon Mire shows little change in plant macrofossils (Figure 14). The record is comprised of partially-decomposed *Scopodium cossonii* (80–90.5%) with some herbs (4.76–5%) and *Calliergon richardsonii* (4.76–10%).

Polygon Mire raised center

Plant macrofossil
analysis: M. Galka

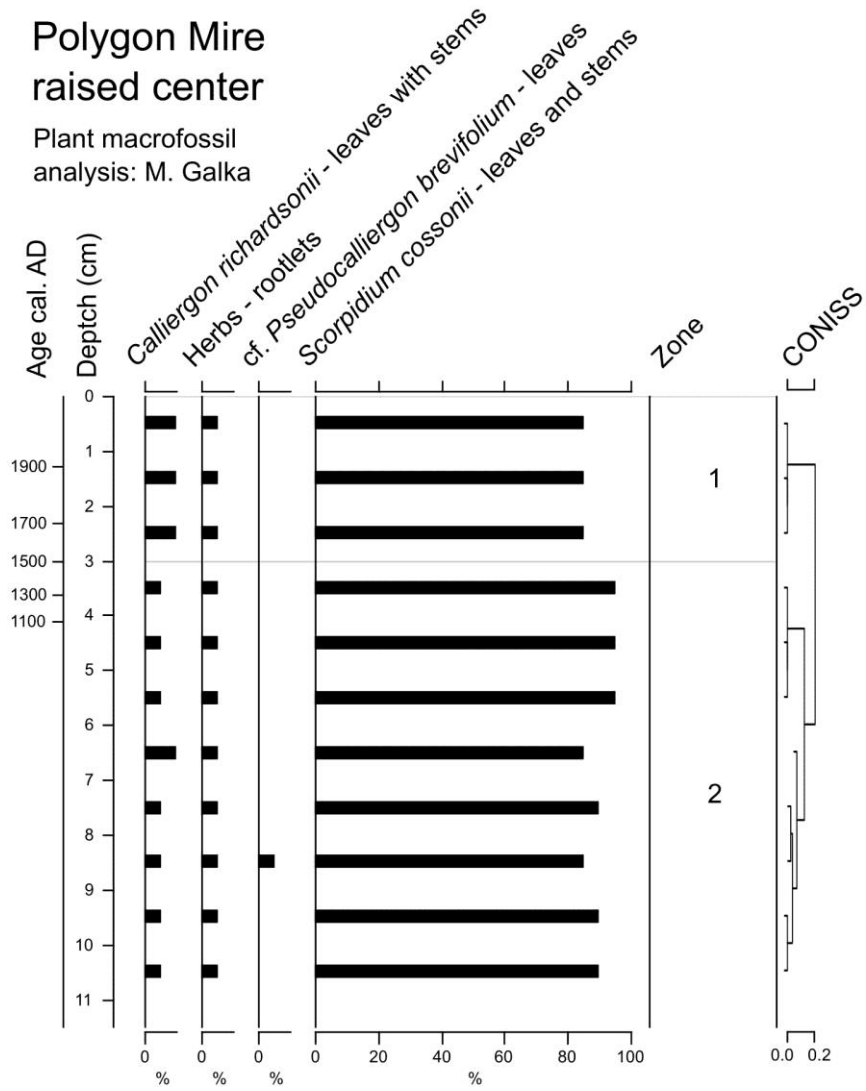


Figure 14. Abundance (%) of plant macrofossils for the Polygon Mire raised centre monolith.

3.2.2 POLYGON MIRE TROUGH

3.2.2.1 AGE-DEPTH MODEL

The Polygon Mire trough monolith has seven radiocarbon dates with calibrated mean ^{14}C dates ranging from AD 677–1998 (Table 3). The monolith demonstrates two age reversals in the chronology, both from bulk peat dates that are removed from the linear interpolation age-depth model (Figure 15). The age-depth model suggests the top 4–5 cm of material has accumulated since ~AD 1998.

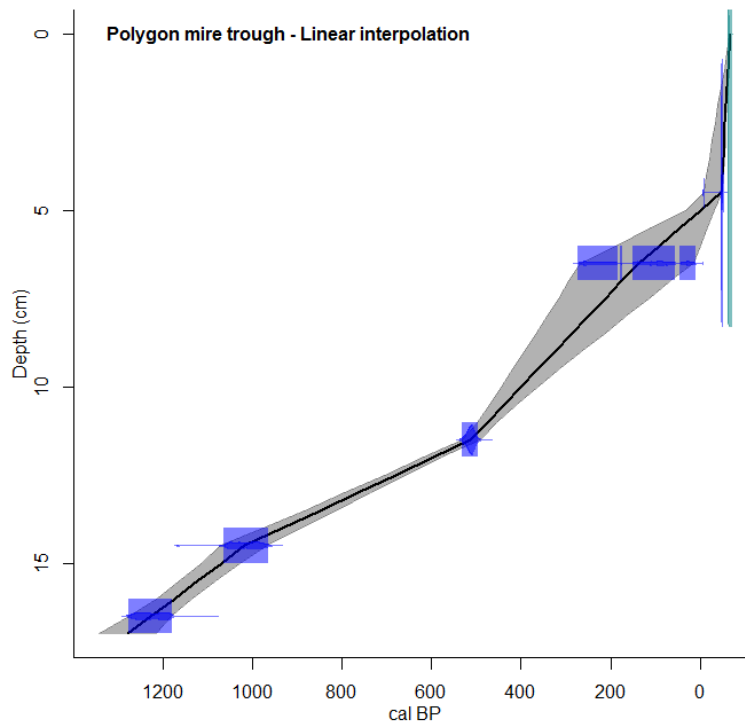
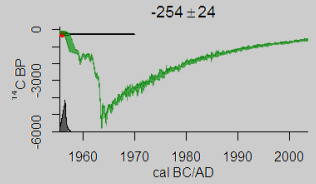
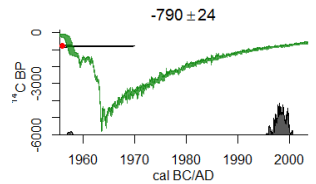
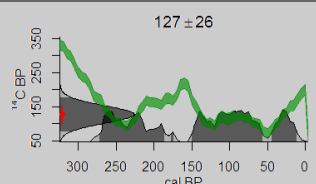
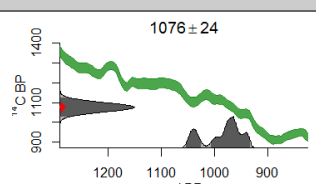
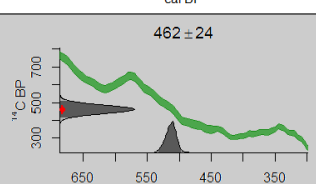
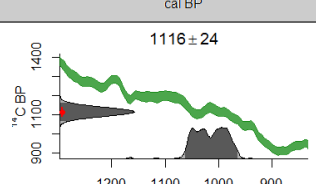
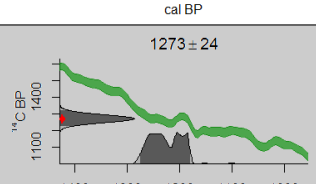


Figure 15. Age-depth model for the Polygon Mire trough monolith. The model was constructed using linear interpolation between dates. Black line = best age-depth model, grey = 95% confidence interval of age-depth model, blue = calibrated distributions of ^{14}C dates.

Table 3. Radiocarbon ^{14}C dating summary table from the Polygon Mire trough monolith, including individual date calibration plots. ‡ = Suess effect.

Site/ Depth (cm)	Lab ID	Material	^{14}C age	±	Calibration range (years BP or AD)	Calibrated median age (years BP or AD)	Calibration plots	Age- depth model
Polygon Mire trough 1-2	UOC- 6182	Bulk peat	Modern	24	1955-1957 cal. AD (95.4%)	AD 1956		No
Polygon Mire trough 4-5	UOC- 6183	Brown moss (stems + leaves)	Modern	24	1957 cal. AD (2.2%) 1996-2000 cal. AD (93.3%)	AD 1998		Yes
Polygon Mire trough 6-7	UOC- 6184	Bulk peat	127 BP	26	273-185 cal. BP (34.3%) 178-174 cal. BP (0.7%) 151-56 cal. BP (45.6%) 45-10 cal. BP (14.8%) ‡	121 BP OR AD 1829		Yes
Polygon Mire trough 9-10	UOC- 6185	Bulk peat	1076 BP	24	1054-1024 cal. BP (21.9%) 1009-932 cal. BP (73.5%)	976 BP OR AD 974		No
Polygon Mire trough 11-12	UOC- 6186	<i>Scorpidium</i> cf. <i>cossoni</i> , (stem + leaves); <i>Wamstorfia</i> <i>sarmentosa</i> (stem + leaves)	462 BP	24	535-495 cal. BP (95.4%)	513 BP OR AD 1437		Yes
Polygon Mire trough 14-15	UOC- 6187	Bulk peat	1116 BP	24	1065-962 cal. BP (95.4%)	1016 BP OR AD 934		Yes
Polygon Mire trough 16-17	UOC- 6188	<i>Scorpidium</i> cf. <i>cossoni</i> , (stem + leaves); <i>Wamstorfia</i> <i>sarmentosa</i> (stem + leaves)	1273 BP	24	1277-1179 cal. BP (95.4%)	1229 BP OR AD 721		Yes

3.2.2.2 PHYSICAL PROPERTIES

The record from the Polygon Mire trough monolith (17 cm; Figure 16) is more dynamic in comparison to the raise centre. The lower phase (7–17 cm) consists of a light-brown, slightly peat-like soil where carbon accumulation is very low ($6.2 \pm 2.1 \text{ g m}^{-2} \text{ yr}^{-1}$), organic matter is low ($27.8 \pm 8.7\%$), bulk density is relatively high ($0.51 \pm 0.16 \text{ g cm}^{-3}$) and organic matter bulk density remains relatively high ($0.13 \pm 0.02 \text{ g cm}^{-3}$). In the upper phase (0–7 cm) organic matter increases (max: 77.4%) and bulk density decreases (min: 0.04 g cm^{-3}) shifting to more peatland-like conditions. Moisture content correlates with these trends in organic matter content. Carbon accumulation increased dramatically ~AD 2000 with recent rates ranging from $45.7\text{--}102.8 \text{ g m}^{-2} \text{ yr}^{-1}$. Coincident with this increase carbon accumulation from ~AD 2000 is the start of a steady decrease in organic matter bulk density until present (max: 0.09 g cm^{-3} , min: 0.03 g cm^{-3}).

Polygon Mire trough

Physical properties
analysis: T. Sim

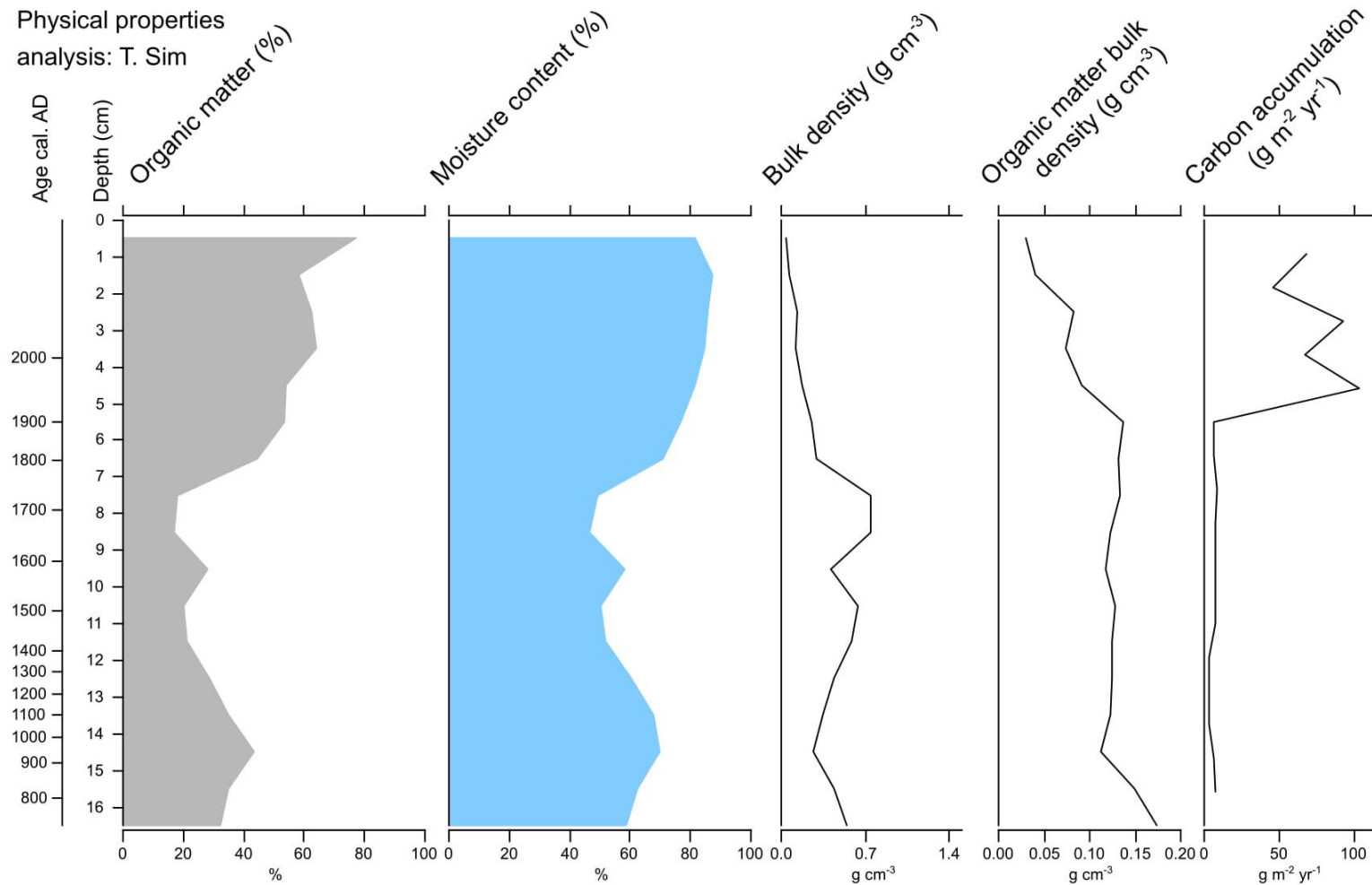


Figure 16. Physical properties summary stratigraphic diagram for the Polygon Mire trough monolith.

4.2.2.3 TESTATE AMOEBAE

The testate amoeba record represents the upper phase of the monolith (0–7 cm; Figure 17), below which was barren of sub-fossils. In zone 3 (5–7 cm) prior to ~AD 1950 unclear/wide-tolerance taxa dominate, primarily *C. aerophila* type (33.8–38.6%) and *Diffflugia* “small” type (19.3–26.2%). In zone 2 (2–5 cm) *Corythion-Trinema* type and *C. aerophila* decrease from 37% to 7.5% and from 50% to 32.1% respectively, while Vaginicolidae and *D. oblonga* type increase from 5.6% to 1.8% and 0% to 24.5% respectively – indicating wetting conditions from ~AD 2000. Zone 3 (0–2 cm) is dominated by the wet taxa: *Arcella hemisphaerica* (15.7–28.3%), *D. oblonga* (11.3–25.5%) and Vaginicolidae (27.5–47.2%).

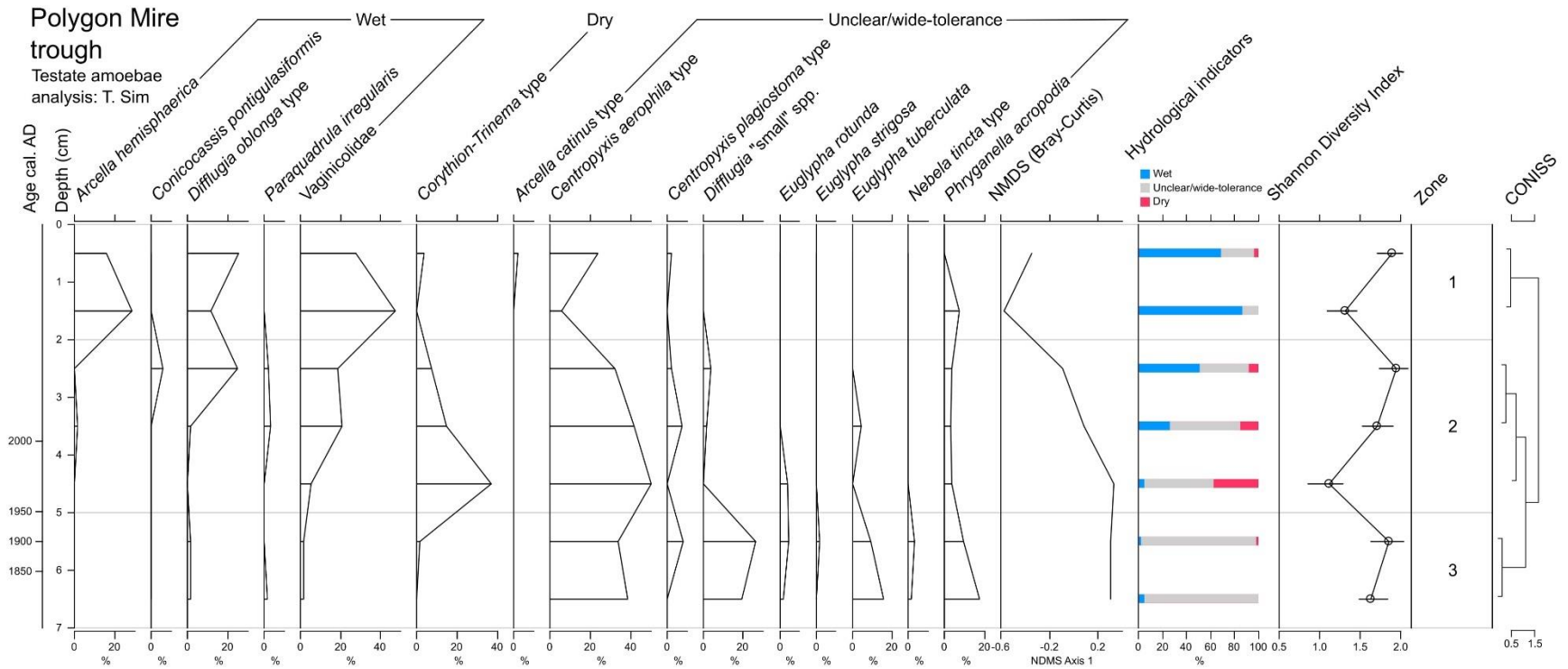


Figure 17. Relative abundance (%) of testate amoebae for the Polygon Mire trough monolith. Hydrological indicator values classified in Table 1.

4.2.2.4 PLANT MACROFOSSILS

Zones 3 and 4 of the Polygon Mire trough monolith (7–17 cm) represents the gradual transition (~AD 750–1800) from *S. cossonii* (40–85%) and *Warnstorfia sarmentosa* (0–35%) moss to a more Cyperaceae (0–30%) and herb-dominated (0–30%) wetland (Figure 18). In zone 2 (4–7 cm) from ~AD 1800–2000 the vegetation is Cyperaceae (20–40%) and herb-dominated (30–40%), with a Brown moss sp. fraction (10–30%). Then there is a rapid shift in zone 1 around ~AD 2000 to a moss-dominated ecosystem of mainly *S. cossonii* (20–70%), *Callergon* spp. (10–30%) and *Campylium* cf. *stellatum* (10–20%).

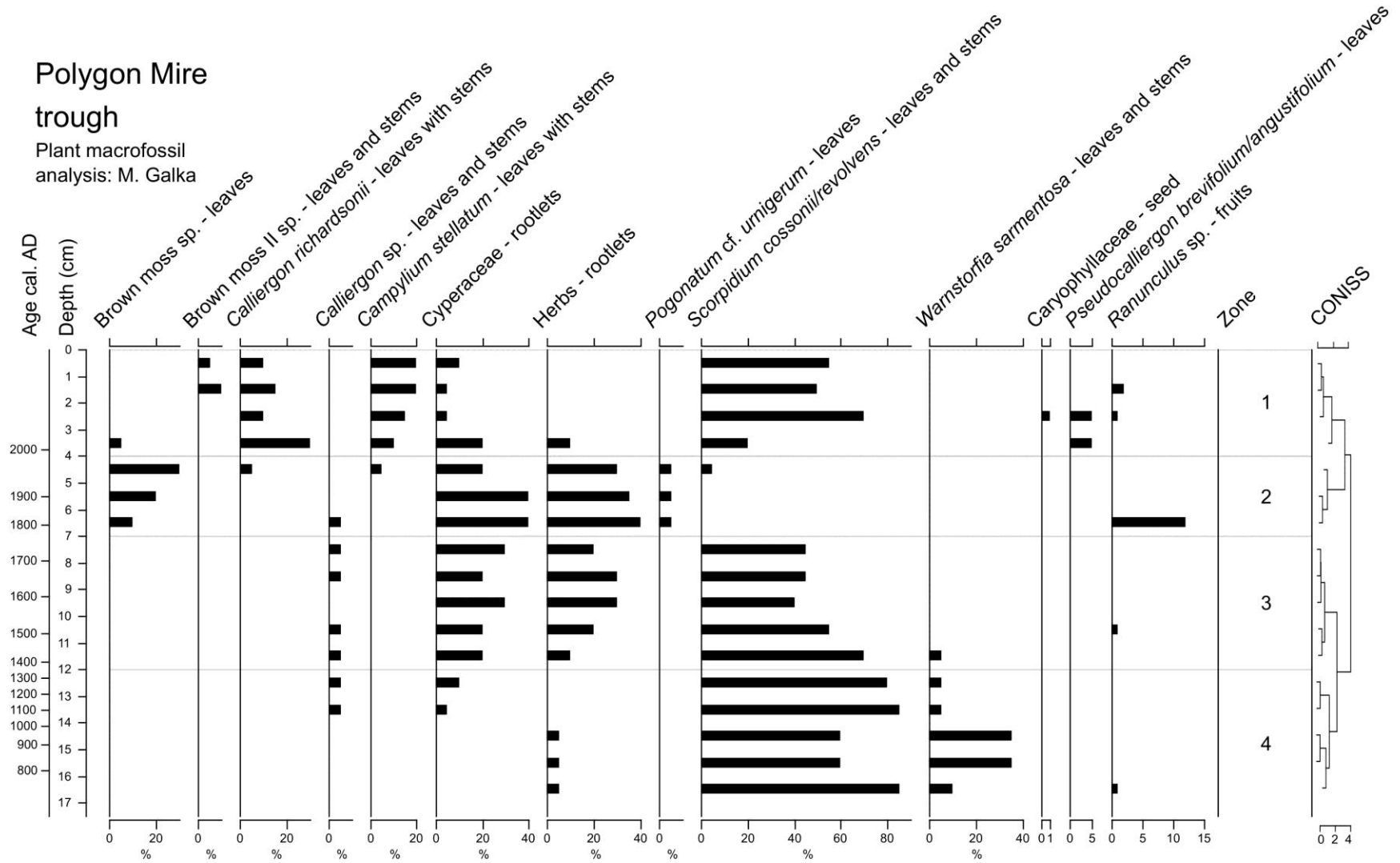


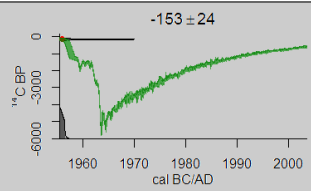
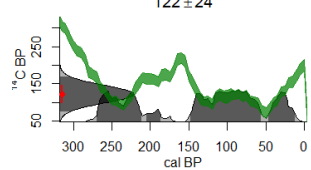
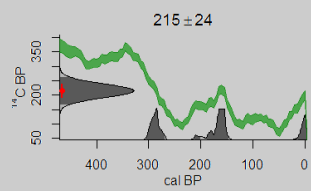
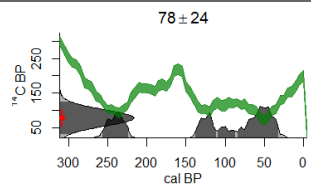
Figure 18. Abundance (%) of plant macrofossils for the Polygon Mire trough monolith.

3.2.3 VALLEY FEN

3.2.3.1 AGE-DEPTH MODEL

The Valley Fen monolith has four radiocarbon dates with calibrated mean ^{14}C dates ranging from AD 1735–1956 (Table 4). The base date (9–10 cm; AD 1850) is an age reversal and is excluded from the polynomial regression age-depth model (Figure 19).

Table 4. Radiocarbon ^{14}C dating summary table from the Valley Fen monolith, including individual date calibration plots. ‡ = Suess effect.

Site/ Depth (cm)	Lab ID	Material	^{14}C age	±	Calibration range (years BP or AD)	Calibrated median age (years BP or AD)	Calibration plots	Age- depth model
Valley Fen 3-4	UOC- 6189	Bulk peat	Modern	24	1955-1956 cal. AD (95.4%)	AD 1956		Yes
Valley Fen 5-6	UOC- 6190	Brown moss (stems)	122 BP	24	270-186 cal. BP (32.1%) 149-55 cal. BP (48.6%) 48-11 cal. BP (14.7%) ‡	115 BP OR AD 1835		Yes
Valley Fen 8-9	UOC- 6191	Bulk peat	215 BP	24	305-268 cal. BP (35.5%) 213-198 cal. BP (3.4%) 189-147 cal. BP (42.0%) 14calBP- >Modern (14.6%) ‡	169 BP OR AD 1781		Yes
Valley Fen 9-10	UOC- 6192	Brown moss (stems)	78 BP	24	257-222 cal. BP (24.4%) 139-31 cal. BP (71.0%) ‡	100 BP OR AD 1850		No

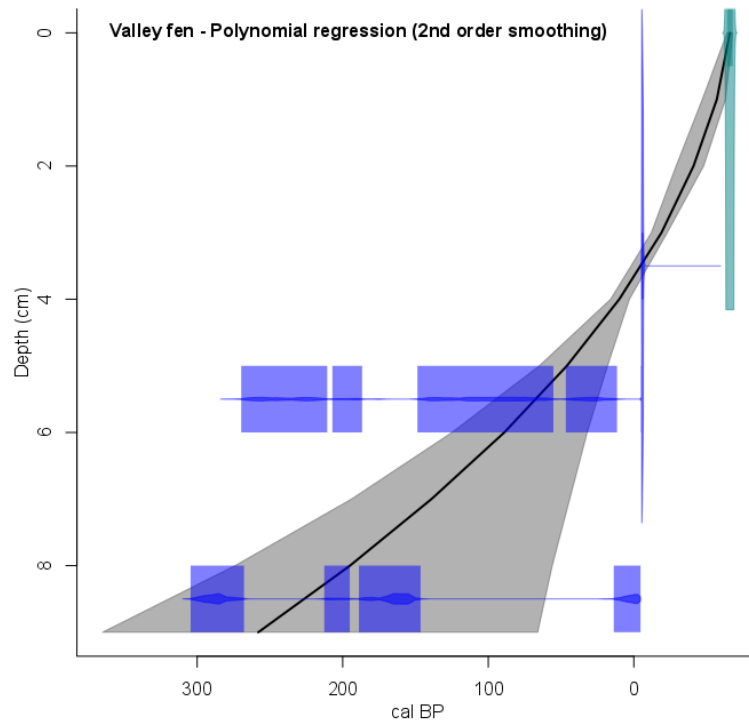


Figure 19. Age-depth model for the Valley Fen monolith. The model was constructed using a polynomial regression (2nd order smoothing) between dates. Black line = best age-depth model, grey = 95% confidence interval of age-depth model, blue = calibrated distributions of ¹⁴C dates.

3.2.3.2 PHYSICAL PROPERTIES

The Valley Fen monolith (13 cm) has three main phases. At the base of the record (9–13 cm) is a pale-coloured mineral layer of extremely low organic matter content (7.2–11.6%) and high bulk density (1.08–1.52 g cm⁻³) (Figure 20). The low organic matter content in this phase suggests that conditions caused plant productivity to be lower than decomposition rates. The transition to the middle section of the record (4–9 cm) shows a sharp increase in organic matter content ~AD 1800 (11.6% to 33.4%) and a decrease in bulk density (1.08 g cm⁻³ to 0.38 g cm⁻³). Throughout the middle section there is a gradual increase in organic matter content to 56.5%, an increase in carbon accumulation (10.9 to 20.1 g m⁻² yr⁻¹) and a decrease in bulk density to 0.23 g cm⁻³. In the top phase of the monolith (0–4 cm) from ~AD 1950 onwards, the wetland demonstrates properties more characteristic of a peatland. This is in terms of increased organic matter content to 78.8% and increased carbon accumulation to 61.3 g cm⁻² yr⁻¹. Additionally, bulk density decreases further to 0.06 g cm⁻³ alongside a decrease in organic matter bulk density to 0.05 g cm⁻³.

Valley Fen

Physical properties
analysis: T. Sim

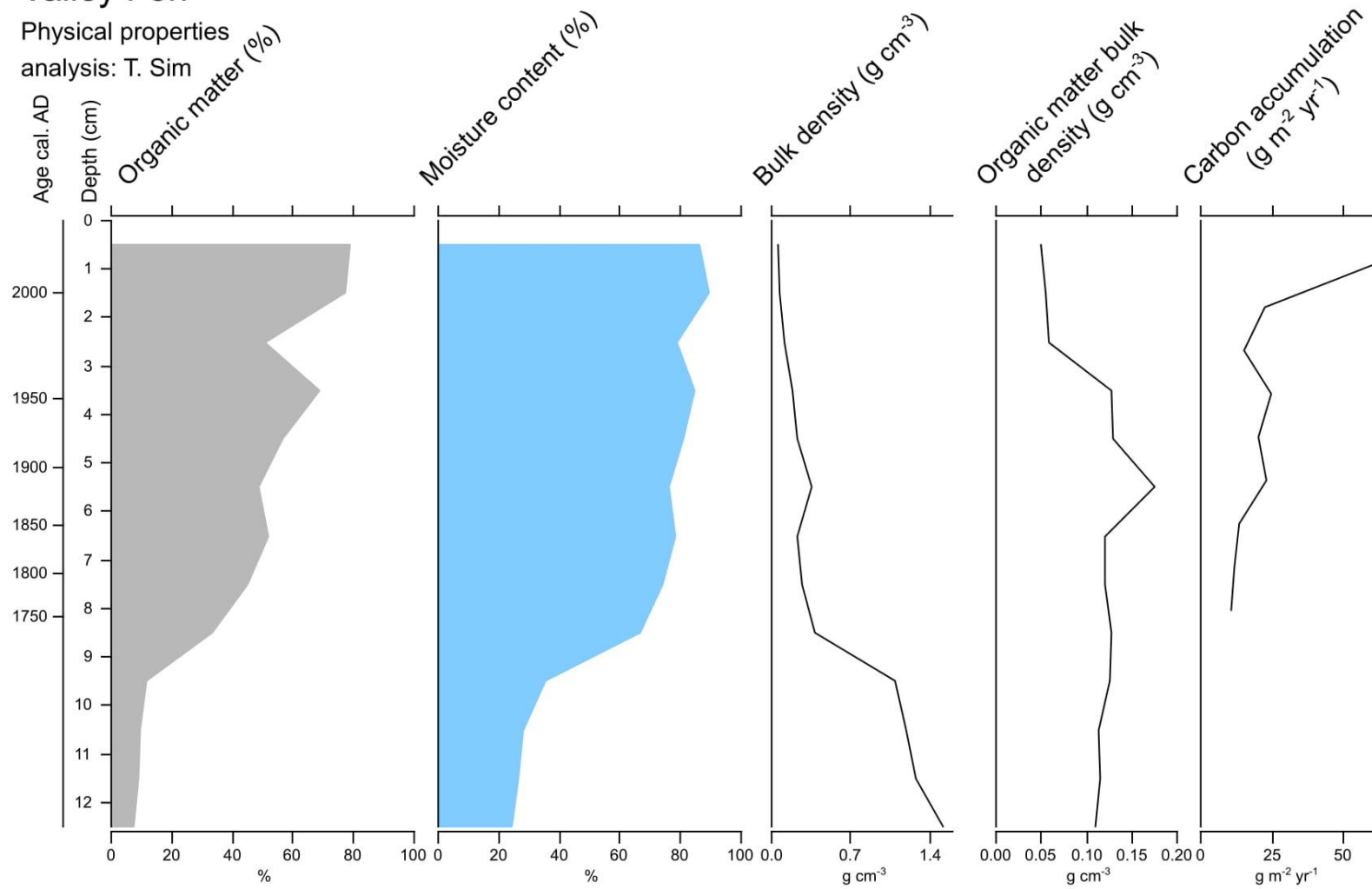


Figure 20. Physical properties summary stratigraphic diagram for the Valley Fen monolith.

3.2.3.3 TESTATE AMOEBAE

The Valley Fen testate amoeba record (Figure 21) spans the majority of the monolith (0–10 cm), excluding the minerogenic sediments at the base. The record demonstrates a general increase in both wet and dry indicators up the monolith. Zone 3 (6–10 cm) prior to ~AD 1850 is dominated by *C. aerophila* type (51.9–70%) and *Centropyxis plagiostoma* (9.6–16.4%). Zone 2 (3–6 cm) from ~AD 1850–1950 experiences an increase in wet taxa, primarily in the form of *Centropyxis aculeata* from 2% to 22% and the limited occurrence of the dry taxa classification of *Corythion-Trinema* (2–6%). In zone 1 (0–3 cm) from ~AD 1950 onwards the wet taxon *Paraquadrula irregularis* dominates (28.8–40.8%), *Corythion-Trinema* increases to a maximum of 13.7%.

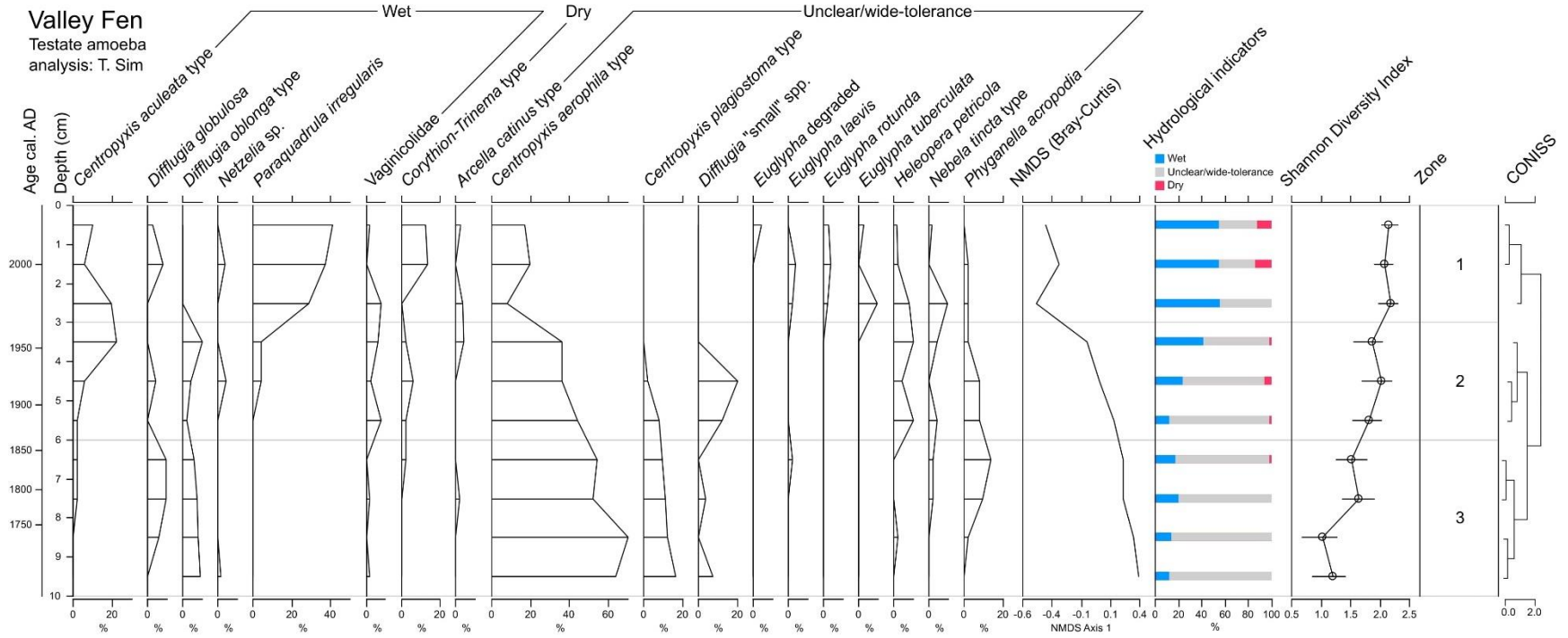


Figure 21. Relative abundance (%) of testate amoebae for the Valley Fen monolith. Hydrological indicator values classified in Table 1.

3.2.3.4 PLANT MACROFOSSILS

The base of the Valley Fen monolith in zone 3 (9–13 cm) before ~AD 1750 is dominated by sedge (Cyperaceae) vegetation (> 75%) (Figure 22). Zone 2 (4–9 cm) from ~AD 1750–1950 is dominated by Brown moss spp. (60–75%), *Calliergon* moss (< 20%) and *Hamatocaulis vernicosus* (< 10%). In zone 3 (0–4 cm) from ~AD 1950, *Tomentypnum nitens* (30–50%), *Cinclidium stygium* (0–20%) and *Aulacomnium palsture* (< 5%) now dominate. These mosses (including *T. nitens*, *C. stygium* and *A. palsture*) may have been present within the Brown moss spp. classification, however decomposition made species-level identification impossible.

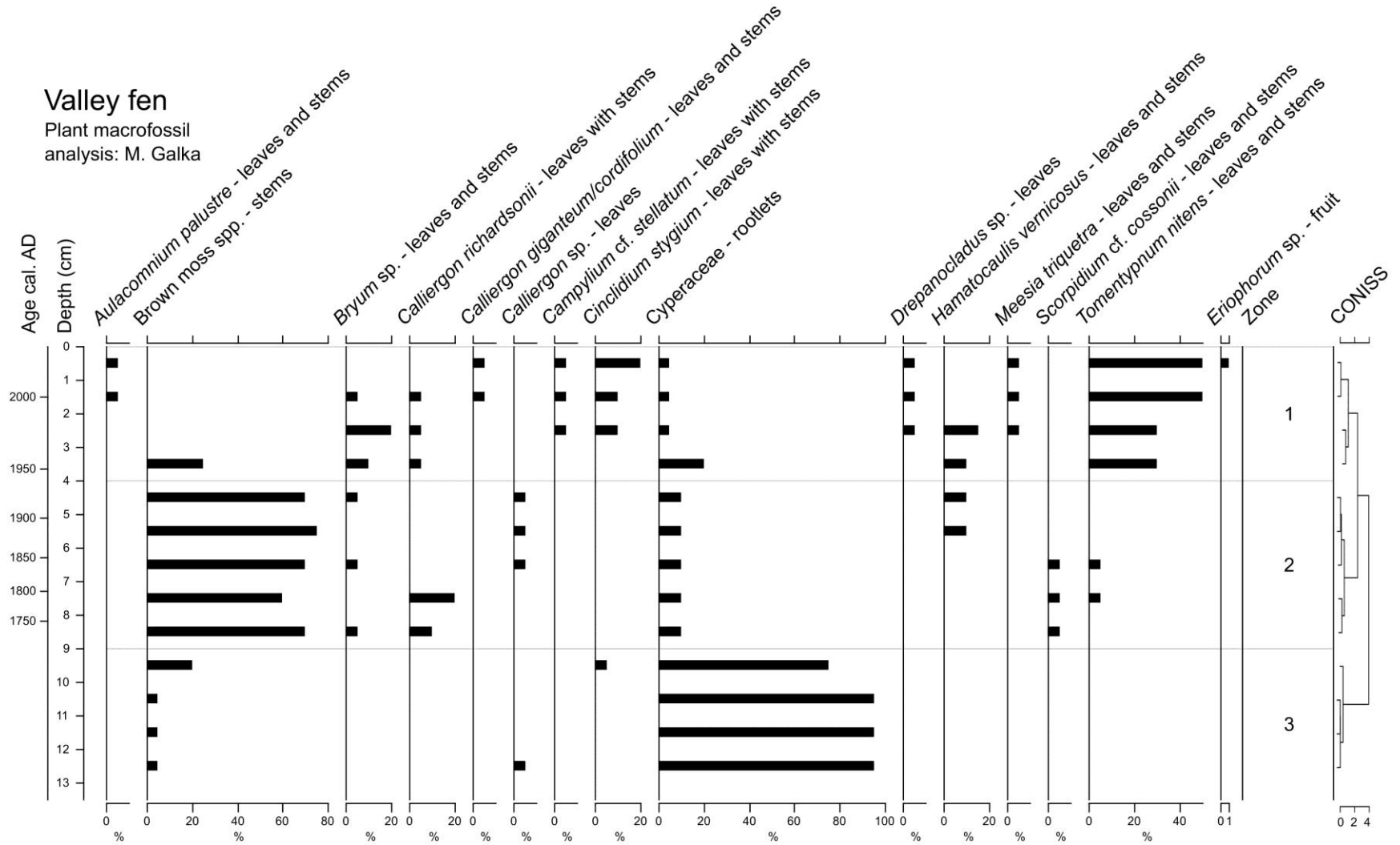


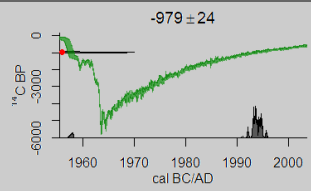
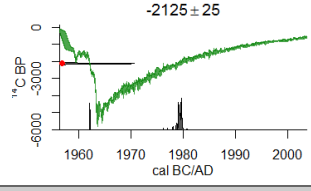
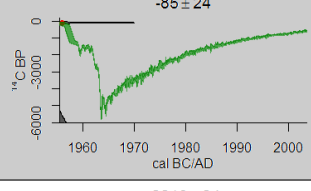
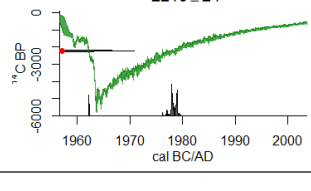
Figure 22. Abundance (%) of plant macrofossils for the Valley Fen monolith.

3.2.4 COASTAL FEN A

3.2.4.1 AGE-DEPTH MODEL

The Coastal Fen A monolith has four radiocarbon dates with calibrated mean ^{14}C dates ranging from AD 1956–1991 (Table 5). The base date (11–12 cm; AD 1977) is an age reversal and is excluded from the cubic spline age-depth model (Figure 23).

Table 5. Radiocarbon ^{14}C dating summary table from the Valley Fen monolith, including individual date calibration plots. ‡ = Suess effect.

Site/ Depth (cm)	Lab ID	Material	^{14}C age	±	Calibration range (years BP or AD)	Calibrated median age (years AD)	Calibration plots	Age- depth model
Coastal Fen A 2-3	UOC- 6193	Bulk peat	Modern	24	1957-1958 cal. AD (5.9%) 1992-1995 cal. AD (89.5%)	AD 1994		Yes
Coastal Fen A 5-6	UOC- 6194	Selaginella (leaf); bud scale, <i>Salix</i> sp. (leaf)	Modern	25	1961-1962 cal. AD (4.3%) 1978-1980 cal. AD (91.1%)	AD 1979		Yes
Coastal Fen A 9-10	UOC- 6195	Bulk peat	Modern	24	1954-1956 cal. AD (95.4%)	AD 1956		Yes
Coastal Fen A 11-12	UOC- 6196	<i>Carex</i> sp. (fruits); Cyperacea e stem bases	Modern	24	1962 cal. AD (5.3%) 1976-1979 cal. AD (89.7%)	AD 1978		No

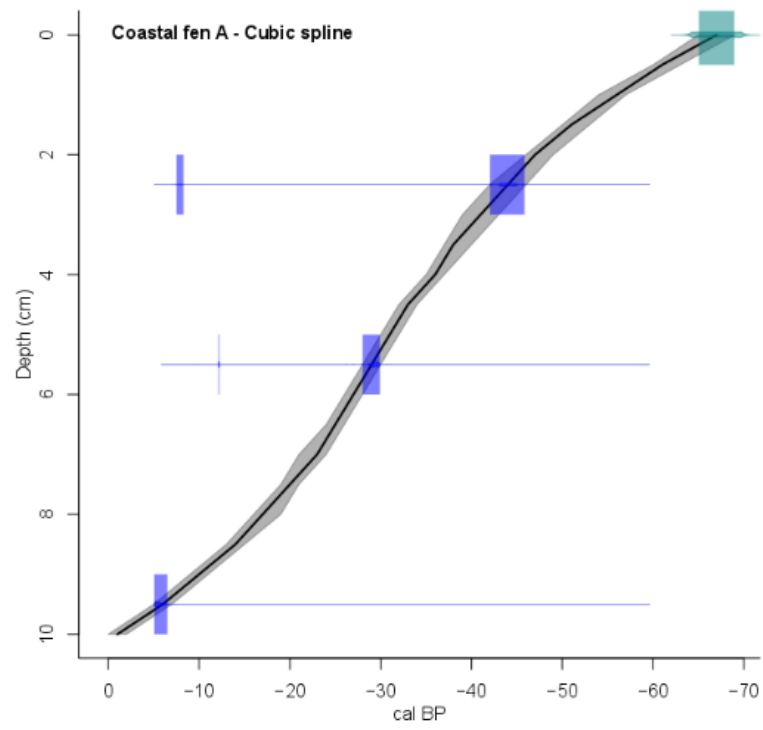


Figure 23. Age-depth model for the Coastal Fen A monolith. The model was constructed using a cubic spline between dates. Black line = best age-depth model, grey = 95% confidence interval of age-depth model, blue = calibrated distributions of ¹⁴C dates.

3.2.4.2 PHYSICAL PROPERTIES

The Coastal Fen A monolith indicates two distinct phases in terms of physical properties (Figure 24). The lower phase (12–17 cm) occurring at least before AD 1956 is characterised by a pale-coloured minerogenic layer, with a low organic matter content (3.4–25.6%), and a high bulk density (max: 1.28 g cm^{-3}) which decreases up the succession (min: 0.38 g cm^{-3}). The upper phase (0–12 cm) is characterised by a darker-coloured peaty layer of poorly decomposed plant material. This upper phase experiences a sharp rise in organic matter content that remains consistently high ($86.7 \pm 5.6\%$) alongside a relatively low bulk density ($0.11 \pm 0.02 \text{ g cm}^{-3}$). Carbon accumulation is modelled from 0–10 cm and is consistently high ($84.5 \pm 24.4 \text{ g m}^{-2} \text{ yr}^{-1}$) peaking ~AD 1980 at $122.2 \text{ g m}^{-2} \text{ yr}^{-1}$.

Coastal Fen A

Physical properties
analysis: T. Sim

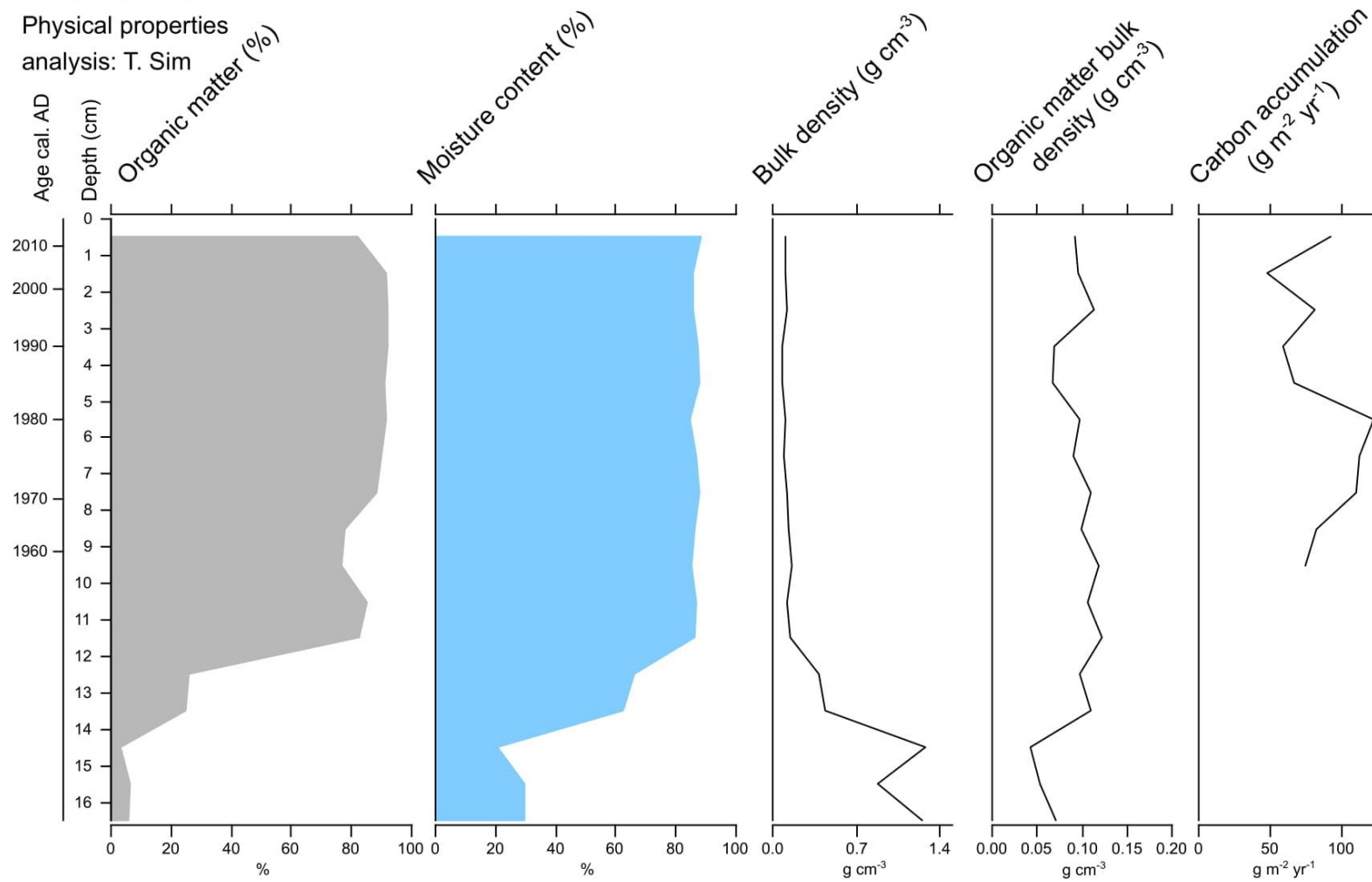


Figure 24. Physical properties summary stratigraphic diagram for the Coastal Fen A monolith.

3.2.4.3 TESTATE AMOEBAE

The testate amoeba record for the Coastal Fen A monolith spans 0–12 cm (Figure 25), excluding the extremely minerogenic base. The record is consistently composed of a high percentage of unclear/wide-tolerance taxa ($79 \pm 8.1\%$), complicating interpretation of trends in past hydrology. Zone 3 prior to ~AD 1970 is dominated by *C. aerophila* type ($21.2 \pm 9\%$) and increasing *N. tinctoria* type (3.4–30.8%). The wet indicator Vaginicolidae gradually decreases from 13.8% to 3.8%. In zone 2 from ~AD 1970–2000 *C. aerophila* type abundance drops and remains low ($5.8 \pm 3.4\%$), *N. tinctoria* type abundance drops and sporadically increases (5.9–42.3%) and wet taxon *C. aculeata* is generally low (4–9.6%), but peaks ~AD 1975 at 21.6%. The *Euglypha* genus increases in zone 2, including *E. rotunda* (1.9–17.6%), *E. tuberculata* (7.4–16%) and *Euglypha* degraded (2–9.2%). In zone 1 since ~AD 2000 the record is dominated by *E. tuberculata* and *Netzelia* sp. increasing to 42% and 24% respectively.

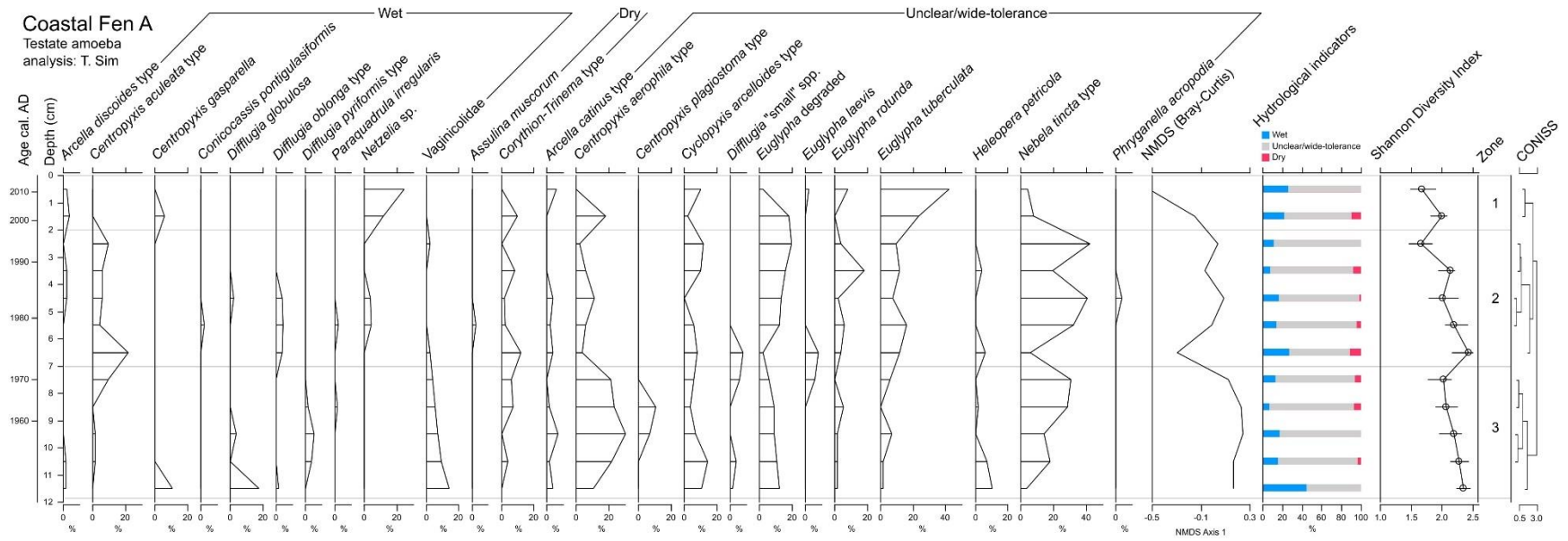


Figure 25. Relative abundance (%) of testate amoebae for the Coastal Fen A monolith. Hydrological indicator values classified in Table 1.

3.2.4.4 PLANT MACROFOSSILS

The vegetation in Coastal Fen A consists of three main zones (Figure 26). In zone 3 (9–16 cm) prior to AD 1956 there is a dominance of Cyperaceae (50–75%) and herbs (20–45%). In zone 2 (2–9 cm) ~AD 1960 there is a spike in the moss *Calliergon richardsonii* to 70% and from ~AD 1960–2000 a transition to shrub-dominance (0–80%) alongside a moderate herb abundance ($22.1 \pm 9\%$). Since ~AD 2000 in Zone 1 (0–2 cm) there is a shift to moss-dominance in the form of *C. richardsonii* (50%) and *Brachythecium mildeanum* (10–40%).

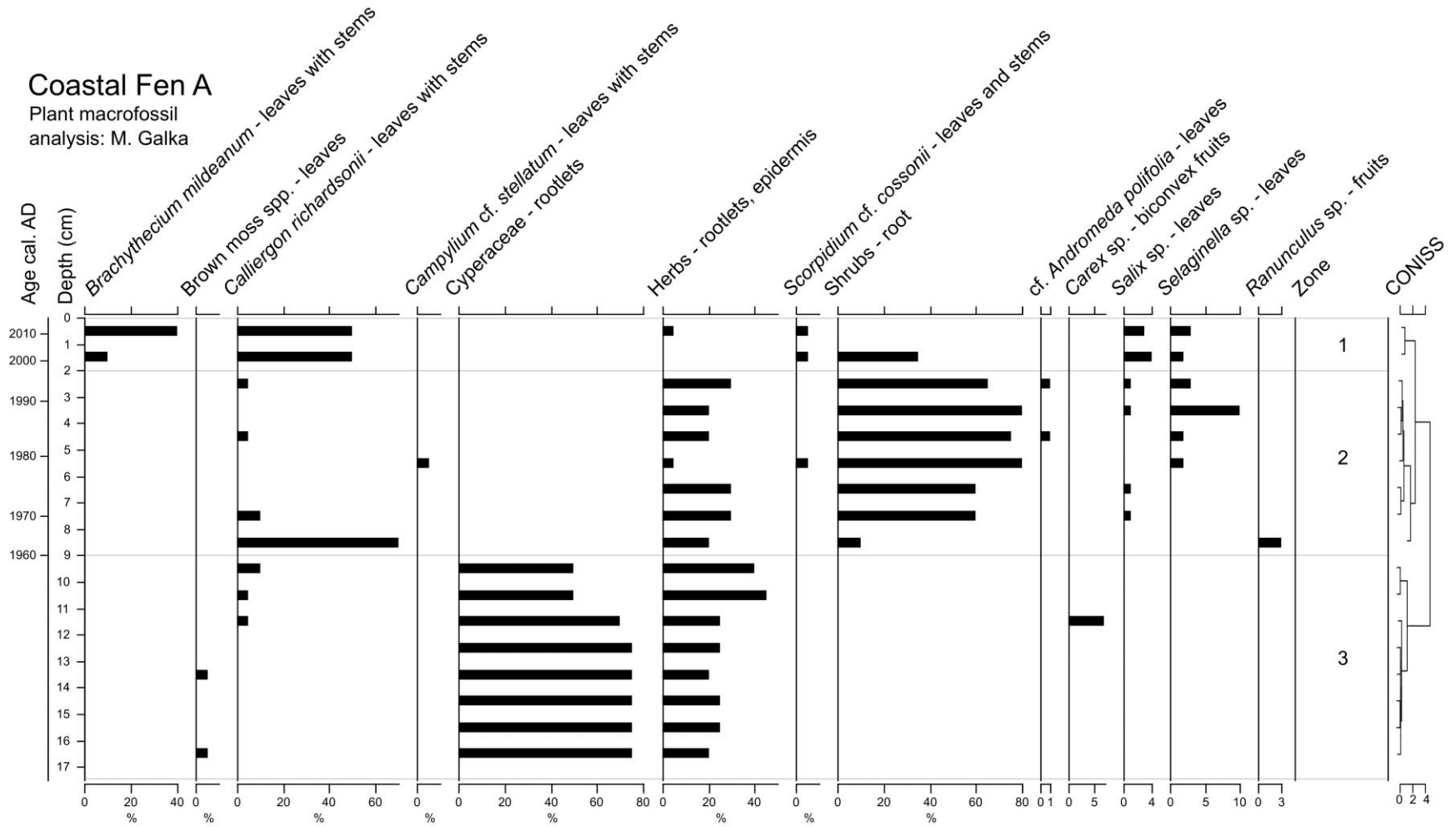


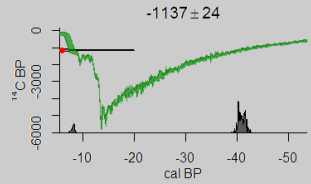
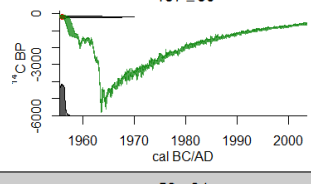
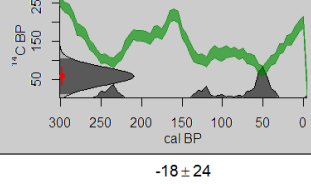
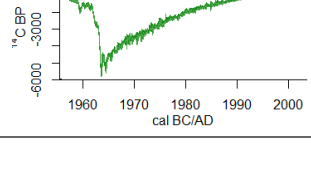
Figure 26. Abundance (%) of plant macrofossils for the Coastal Fen A monolith.

3.2.5 COASTAL FEN B

3.2.5.1 AGE-DEPTH MODEL

The Coastal Fen B monolith has four radiocarbon dates with calibrated mean ^{14}C dates ranging from AD 1892–1987 (Table 6). The base date (9–10 cm; AD 1955) is an age reversal and is excluded from the cubic spline age-depth model (Figure 27), overall demonstrating similar chronology to the Coastal Fen A monolith (Table 5; Figure 23).

Table 6. Radiocarbon ^{14}C dating summary table from the Coastal Fen B monolith, including individual date calibration plots. † = Suess effect.

Site/ Depth (cm)	Lab ID	Material	^{14}C age	±	Calibration range (years BP or AD)	Calibrated median age (years BP or AD)	Calibration plots	Age- depth model
Coastal Fen B 2-3	UOC- 6197	Bulk peat	Modern	24	1957-1958 cal. AD (12.1%) 1989-1992 cal. AD (83.3%)	AD 1991	 -1137 ± 24	Yes
Coastal Fen B 6-7	UOC- 6198	<i>Calliergon richardsonii</i> (leaves + stems)	Modern	30	1955-1956 cal. AD (95.4%)	AD 1956	 -187 ± 30	Yes
Coastal Fen B 8-9	UOC- 6199	<i>Calliergon richardsonii</i> (leaves + stems)	58 BP	24	255-223 cal. BP (21.3%) 138-96 cal. BP (19.1%) 83-31 cal. BP (55.0%) †	65 BP OR AD 1885	 58 ± 24	Yes
Coastal Fen B 9-10	UOC- 6200	Bulk peat	Modern	24	1954-1957 cal. AD (92.7%)	AD 1955	 -18 ± 24	No

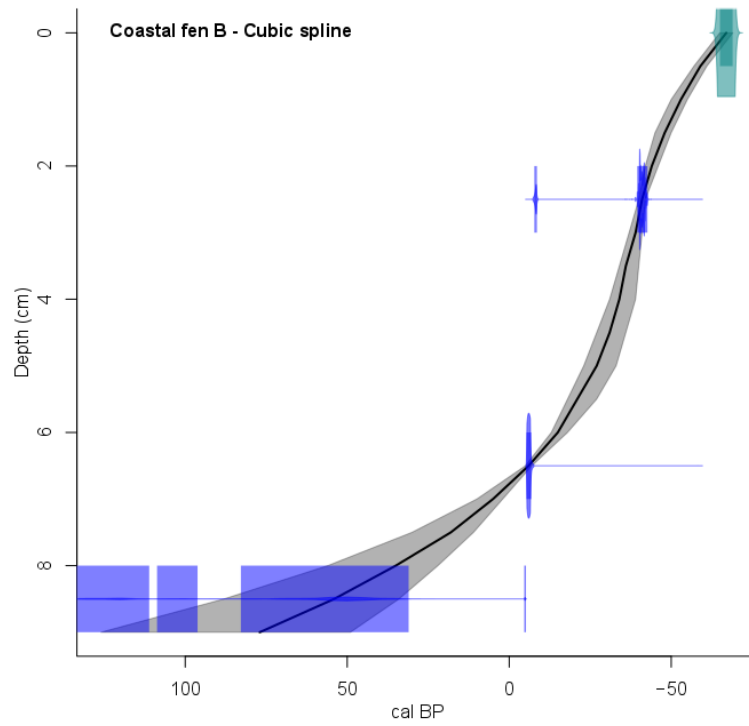


Figure 27. Age-depth model for the Coastal Fen B monolith. The model was constructed using a cubic spline between dates. Black line = best age-depth model, grey = 95% confidence interval of age-depth model, blue = calibrated distributions of ¹⁴C dates.

3.2.5.2 PHYSICAL PROPERTIES

The Coastal Fen B monolith indicates two distinct phases in terms of physical properties (Figure 28) and is very similar to the Coastal Fen A record (Figure 24). The lower phase (10–16 cm) occurring prior to ~AD 1900, is characterised by a pale-coloured minerogenic layer with a low organic matter content (mostly 3.4–25.6%), and a high bulk density (max: 2.44 g cm⁻³) decreasing up the monolith (min: 0.27 g cm⁻³). There is a spike in organic matter content (45.6%) at 10–11 cm and in bulk density (1.29 g cm⁻³) at 9–10 cm. The upper phase (0–10 cm) is characterised by a darker-coloured peaty section of partially decomposed plant material and a marked increase in organic matter content that remains consistently high (87.3 ± 3.9%) alongside a relatively low bulk density from 0–9 cm (0.12 ± 0.02 g cm⁻³). Carbon accumulation is modelled from 0–9 cm and is consistently high (50.9 ± 25.1 g m⁻² yr⁻¹), peaking ~AD 1980 at 98.2 g m⁻² yr⁻¹.

Coastal Fen B

Physical properties
analysis: T. Sim

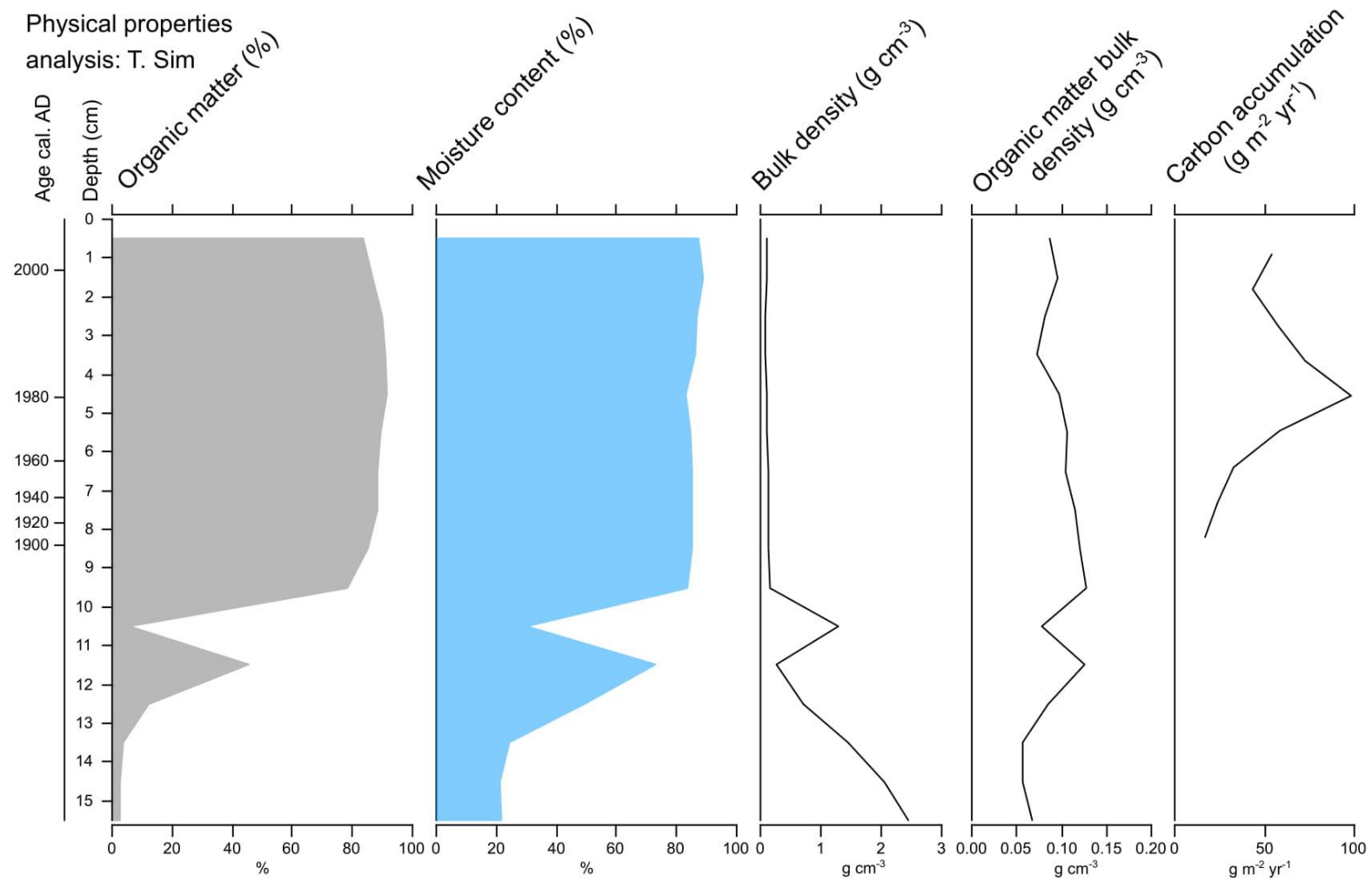


Figure 28. Physical properties summary stratigraphic diagram for the Coastal Fen B monolith.

3.2.5.3 TESTATE AMOEBAE

The testate amoeba record for the Coastal Fen B monolith spans 0–10 cm (Figure 29), excluding the extremely minerogenic base. The record is consistently composed of a high relative abundance of unclear/wide-tolerance taxa ($75.6 \pm 12.6\%$). As with the Coastal Fen A monolith, this complicates interpretation of trends in past hydrology. Zone 3 prior to ~AD 1950 is dominated by *C. aerophila* type (16–25.5%) and increasing *N. tinctoria* type (6–54%). In zone 2 from ~AD 1950–2000, *C. aerophila* type peaks at 35.3% and gradually decreases to 2%. *N. tinctoria* type drops before increasing (11.8–44%) and wet taxon *C. aculeata* is generally relatively low (2–18%), but peaks ~AD 1970 at 29.4%. The *Euglypha* genus increases in zone 2, including *E. rotunda* (0–19.6%), *E. tuberculata* (0–5.9%) and *Euglypha* degraded (9.8–23.5%). In zone 1 since ~AD 2000 the record is dominated by *Corythion-Trinema*, *E. rotunda* and *Netzelia* sp. increasing to 29.6%, 22.2% and 14.8% respectively.

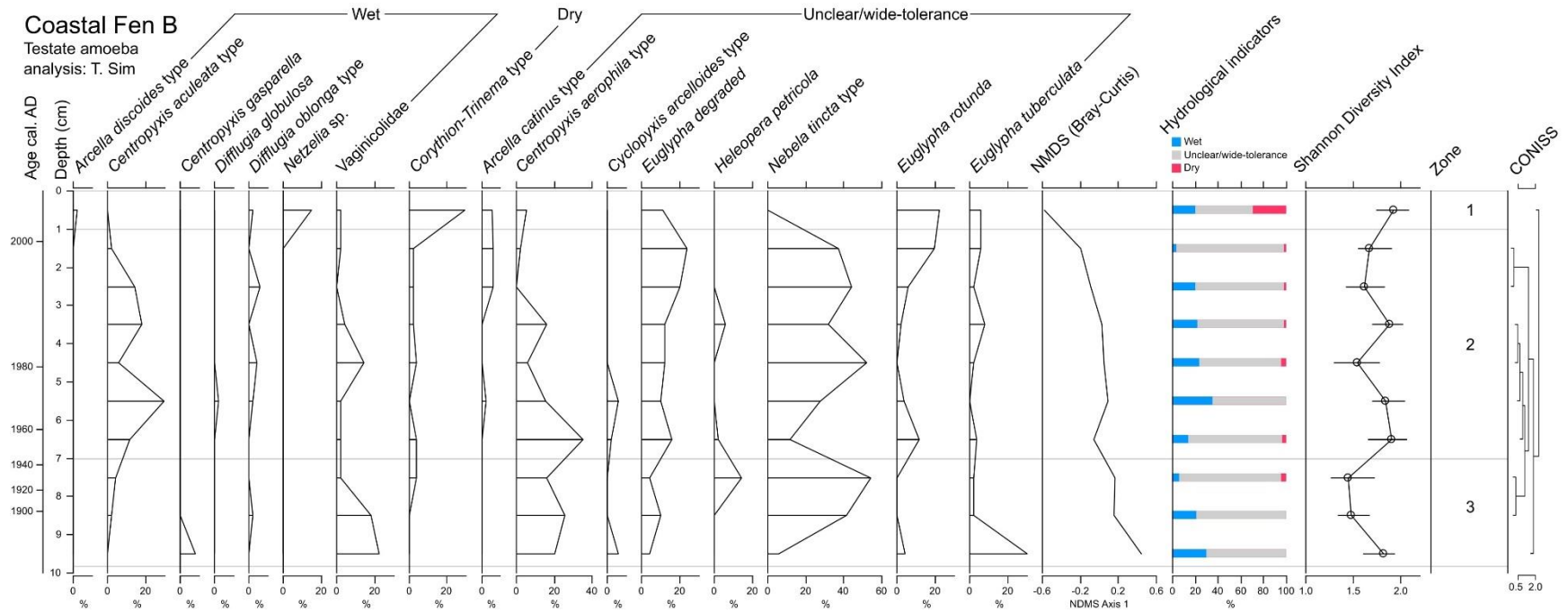


Figure 29. Relative abundance (%) of testate amoebae for the Coastal Fen B monolith. Hydrological indicator values classified in Table 1.

3.2.5.4 PLANT MACROFOSSILS

The vegetation in Coastal Fen B consists of three main zones (Figure 30), as in Coastal Fen A. In zone 3 (9–16 cm) prior to ~AD 1900 Cyperaceae (75%) and herbs (20–25%) dominate. In zone 2b (6–9 cm) from ~AD 1900–1960, shrubs (20–55%) begin to dominate and *C. richardsonii* (30–40%) is present in moderate abundance. From ~AD 1960–2000 in zone 2a (1–6 cm) shrubs dominate (80–90%) with minimal herbs (5%). In zone 1 (0–1 cm) since ~AD 2000 there is a shift to the mosses *C. richardsonii* (70%), *Campylium* cf. *stellatum* (10%) and *Drepanocladus polygamous* (5%).

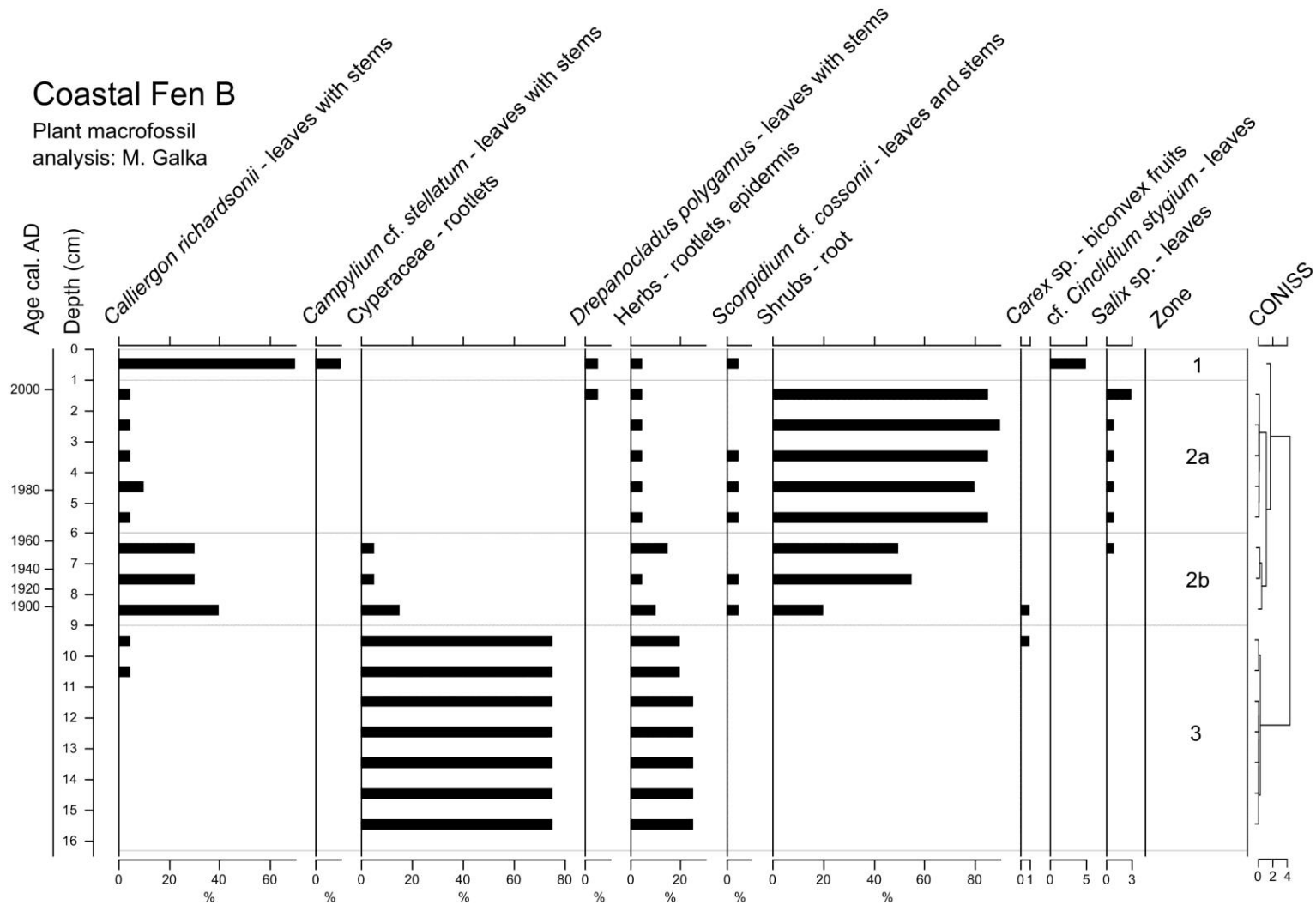


Figure 30. Abundance (%) of plant macrofossils for the Coastal Fen B monolith.

3.2.6 PALAEOENVIRONMENTAL SUMMARY

All palaeoenvironmental data from each monolith is summarised below and the stratigraphic location of the change point in GDD₀ for each site is highlighted (Figure 31). This summary aims to allow for clearer and more holistic interpretation. All three wetland sites (4/5 monoliths) experienced some form of ecosystem shift following a mid-twentieth century increase in GDD₀.

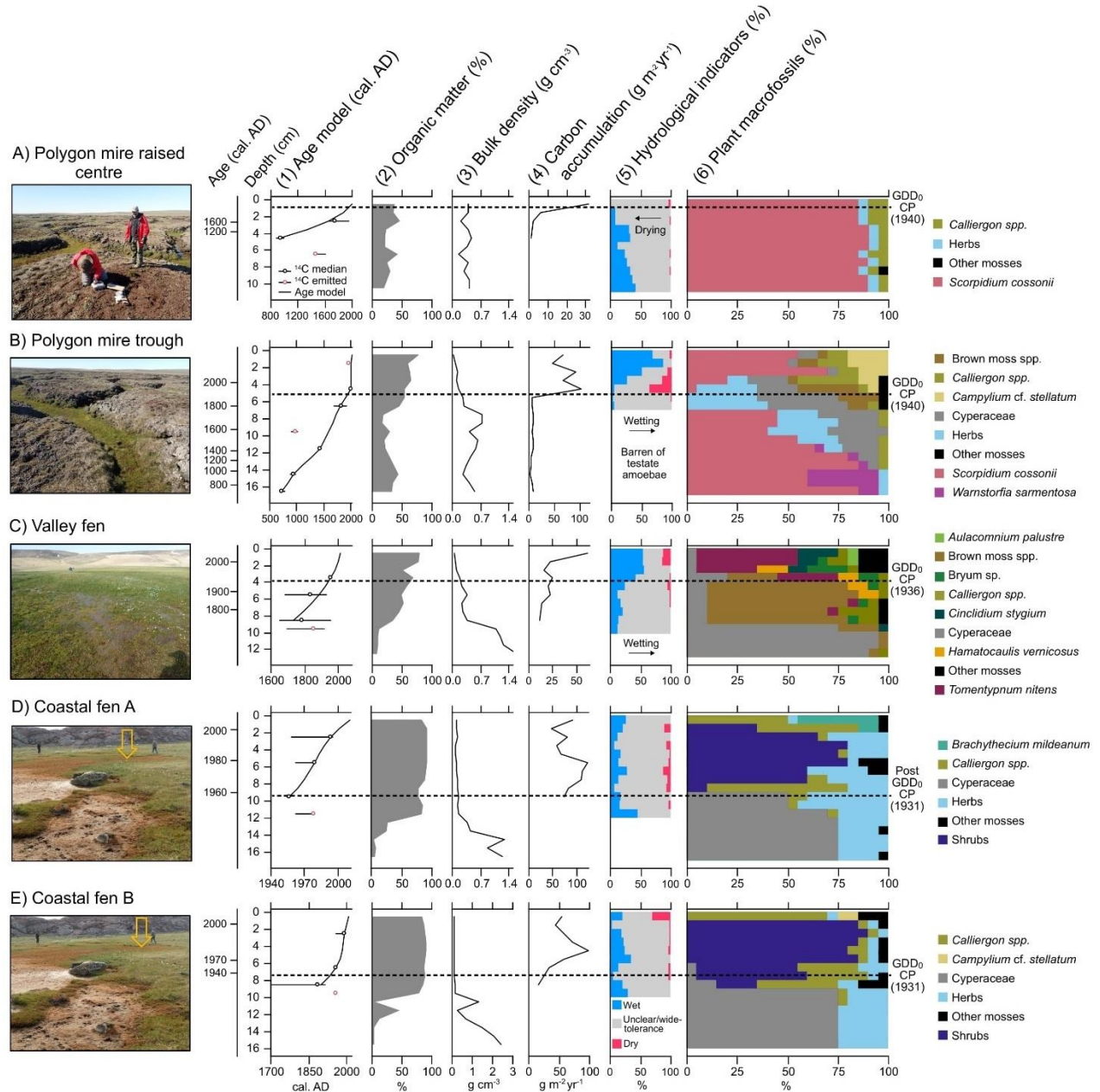


Figure 31. Summary stratigraphic diagram of palaeoenvironmental variables from the Polygon Mire raised centre (A), Polygon Mire trough (B), the Valley Fen (C) and Coastal Fen (D and E). GDD₀ CP = Change point in GDD₀ for each site. See Table 1 for hydrological indicator classification.

4. DISCUSSION

4.1 TWENTIETH CENTURY GROWING SEASON LENGTHENING AND WARMING IN THE WESTERN ARCTIC

In contrast to lower latitudes, the Arctic tundra north of the tree line and in the continuous permafrost zone (Figure 5) experiences a short, cool growing season that limits plant growth - although the area is warming rapidly. Twentieth century climatic warming has been documented in historical weather station records (beginning ~AD 1950) near to my study sites, and across the Arctic (Hassol et al., 2004). The Cambridge Bay and Sachs Harbour stations show the most pronounced warming rates of $0.03^{\circ}\text{C yr}^{-1}$ and $0.05^{\circ}\text{C yr}^{-1}$, in contrast to $0.01^{\circ}\text{C yr}^{-1}$ at the highest latitude station of Mould Bay (Figure 32a). Re-analysis data demonstrates that there is a pronounced increase in GDD_0 across all three wetland sites, with changepoints in the data detected 1931–1940 (Figures 10 and 32b). These increases in GDD_0 have occurred from lengthening and slight warming of the growing season. Elsewhere in the Canadian High Arctic ($n = 4$) increases in GDD_0 have been observed over the past few decades (Woo & Young, 2014).

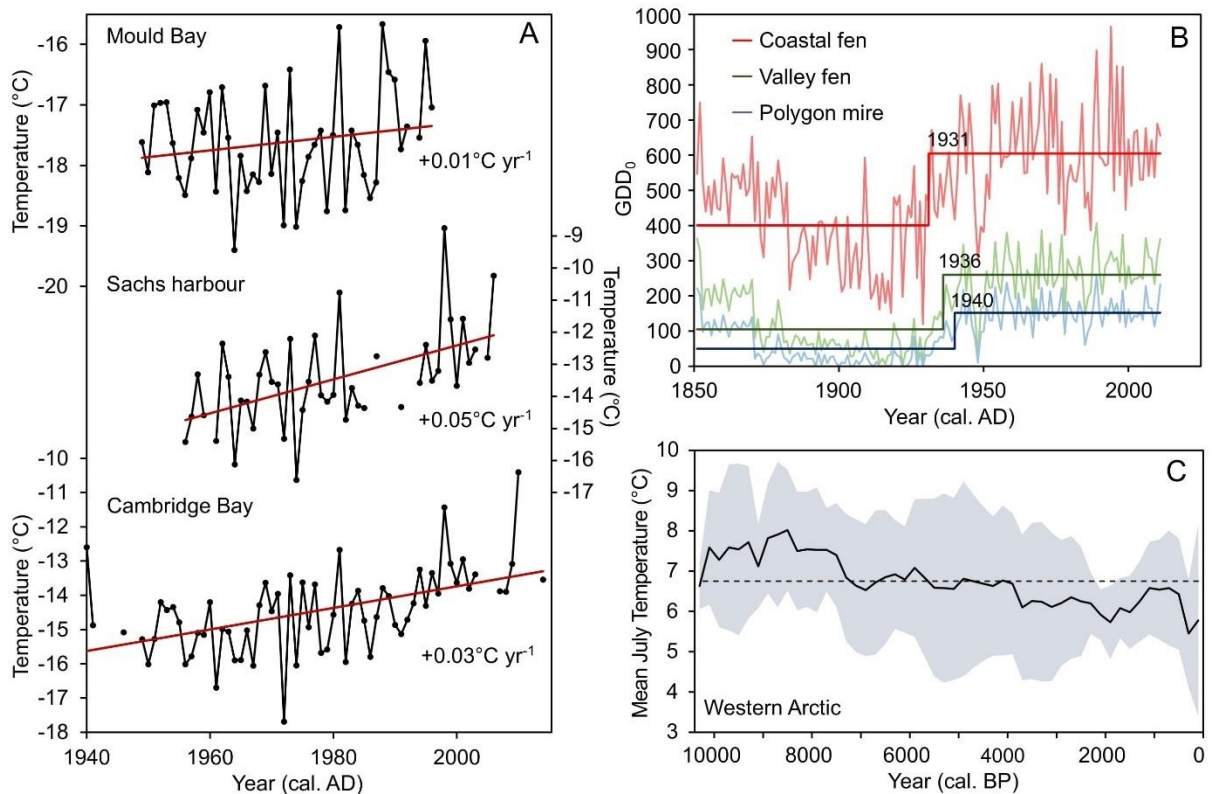


Figure 32. Climatic data showing recent warming for my sites in the western Canadian Arctic study region. A) Historical temperature data from nearby weather stations, see Figure 5 for station locations – data sourced from Climate Explorer and Environment Canada websites. B) GDD_0 = Growing degree days above 0°C for each wetland site 1851–2011 calculated from monthly temperature re-analysis data (Compo et al.,

2011), stepped lines indicate the main change point in the mean and variance of the data for each site. C) Mean July temperature for the western Arctic during the Holocene reconstructed from pollen analysis of lake bed cores interpolated to 200-year intervals. The shaded area representing one standard deviation (Gajewski, 2015; see Figure 5 for core locations).

During previous warm periods there is evidence of substantial peat formation in the High Arctic. Pollen-based temperature reconstructions for the western Arctic show that following a warm period from 10–7 Ka BP there was a general cooling trend through the majority of the Holocene (Gajewski, 2015; Figure 32c). During the early Holocene warm period there is stratigraphic evidence of peatland formation in the Canadian High Arctic (Garneau, 2000) and on Banks Island specifically during previous interglacial periods (Vincent et al., 1983; Evans et al., 2014). The cooling experienced in the latter half of the Holocene - before recent anthropogenic warming - appears to coincide with reduced peat accumulation or a hiatus in the High Arctic, although data is patchy (Ovenden, 1988; Bradley, 1990; Garneau & Alt, 2000).

Future increases in GDD_0 alongside climatic warming may facilitate increased High Arctic peatland formation. In the presence of adequate moisture, GDD_0 and PAR have demonstrated a positive relationship with carbon accumulation in northern peatlands and over the last millennium (Charman et al., 2013; Gallego-Sala et al., 2018). Future Arctic precipitation may increase alongside warming (Kattsov et al., 2007 ;Bintanja & Selten, 2014; Kopec et al., 2016) improving moisture availability, although since ~AD 1950 there was no clear shift in precipitation at the closest weather stations to my sites (Figure A1). Nonetheless, the increase in GDD_0 across all study sites may represent a transition to conditions that are more favourable to peat formation and support the notion for the northern expansion of peatland extent with future warming (e.g. Charman et al., 2015; Gallego-Sala et al., 2018).

4.2 POLYGON MIRE – AUTOGENIC AND ALLOGENIC ECOSYSTEM PROCESSES WITH INCREASED THAW

The response of the Polygon Mire to warming was dictated by wetland microtopography i.e. differing in the raised centre and the surround trough. The raised centre showed a reduction in wet testate amoeba taxa up the core suggesting drying conditions for potentially over 1 Ka (Figure 31.5a). This drying is characteristic of a raised centre within an ice-wedge polygon system (Liljedahl et al., 2016). Although, the raised centre is a very consistent record in terms of *S. cossonii*-dominated vegetation, relatively high bulk density and relatively low organic matter

content (Figure 31a). Carbon accumulation does appear to increase recently, but this could be an artefact of the age-depth. Increased organic matter bulk density (max: 0.15 g cm^{-3} ; Figure 12) in the top 2 cm of the monolith is likely to represent greater decomposition of peat (Chambers et al., 2011) and therefore could indicate a lack of recent peat accumulation. A cessation in peat accumulation is supported by limited contemporary vegetation observed in the field on the raised centre mounds (see Figure 33). Ultimately, the raised centre shows no clear response to twentieth century warming.

A possible explanation for the lack of an obvious response to recent warming in the palaeo-record and for possible surface compaction is the cessation of peat accumulation following formation of the raised centre – as can occur with palsa mound formation (Blyakharchuk and Sulerzhitsky, 1999). The drying associated with the formation of raised centres and evidenced by the testate amoeba record may have exposed carbon to aerobic decomposition (Schädel et al., 2016), which could explain the low organic matter content, high bulk density and potential degradation of the palaeoenvironmental archive.

In the Polygon Mire trough, the response to increased GDD_0 was clear, but non-linear. My analysis detected a marked increase in GDD_0 at the Polygon Mire in 1940 (Figures 10 and 32b). A further increase in GDD_0 from 1956–2016 at Sachs Harbour on southern Banks Island has been documented and linked to increasing active layer thaw depth on central Banks Island (Fraser et al., 2018). The trough experienced an abrupt transition \sim AD 2000 from sedge and herb-dominance to a moss-dominated (*S. cossonii*) vegetation, alongside a dramatic increase in wetness (Figure 31b). I suggest these shifts in vegetation and hydrology are likely because of ice-wedge degradation with warming. This theory is evidenced by the findings of Jorgenson et al. (2015) from a contemporary study in Alaska of ice-wedge polygon degradation with warming. Under initial ice-wedge degradation Jorgenson et al. (2015) observed sedge-dominated troughs and with advanced ice-wedge degradation wetter aquatic moss-dominated troughs. The timescale of this ecosystem shift suggests a delayed response in the Polygon Mire to an increase in GDD_0 , perhaps indicating a threshold of ice-wedge thaw was reached \sim AD 2000 to initiate trough wetting and moss-dominance. This decadal or sub-decadal timescale of trough wetting in polygon landscapes in response to warming is supported by observations from across the Arctic since the mid-twentieth century (Jorgensen et al., 2015; Liljedahl et al., 2016; Fraser et al., 2018).

The establishment of moss vegetation under wetter conditions (Figure 31b) may represent a negative ecological feedback to ice-wedge thaw. Since ~AD 2000 with the establishment of moss vegetation, organic matter content (53.8–77.4%) and carbon accumulation (45.7–102.8 g m⁻² yr⁻¹) have increased to high levels. The moss and peat accumulation may act an insulating layer alongside slumped material from trough banks to retard further thaw (Jorgenson et al., 2006; 2015). The slumping process was observed onsite (Figure 33) and is evidenced by an older bulk peat ¹⁴C date (1–2 cm; AD 1956 ± 1) that is likely to have been influenced by the addition of older slump material, above a reliable plant macrofossil ¹⁴C date (4–5 cm; AD 1998 ± 2; Table 3). Under advanced ice-wedge degradation and the establishment of hydrological connectivity between troughs, landscape scale drainage can be initiated (Liljedahl et al., 2016). Drainage could then expose partially decomposed carbon to increased aerobic decomposition – elevating CO₂ emissions (Schädel et al., 2016). However, these negative autogenic ecological (vegetation) and allogenic geomorphological (slumping) feedbacks could contribute to the deceleration of ice-wedge degradation and delay the associated increase in carbon emissions. These feedbacks highlight the importance of considering autogenic factors in polygon mires alongside climate change (Vardy et al., 2005).

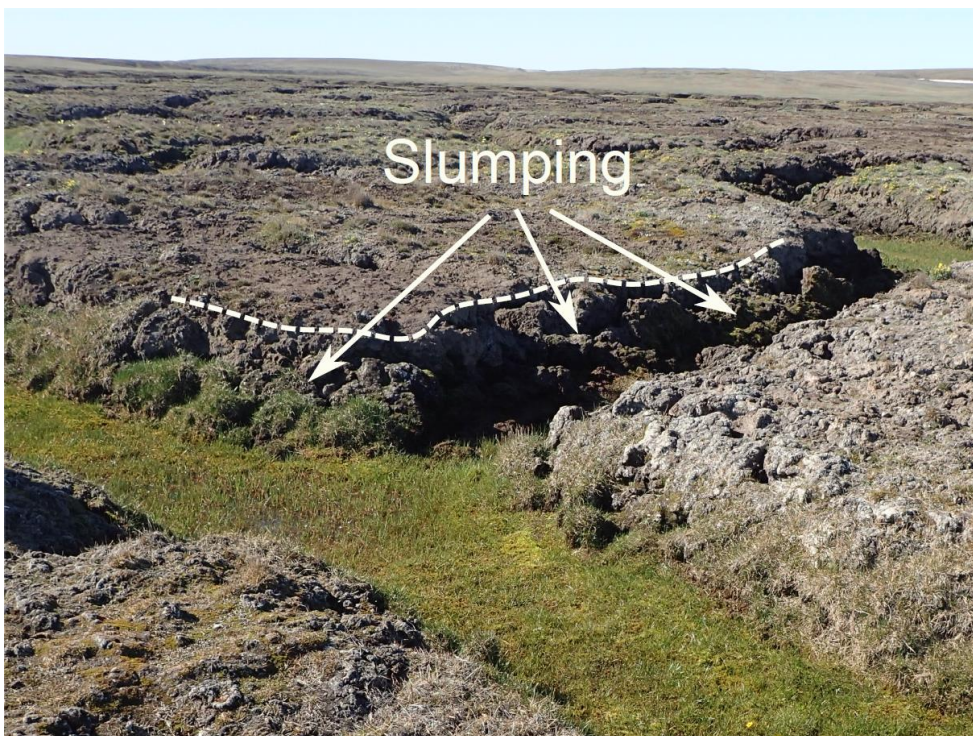


Figure 33. Site photo taken mid-July 2016 at the Polygon Mire site (74.46 °N, 121.04 °E) showing slumping of raised polygon centres into adjacent troughs.

The previous periods of sedge and herb-dominance and moss-dominance in the trough record (Figure 31.6b) may relate to previous ice-wedge degradation and stabilisation cycles. However, accurate interpretation of these previous trough vegetation shifts in this active geomorphological system is limited by the absence of a testate amoeba hydrological record (monolith barren of testate amoeba below 7 cm) and an extremely precise dating chronology. Further work is required to quantify how these dual-state systems will continue to change in response to continued warming, however my results demonstrate a clear ecosystem shift in response to twentieth century warming.

4.3 VALLEY FEN – INCREASING EXTREMES IN GROWING SEASON HYDROLOGY

The short growing season of around three months in the High Arctic results in a highly seasonal hydrological cycle, which my results suggest is being influenced by warming. An increase in GDD₀ at the Valley Fen from AD 1936 (Figure 10 and Figure 32b) is followed ~AD 1950 by a marked increase in wet testate amoeba taxon and slight increase in dry taxon (Figure 31.5c). At the start of the summer when temperatures rise above 0°C there is a large influx of water to the catchment from the thaw of ice and snowbanks that have accumulated over the winter (Glenn & Woo, 1997). The increase in wet testate amoeba taxa is likely as a result of increased ice and snow pack melt under recent warming conditions – a process that has been observed in other Arctic and alpine regions (Fontana et al., 2010; Woo & Young, 2014). Increased groundwater flow to the wetland through the surrounding Devonian limestone bedrock of the Mercy Bay Member is evidenced by the increased abundance of the calcite based testate amoeba *Paraquadrula irregularis* since ~AD 1980 (28.8–40.8%; Figure 21). The increase in dry testate amoeba taxa may represent increasingly dry conditions towards the end of the growing season as a result of increased evapotranspiration over the course of a longer and warmer summer (Oechel et al., 1998; Woo & Young, 2014). This increased variability in seasonal hydrology ~AD 1950 following the GDD₀ changepoint is further supported by the presence of the hummock mosses *T. nitens* (30–50%) and of *A. palsture* (< 5%). These mosses have broad climatic and ecological ranges (Nicholson & Gignac, 1995; Minke et al., 2009) making them suitable for the increasingly variable growing season hydrology. *T. nitens* specifically has been observed in both wet High Arctic (Steere & Scotter, 1979) and dry Boreal fens (Gignac et al., 1991), suggesting a certain resilience to warming temperatures alongside more variable hydrology.

Under the likely scenario of further Arctic warming in the twenty-first century (Christensen et al., 2013), alterations to the hydrology of patchy wetlands may threaten future persistence. Greater summer snow melt may increase inundation in the short term. However, there is likely to become a point where snow banks become sufficiently depleted to no longer have the capacity to sustain wetlands (Woo & Young, 2006). Snow patches were still present at the Valley Fen in July 2016 (Figure 34) suggesting this point of depletion may not yet have been reached, although quantifying the extent and rate of change of snow bank extent over time requires retrospective remote sensing analysis and monitoring.

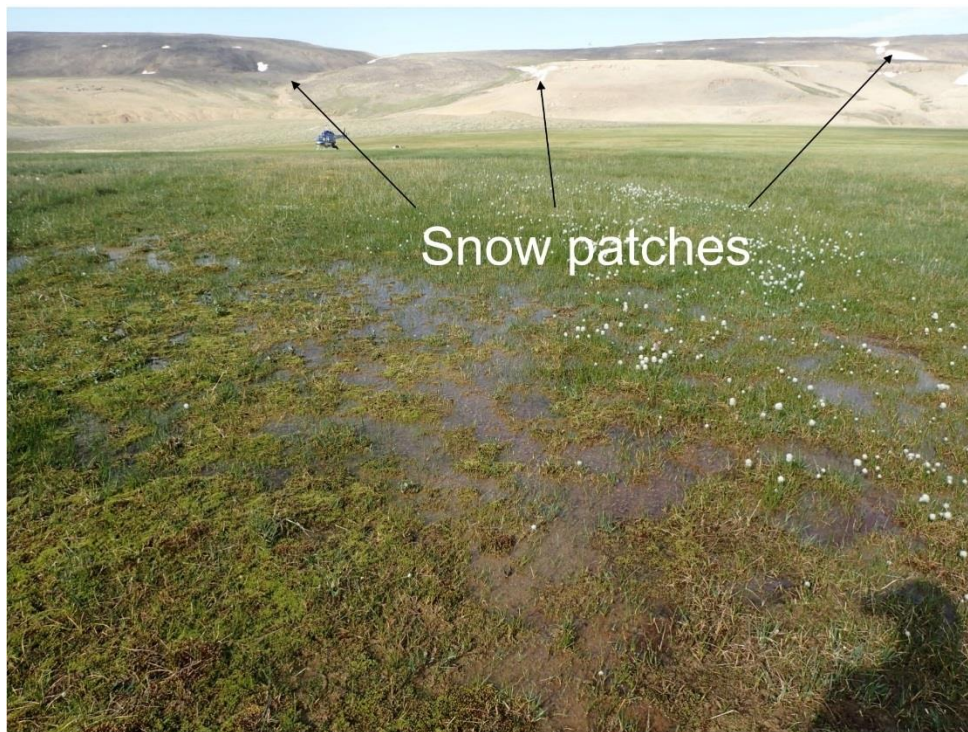


Figure 34. Site photo taken mid-July 2016 at the Valley Fen site (74.05 °N, 118.43 °E) showing snow patches on the hilltops of the surrounding catchment.

Furthermore, increased future permafrost thaw and thickening of the active layer may increase permeability and compromise wetland water retention capacity (Avis et al., 2011). Under this scenario of drying, CO₂ emissions from aerobic decomposition are likely to increase and the wetland is likely to become a carbon source (Oechel et al., 1998). Carbon accumulation rates since ~AD 1950 remain consistent around 20 g m⁻² yr⁻¹ before a dramatic recent increase to 61.3 g m⁻² yr⁻¹ (Figure 31.4c. This increase hints at a potential increase in productivity with increased GDD₀, but this increase should be treated with caution because incomplete decomposition was not accounted for. Nonetheless, stable carbon accumulation indicates that the wetland

ecosystem has not reached a moisture limited point where carbon loss to aerobic decomposition outweighs carbon input from litter.

My results demonstrate a clear ecosystem shift in response to twentieth century climate warming. The testate amoeba record suggests a clear shift in hydrology with increased early growing season inundation from snowmelt, followed by increased drying towards the end of the growing season with increased evapotranspiration. This complex hydrological cycle is supported by the presence of generalist mosses that may also have been influenced by warming conditions. The balance of possible increases in twenty-first century Arctic late-autumn and winter precipitation (Kattsov et al., 2007; Bintanja & Selten, 2014) against summer evapotranspiration losses and permafrost thaw alterations to the water retention capacity of wetland systems is likely to determine the future sustainability and carbon accumulation capacity of this Valley Fen and other Arctic patchy wetlands.

4.4 COASTAL FEN – WARMING AND GRAZING INDUCED ECOSYSTEM STATE SHIFTS

The timing and magnitude of the ecosystem shift from sedges to shrubs is well established in both Coastal Fen records by ~AD 1950 and is likely to be linked to both climate and isostatic uplift. The shrubification of this coastal wetland ~AD 1950 (Figure 31d and 31e) is coincident with an increase in GDD₀ from AD 1931 (Figure 10 and 32b). The northern expansion of shrub communities and increase in plant growth in response to recent climatic warming has been widely documented across the tundra (Tape et al., 2006; Myers-Smith et al., 2011; Elmendorf et al., 2012). Furthermore, climatic warming has been directly linked to increased shrub and decreased sedge abundance in an Alaskan coastal wetland (Carlson et al., 2018). Isostatic uplift is relatively rapid in northern Canada, and has been estimated at 4.2 mm yr⁻¹ at the Coastal Fen site (Peltier, 2004; Geruo et al., 2013). This isostatic uplift may have played a role in lowering the water table, increasing dryness to facilitate sedge to shrub succession (Klinger & Short, 1996). However, in my testate amoeba data, any hydrological shift associated with an increased abundance of shrubs is unclear. I hypothesise that the increase in GDD₀ in combination with ongoing isostatic uplift are the most plausible mechanisms driving this ecosystem shift. The climatic element of this mechanism is further supported by evidence of a recent increase in shrub taxa in Subarctic permafrost peatlands in Sweden (Gałka, et al., 2017b) and Alaska (Gałka et al., 2018) - areas of limited isostatic uplift (Peltier, 2004; Geruo et al., 2013).

The contemporary wetland ecosystem demonstrates minimal shrub cover and contains several large bare vegetated sections and patches of dead moss (Figure 35A and 35B). Both Coastal Fen monoliths demonstrates a recent shift to mosses ~AD 2000. In the absence of any obvious shift in precipitation from the nearby Cambridge Bay weather station since AD 2000 (Figure A1) I suggest that moss-dominance has resulted from an external forcing factor and the apparent increase in wetness suggested by the plant macrofossil record – not corroborated by the testate amoeba record - is an autogenic response to this establishment of a moss-dominance. Wildfire has previously been seen to reduce shrub cover in similar environments (Higuera et al., 2008; Mack et al., 2011), but the absence of macro-charcoal indicates that fire was not an important driver of this marked vegetation shift.

An alternative theory for the reappearance of moss since ~AD 2000 (Figure 31d and 31e) is linked to increased grazing by Arctic geese e.g. lesser snow geese (*Chen caerulescens*) and Ross's geese (*Anser rossii*). My Coastal Fen site is located ~20 km northwest of Queen Maud Gulf Migratory Bird Sanctuary (QMBS), a major summer nesting site for Arctic geese (Cooch et al., 2001). Similarly, bird presence is unambiguously confirmed at the Coastal Fen site by an abundance of tracks and excrement (Figure 35C and 35D). Arctic geese populations have been increasing alongside improved food provision from increased agricultural production in the wintering grounds of the southern United States (Jefferies et al., 2004; Fox et al., 2005). This increased agricultural production is driven primarily by non-climatic factors such as widespread application of nitrogen fertiliser and agricultural subsidy policies (Jefferies et al., 2004). Arctic geese populations appear to continue increasing despite population reduction efforts in the form of relaxed hunting regulations (Alisauskas et al., 2011).

The QMBS has seen Arctic geese nesting populations rise from an estimated 44,300 in 1965 to 2,251,900 in 2006, with over 50% of this increase occurring since 1998 (Kerbes et al., 2014), albeit concentrated to eastern half of the sanctuary further from my site. Increasing snow geese populations in eastern QMBS have been correlated with decreasing vegetation cover. In particular an increasing snow geese numbers have been linked with a reduction in shrub cover relating to foraging and nest construction demands, and increasing areas of bare peat (five-fold increase in extent 1988–2011) or mineral substrate (Alisauskas et al., 2006; Conkin & Alisauskas, 2017). Consequently, snow geese may seek out more pristine and warming habitats further

north – such as my site – and begin to degrade them, providing a credible explanation for the presence of large bare patches or dead vegetation (Figure 35A and 35B).

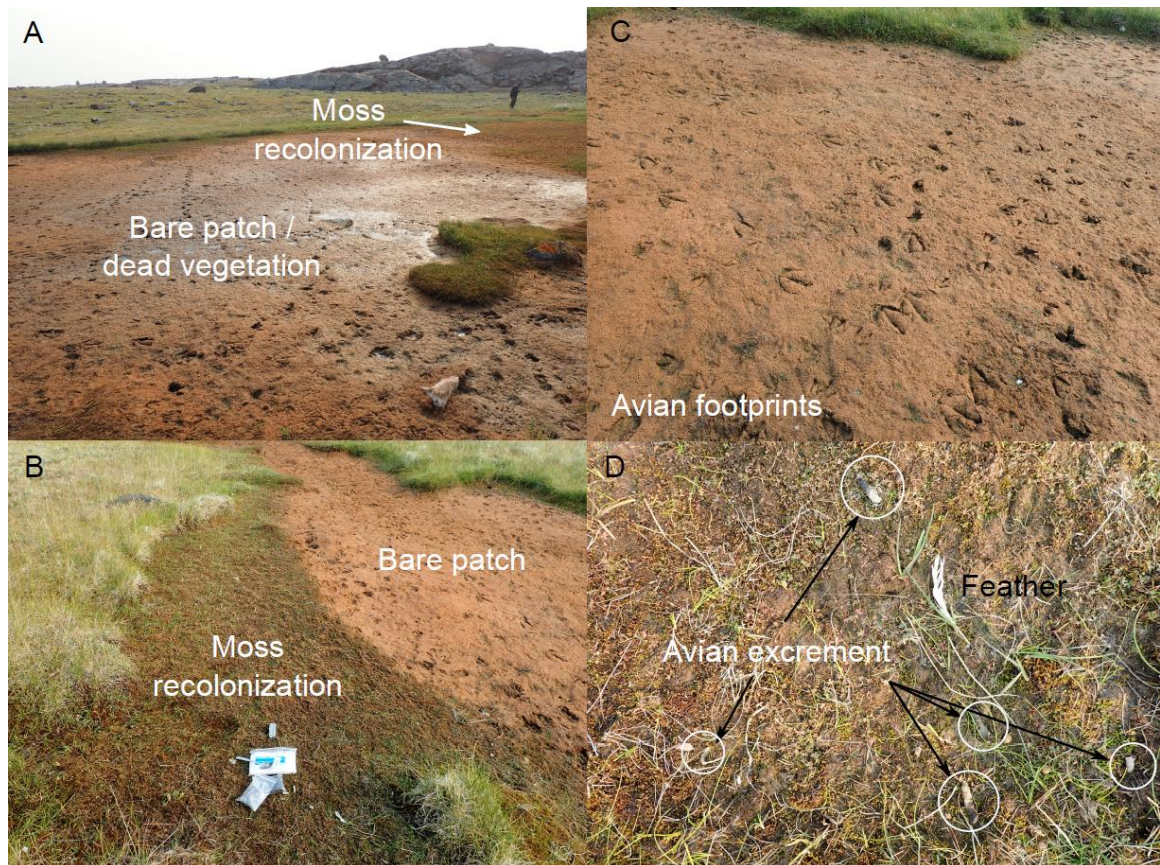


Figure 35. Site photos taken mid-August 2017 at the Coastal Fen site (68.65 °N, 105.45 °E). A) Large bare patch including some dead vegetation with the early stages of moss recolonization in the top right. B) Moss recolonization towards edge of the disturbed area. C) Clear avian footprints in a bare patch. D) Avian excrement and a feather observed at the site.

Moreover, snow geese have demonstrated a preference for herbivory of vascular plants and therefore across the coastal wetlands of northern Canada, areas subjected to destructive grazing often experience an increase in moss vegetation abundance (Abraham & Jefferies, 1997; Alisauskas et al., 2006). However, conversions of moss-cover to bare peat have also been documented in response to intensifying snow geese herbivory (Conkin and Alisauskas, 2017), perhaps suggesting an ecological threshold. Nonetheless, vegetation recolonization in disturbed wetlands is typically concentrated to smaller patches towards the edge of the disturbance (Speed et al., 2010). Either edge recolonization following snow geese disturbance or selective snow geese herbivory provides a plausible explanation for the dramatic shift from a shrub to moss-dominance ecosystem ~AD 2000 (Figure 31d and 31e; Figure 35 A and 35B).

At the Coastal Fen site, the clear ecosystem state shift to shrub-dominance is coincident with high carbon accumulation that peaks ~AD 1980 at over $100 \text{ g m}^{-2} \text{ yr}^{-1}$ (Figure 31.4d and 31.4.e). This ecosystem shift provides evidence for an increase in carbon accumulation at high latitudes and for the potential of a northward migration of peatlands with longer and warmer growing seasons under twenty-first century warming – as is predicted by Charman et al. (2015) and Gallego-Sala et al. (2018). Similarly, regional isostatic uplift (Peltier, 2004; Geruo et al., 2013) may further increase the area of coastal wetlands. This may to some extent mitigate losses from degrading peatlands further south (Charman et al., 2015; Gallego-Sala et al., 2018). However, subsequent destructive grazing by Arctic geese from ~AD 2000 appears to have curtailed carbon accumulation rates since ~AD 1980 (Figure 31d and 31e), highlighting the complexity of Arctic wetland systems. The recolonization of moss consists mainly of *C. richardsonii* (> 50%) and in CFA also *Brachythecium mildeanum* (up to 40%). *Calliergon* spp. mosses are typical of High Arctic conditions and characteristic of pools or lawns under wet rich fen conditions (Vitt & Chee, 1990). *B. mildeanum* is rare in northern Canada, typical of low hummocks in Boreal moderate rich fens (Chee & Vitt, 1989; Nicholson & Gignac, 1995), suggesting that despite grazing pressures climatic warming is pushing the distribution of this species northwards.

My results demonstrate a marked response in this coastal wetland to twentieth century warming, with a shift to a more productive shrub-dominated ecosystem with increased GDD_0 . However, potential recent increases in bird grazing appear to have reduced vegetation cover, curtailed carbon accumulation and facilitated a degree of moss recolonization - highlighting the complexity of Arctic wetland systems. Wetter habitats have demonstrated greater resilience to grazing pressures (Speed et al., 2010), therefore if adequate moisture is retained in the fen there may be potential for a moss-dominated wetland system to continue accumulating carbon (Charman et al., 2013). The future carbon balance of Arctic coastal wetlands is likely to be dependent upon the ability of mosses and other vegetation to recolonize bare patches, changes to precipitation and the trajectory of future Arctic geese populations - I suggest these areas are a priority for future research.

5. CONCLUSION

The findings of this study have shown that twentieth century warming of the western Canadian Arctic has caused an increase in growing degree days above 0°C (GDD₀) across all my study sites. All sites demonstrated a marked ecosystem shift in response to this warming, however the pathways of these responses were diverse between different wetland types. In the absence of long-term monitoring data my high-resolution palaeoecological approach – the first of its kind in the High Arctic - allowed me to identify a diverse array of marked ecosystem shifts at each of my Arctic wetland sites in response to this recent warming.

The raised centre of the Polygon Mire was the only monolith across all study sites not to demonstrate a clear response to increased GDD₀. A cessation of peat accumulation coincident with drying following the formation of the raised centre structure may have occurred prior to 1 Ka BP and could explain the absence of an ecological response to recent warming in the raised centre palaeo-record. In contrast, the Polygon Mire trough shows a marked shift ~AD 2000 from a sedge, herb and moss ecosystem to one dominated by brown mosses - likely in response to wetting from ice-wedge degradation under warming conditions. This moss establishment may represent a negative ecological feedback limiting further ice-wedge degradation via insolation, reducing or delaying the influence of climate warming and potentially mitigating carbon losses. This diversity in responses between the two sections of the wetland highlights the importance of considering the microtopography of ice-wedge polygon systems.

In the Valley Fen, a marked increase in GDD₀ from ~AD 1950 appears to have altered the seasonal hydrology. I hypothesise elevated melt with warming has increased inundation early in the summer, but greater evaporation losses have led to drying towards the end. This hydrological trend is supported by coincidence with generalist mosses (*T. nitens* and *A. palsture*) tolerant to these conditions. Changing wetland hydrology has so far not been detrimental to carbon accumulation rates, but adequate water retention is likely to be key in the future sustainability of Arctic patchy wetlands under a warming climate.

The Coastal Fen site experienced an ecosystem shift ~AD 1950 from a minerogenic sedge-dominated fen to an organic-rich shrub-dominated fen with high carbon accumulation and is coincident with a dramatic increase in GDD₀, alongside more gradual isostatic uplift. This provides evidence for the northern migration of ecotones and highlights the potential for

warming Arctic wetlands to mitigate carbon losses from degrading peatlands further south. However, increased destructive grazing by Arctic snow geese at the Coastal Fen since ~AD 2000 may have reduced vegetation cover and facilitated a degree of moss recolonization. This recolonization includes a predominantly Boreal moss (*B. mildeanum*), evidencing the influence of warming on ecology despite changing grazing pressures. Although, large uncertainties remain over the future trajectory of Arctic coastal wetlands.

The findings of this study provide direction to future contemporary studies and should be tested by further palaeoenvironmental investigations. Longer and warmer growing seasons in the twenty-first century are likely to cause increased carbon accumulation in wetlands if adequate moisture can be maintained and may facilitate the transition of High Arctic wetlands to productive peatland systems. Although, while my results clearly identify marked ecosystem shifts in High Arctic wetlands in response to twentieth century warming, they also highlight the complexity and diversity in the pathways of these responses across wetland types. The clear, yet complex response of Arctic wetlands to climate warming and non-climate factors (e.g. bird grazing) recorded in this study should be considered in the prediction of twenty-first century peatland distribution and carbon accumulation under further climate warming.

REFERENCES

- Abbott, B.W., Jones, J.B., Schuur, E.A.G., Chapin III, F.S., Bowden, W.B., Bret-Harte, M.S., Epstein, H.E., Flannigan, M.D., Harms, T.K., Hollingsworth, T.N., Mack, M.C., McGuire, A.D., Natali, S.M., Rocha, A. V, Tank, S.E., Turetsky, M.R., Vonk, J.E., Wickland, K.P., Aiken, G.R., Alexander, H.D., Amon, R.M.W., Benscotter, B.W., Bergeron, Y., Bishop, K., Blarquez, O., Ben Bond-Lamberty, B., Breen, A.L., Buffam, I., Cai, Y., Carcaillet, C., Carey, S.K., Chen, J.M., Chen, H.Y.H., Christensen, T.R., Cooper, L.W., Cornelissen, J.H.C., de Groot, W.J., DeLuca, T.H., Dorrepaal, E., Fetcher, N., Finlay, J.C., Forbes, B.C., French, N.H.F., Gauthier, S., Girardin, M.P., Goetz, S.J., Goldammer, J.G., Gough, L., Grogan, P., Guo, L., Higuera, P.E., Hinzman, L., Hu, F.S., Hugelius, G., Jafarov, E.E., Jandt, R., Johnstone, J.F., Jan Karlsson, J., Kasischke, E.S., Kattner, G., Kelly, R., Keuper, F., Kling, G.W., Kortelainen, P., Kouki, J., Kuhry, P., Laudon, H., Laurion, I., Macdonald, R.W., Mann, P.J., Martikainen, P.J., McClelland, J.W., Molau, U., Oberbauer, S.F., Olefeldt, D., Paré, D., Parisien, M.-A., Payette, S., Peng, C., Pokrovsky, O.S., Rastetter, E.B., Raymond, P.A., Reynolds, M.K., Rein, G., Reynolds, J.F., Robards, M., Rogers, B.M., Schädel, C., Schaefer, K., Schmidt, I.K., Shvidenko, A., Sky, J., Spencer, R.G.M., Starr, G., Striegl, R.G., Teisserenc, R., Tranvik, L.J., Virtanen, T., Welker, J.M. and Zimov, S. 2016. Biomass offsets little or none of permafrost carbon release from soils, streams, and wildfire: an expert assessment. *Environmental Research Letters*. **11**(3), p.034014.
- Abraham, K.F. and Jefferies, R.L. 1997. High goose populations: Causes, impacts and implications *In*: B. D. J. Batt, ed. *Arctic ecosystems in peril: Report of the Arctic Goose Habitat Working Group. Arctic Goose Joint Venture Special Publication*. Ottawa, Ontario: Canadian Wildlife Service, pp.7–72.
- Åkerman, H.J. and Johansson, M. 2008. Thawing permafrost and thicker active layers in sub-arctic Sweden. *Permafrost and Periglacial Processes*. **19**(3), pp.279–292.
- Alisauskas, R.T., Charlwood, J.W. and Kellett, D.K. 2006. Vegetation Correlates of the History and Density of Nesting by Ross's Geese and Lesser Snow Geese at Karrak Lake, Nunavut. *Arctic*. **59**, pp.201–210.
- Alisauskas, R.T., Rockwell, R.F., Dufour, K.W., Cooch, E.G., Zimmerman, G., Drake, K.L., Leafloor, J.O., Moser, T.J. and Reed, E.T. 2011. Harvest, survival, and abundance of midcontinent lesser snow geese relative to population reduction efforts. *Wildlife Monographs*. **179**(1), pp.1–42. <http://doi.wiley.com/10.1002/wmon.5>.
- Amesbury, M.J., Barber, K.E. and Hughes, P.D.M. 2011. The methodological basis for fine-resolution, multi-proxy reconstructions of ombrotrophic peat bog surface wetness. *Boreas*. **40**(1), pp.161–174. <http://doi.wiley.com/10.1111/j.1502-3885.2010.00152.x>.
- Amesbury, M.J., Mallon, G., Charman, D.J., Hughes, P.D.M., Booth, R.K., Daley, T.J. and Garneau, M. 2013. Statistical testing of a new testate amoeba-based transfer function for water-table depth reconstruction on ombrotrophic peatlands in north-eastern Canada and Maine, United States. *Journal of Quaternary Science*. **28**(1), pp.27–39. <http://doi.wiley.com/10.1002/jqs.2584>.
- Arlen-Pouliot, Y. and Bhiry, N. 2005. Palaeoecology of a palsa and a filled thermokarst pond in a permafrost peatland, subarctic Québec, Canada. *The Holocene*. **15**(3), pp.408–419.

- Avis, C.A., Weaver, A.J. and Meissner, K.J. 2011. Reduction in areal extent of high-latitude wetlands in response to permafrost thaw. *Nature Geoscience*. **4**(7), pp.444–448.
- Beilman, D.W., MacDonald, G.M., Smith, L.C. and Reimer, P.J. 2009. Carbon accumulation in peatlands of West Siberia over the last 2000 years. *Global Biogeochemical Cycles*. **23**(1). <http://doi.wiley.com/10.1029/2007GB003112>.
- Beilman, D.W. and Robinson, S.D. 2003. Peatland permafrost thaw and landform type along a climatic gradient *In: Proceedings of the 8th International Conference on Permafrost*. Zurich: Balkema, pp.61–65.
- Beilman, D.W., Vitt, D.H. and Halsey, L.A. 2001. Localized Permafrost Peatlands in Western Canada: Definition, Distributions, and Degradation. *Arctic, Antarctic, and Alpine Research*. **33**(1), p.70.
- Belyea, L.R. 2009. Nonlinear Dynamics of Peatlands and Potential Feedbacks on the Climate System *In: Carbon Cycling in Northern Peatlands.*, pp.5–18.
- Belyea, L.R. and Baird, A.J. 2006. Beyond ‘The Limits to Peat Bog Growth’: Cross-Scale Feedback in Peatland Development. *Ecological Monographs*. **76**(763), pp.299–322.
- Beyens, L. and Chardez, D. 1995. An Annotated List of Testate Amoebae Observed in the Arctic between the Longitudes 27° E and 168° W. *Archiv für Protistenkunde*. **146**(2), pp.219–233.
- Beyens, L., Chardez, D., De Baere, D., De Bock, P. and Jaques, E. 1990. Ecology of terrestrial testate amoebae assemblages from coastal Lowlands on Devon Island (NWT, Canadian Arctic). *Polar Biology*. **10**(6), pp.431–440.
- Bick, H. 1972. *Ciliated Protozoa: An illustrated guide to the species used as biological indicators in freshwater biology* Geneva.
- Bindoff, N.L., Stott, P.A., AchutaRao, K.M., Allen, M.R., Gillett, N., Gutzler, D., Hansingo, K., Hegerl, G., Hu, Y., Jain, S., Mokhov, I.I., Overland, J., Perlwitz, J., Sebbari, R. and Zhang, X. 2013. Detection and Attribution of Climate Change: from Global to Regional *In: T. F. Stocker, D. Qin, G.-K. Plattner, M. Tignor, S. K. Allen, J. Boschung, A. Nauels, Y. Xia, V. Bex and P. M. Midgley, eds. Climate Change 2013: The Physical Science Basis. Contribution of Working Group I to the Fifth Assessment Report of the Intergovernmental Panel on Climate Change*. Cambridge, United Kingdom and New York, NY, USA: Cambridge University Press, pp.867–952.
- Bintanja, R. and Selten, F.M. 2014. Future increases in Arctic precipitation linked to local evaporation and sea-ice retreat. *Nature*. **509**(7501), pp.479–482.
- Blaauw, M. 2010. Methods and code for ‘classical’ age-modelling of radiocarbon sequences. *Quaternary Geochronology*. **5**(5), pp.512–518.
- Blyakharchuk, T.A. and Sulerzhitsky, L.D. 1999. Holocene vegetational and climatic changes in the forest zone of Western Siberia according to pollen records from the extrazonal palsa bog Bugristoye. *The Holocene*, **9**(5), pp.621–628
- Bobrov, A.A., Charman, D.J. and Warner, B.G. 1999. Ecology of Testate Amoebae (Protozoa: Rhizopoda) on Peatlands in Western Russia with Special Attention to Niche Separation in

Closely Related Taxa. *Protist.* **150**(2), pp.125–136.

- Bockheim, J. ., & Tarnocai, C. (1998). Recognition of cryoturbation for classifying permafrost-affected soils. *Geoderma*, *81*(3–4), 281–293. [https://doi.org/10.1016/S0016-7061\(97\)00115-8](https://doi.org/10.1016/S0016-7061(97)00115-8)
- Booth, R.K. 2008. Testate amoebae as proxies for mean annual water-table depth in Sphagnum-dominated peatlands of North America. *Journal of Quaternary Science.* **23**(1), pp.43–57. <http://doi.wiley.com/10.1002/jqs.1114>.
- Booth, R.K., Lamentowicz, M. and Charman, D.J. 2010. Preparation and analysis of testate amoebae in peatland palaeoenvironmental studies. *Mires and Peat.* **7**(02), pp.1–7.
- Bradley, R.S. 1990. Holocene paleoclimatology of the Queen Elizabeth Islands, Canadian High Arctic. *Quaternary Science Reviews.* **9**(4), pp.365–384.
- Brown, J., Ferrians, O., Heginbottom, J.A. and Melnikov, E. 2002. *Circum-Arctic Map of Permafrost and Ground-Ice Conditions, Version 2*. Boulder, Colorado, USA: National Snow and Ice Data Center.
- Burgess, M.M., Smith, S.L., Brown, J., Romanovsky, V. and Hinkel, K. 2000. Global Terrestrial Network for Permafrost (GTNet-P): permafrost monitoring contributing to global climate observations.
- Burn, C.R. and Kokelj, S. V. 2009. The environment and permafrost of the Mackenzie Delta area. *Permafrost and Periglacial Processes.* **20**(2), pp.83–105. <http://doi.wiley.com/10.1002/ppp.655>.
- Burton, R.G.O. and Hodgson, J.M. 1987. *Lowland peat in England and Wales*. Harpenden: Soil Survey of England and Wales.
- Carlson, L.G., Beard, K.H. and Adler, P.B. 2018. Direct effects of warming increase woody plant abundance in a subarctic wetland. *Ecology and Evolution.* **8**(5), pp.2868–2879.
- Chambers, F.M., Beilman, D.W. and Yu, Z. 2011. Methods for determining peat humification and for quantifying peat bulk density, organic matter and carbon content for palaeostudies of climate and peatland carbon dynamics. *Mires and Peat.* **7**(07), pp.1–10.
- Charman, D. 2002. *Peatlands and environmental change* Chichester, UK: John Wiley & Sons Ltd.
- Charman, D.J., Amesbury, M.J., Hinchliffe, W., Hughes, P.D.M., Mallon, G., Blake, W.H., Daley, T.J., Gallego-Sala, A. V. and Mauquoy, D. 2015. Drivers of Holocene peatland carbon accumulation across a climate gradient in northeastern North America. *Quaternary Science Reviews.* **121**, pp.110–119.
- Charman, D.J., Beilman, D.W., Blaauw, M., Booth, R.K., Brewer, S., Chambers, F.M., Christen, J.A., Gallego-Sala, A., Harrison, S.P., Hughes, P.D.M., Jackson, S.T., Korhola, A., Mauquoy, D., Mitchell, F.J.G., Prentice, I.C., van der Linden, M., De Vleeschouwer, F., Yu, Z.C., Alm, J., Bauer, I.E., Corish, Y.M.C., Garneau, M., Hohl, V., Huang, Y., Karofeld, E., Le Roux, G., Loisel, J., Moschen, R., Nichols, J.E., Nieminen, T.M., MacDonald, G.M., Phadtare, N.R., Rausch, N., Sillasoo, Ü., Swindles, G.T., Tuittila, E.-S., Ukonmaanaho, L., Väliranta, M., van Bellen, S., van Geel, B., Vitt, D.H. and Zhao, Y. 2013. Climate-related changes in peatland

- carbon accumulation during the last millennium. *Biogeosciences*. **10**(2), pp.929–944.
- Charman, D.J., Blundell, A. and Abrupt Climate Change Over the European Land Mass project members 2007. A new European testate amoebae transfer function for palaeohydrological reconstruction on ombrotrophic peatlands. *Journal of Quaternary Science*. **22**(3), pp.209–221. <http://doi.wiley.com/10.1002/jqs.1026>.
- Charman, D.J., Hendon, D. and Woodland, W.A. 2000. *The identification of testate amoebae (Protozoa: Rhizopoda) in peats: QRA Technical Guide No. 9*. London: Quaternary Research Association.
- Chaudhary, N., Miller, P.A. and Smith, B. 2017. Modelling past, present and future peatland carbon accumulation across the pan-Arctic region. *Biogeosciences*. **14**(18), pp.4023–4044.
- Chee, W.-L. and Vitt, D.H. 1989. The vegetation, surface water chemistry and peat chemistry of moderate-rich fens in central Alberta, Canada. *Wetlands*. **9**(2), pp.227–261.
- Chivers, M.R., Turetsky, M.R., Waddington, J.M., Harden, J.W. and McGuire, A.D. 2009. Effects of Experimental Water Table and Temperature Manipulations on Ecosystem CO₂ Fluxes in an Alaskan Rich Fen. *Ecosystems*. **12**(8), pp.1329–1342.
- Christensen, J.H., Kumar, K.K., Aldrian, E., An, S.-I., Cavalcanti, I.F.A., de Castro, M., Dong, W., Goswami, P., Hall, A., Kanyanga, J.K., Kitoh, A., Kossin, J., Lau, N.-C., Renwick, J., Stephenson, D., Xie, S.-P. and Zhou, T. 2013. Climate Phenomena and their Relevance for Future Regional Climate Change *In*: T. F. Stocker, D. Qin, G.-K. Plattner, M. Tignor, S. K. Allen, J. Boschung, A. Nauels, Y. Xia, V. Bex and P. M. Midgley, eds. *The Physical Science Basis. Contribution of Working Group I to the Fifth Assessment Report of the Intergovernmental Panel on Climate Change*. Cambridge, United Kingdom and New York, NY, USA: Cambridge University Press, pp.1217–1310.
- Christensen, T.R., Johansson, T., Åkerman, H.J., Mastepanov, M., Malmer, N., Friborg, T., Crill, P. and Svensson, B.H. 2004. Thawing sub-arctic permafrost: Effects on vegetation and methane emissions. *Geophysical Research Letters*. **31**(4), p.L04501. <http://doi.wiley.com/10.1029/2003GL018680>.
- Coleman, D.C., Callaham, M.A. and Crossley, D.A. 2017. *Fundamentals of soil ecology* 3rd ed. London, United Kingdom: Academic Press.
- Collins, M., Knutti, R., Arblaster, J., Dufresne, J.-L., Fichet, T., Friedlingstein, P., Gao, X., Gutowski, W.J., Johns, T., Krinner, G., Shongwe, M., Tebaldi, C., Weaver, A.J. and Wehner, M. 2013. Long-term Climate Change: Projections, Commitments and Irreversibility *In*: T. F. Stocker, D. Qin, G.-K. Plattner, M. Tignor, S. K. Allen, J. Boschung, A. Nauels, Y. Xia, V. Bex and P. M. Midgley, eds. *Climate Change 2013: The Physical Science Basis. Contribution of Working Group I to the Fifth Assessment Report of the Intergovernmental Panel on Climate Change*. Cambridge, United Kingdom and New York, NY, USA: Cambridge University Press, pp.1029–1136.
- Compo, G.P., Whitaker, J.S., Sardeshmukh, P.D., Matsui, N., Allan, R.J., Yin, X., Gleason, B.E., Vose, R.S., Rutledge, G., Bessemoulin, P., Brönnimann, S., Brunet, M., Crouthamel, R.I., Grant, A.N., Groisman, P.Y., Jones, P.D., Kruk, M.C., Kruger, A.C., Marshall, G.J., Maugeri, M., Mok, H.Y., Nordli, Ø., Ross, T.F., Trigo, R.M., Wang, X.L., Woodruff, S.D. and Worley, S.J. 2011. The Twentieth Century Reanalysis Project. *Quarterly Journal of the Royal*

Meteorological Society. **137**(654), pp.1–28.

- Conkin, J. and Alisauskas, R.T. 2017. Conversion of tundra to exposed peat habitat by snow geese (*Chen caerulescens caerulescens*) and Ross's geese (*C. rossii*) in the central Canadian Arctic. *Polar Biology*. **40**(3), pp.563–576.
- Cooch, E., Rockwell, R.F. and Brault, S. 2001. Retrospective Analysis of Demographic Responses To Environmental Change : a Lesser Snow Goose Example. *Ecological Monographs*. **71**(3), pp.377–400.
- Corliss, J.O. 1979. *The Ciliated Protozoa : Characterization, Classification and Guide to the Literature*. 2nd ed. Oxford, United Kingdom: Pergamon Press.
- Dorrepaal, E., Toet, S., van Logtestijn, R.S.P., Swart, E., van de Weg, M.J., Callaghan, T. V. and Aerts, R. 2009. Carbon respiration from subsurface peat accelerated by climate warming in the subarctic. *Nature*. **460**(7255), pp.616–619.
- Elmendorf, S.C., Henry, G.H.R., Hollister, R.D., Björk, R.G., Boulanger-Lapointe, N., Cooper, E.J., Cornelissen, J.H.C., Day, T.A., Dorrepaal, E., Elumeeva, T.G., Gill, M., Gould, W.A., Harte, J., Hik, D.S., Hofgaard, A., Johnson, D.R., Johnstone, J.F., Jónsdóttir, I.S., Jorgenson, J.C., Klanderud, K., Klein, J.A., Koh, S., Kudo, G., Lara, M., Lévesque, E., Magnússon, B., May, J.L., Mercado-Díaz, J.A., Michelsen, A., Molau, U., Myers-Smith, I.H., Oberbauer, S.F., Onipchenko, V.G., Rixen, C., Martin Schmidt, N., Shaver, G.R., Spasojevic, M.J., Pórhallsdóttir, Þ.E., Tolvanen, A., Troxler, T., Tweedie, C.E., Villareal, S., Wahren, C.-H., Walker, X., Webber, P.J., Welker, J.M. and Wipf, S. 2012. Plot-scale evidence of tundra vegetation change and links to recent summer warming. *Nature Climate Change*. **2**(6), pp.453–457. <http://www.nature.com/doi/10.1038/nclimate1465>.
- Evans, D.J.A., England, J.H., La Farge, C., Coulthard, R.D., Lakeman, T.R. and Vaughan, J.M. 2014. Quaternary geology of the Duck Hawk Bluffs, southwest Banks Island, Arctic Canada: a re-investigation of a critical terrestrial type locality for glacial and interglacial events bordering the Arctic Ocean. *Quaternary Science Reviews*. **91**, pp.82–123.
- van Everdingen, R.O. 2005. *Multi-language glossary of permafrost and related ground-ice terms*. Boulder, Colorado, USA: National Snow and Ice Data Center/World Data Center for Glaciology.
- Flora of North America Editorial Committee 2007. *Flora of North America North of Mexico, Volume 27: Bryophytes, Part 1: Mosses*. Oxford, United Kingdom: Oxford University Press.
- Fontana, F.M.A., Trishchenko, A.P., Luo, Y., Khlopenkov, K. V, Nussbaumer, S.U. and Wunderle, S. 2010. Perennial snow and ice variations (2000–2008) in the Arctic circumpolar land area from satellite observations. *J. Geophys. Res.* **115**, p.4020.
- Fox, A.D., Madsen, J., Boyd, H., Kuijken, E., Norriss, D.W., Tombre, I.M. and Stroud, D.A. 2005. Effects of agricultural change on abundance, fitness components and distribution of two arctic-nesting goose populations. *Global Change Biology*. **11**(6), pp.881–893. <http://doi.wiley.com/10.1111/j.1365-2486.2005.00941.x>.
- Fraser, R., Kokelj, S., Lantz, T., McFarlane-Winchester, M., Olthof, I. and Lacelle, D. 2018. Climate Sensitivity of High Arctic Permafrost Terrain Demonstrated by Widespread Ice-Wedge Thermokarst on Banks Island. *Remote Sensing*. **10**(6), p.954.

- French, H.M. 2017. *The Periglacial Environment* 4th ed. Chichester, UK: John Wiley & Sons Ltd.
- Frolking, S., Talbot, J., Jones, M.C., Treat, C.C., Kauffman, J.B., Tuittila, E.-S. and Roulet, N. 2011. Peatlands in the Earth's 21st century climate system. *Environmental Reviews*. **19**, pp.371–396.
- Gajewski, K. 2015. Quantitative reconstruction of Holocene temperatures across the Canadian Arctic and Greenland. *Global and Planetary Change*. **128**, pp.14–23.
<https://www.sciencedirect.com/science/article/pii/S0921818115000417>.
- Gałka, M., Swindles, G.T., Szal, M., Fulweber, R. and Feurdean, A. 2018. Response of plant communities to climate change during the late Holocene: Palaeoecological insights from peatlands in the Alaskan Arctic. *Ecological Indicators*. **85**, pp.525–536.
<https://www.sciencedirect.com/science/article/pii/S1470160X17306994>.
- Gałka, M., Szal, M., Watson, E.J., Gallego-Sala, A., Amesbury, M.J., Charman, D.J., Roland, T.P., Edward Turner, T. and Swindles, G.T. 2017b. Vegetation Succession, Carbon Accumulation and Hydrological Change in Subarctic Peatlands, Abisko, Northern Sweden. *Permafrost and Periglacial Processes*. **28**(4), pp.589–604. <http://doi.wiley.com/10.1002/ppp.1945>.
- Gałka, M., Tobolski, K., Lamentowicz, Ł., Ersek, V., Jassey, V.E.J., van der Knaap, W.O. and Lamentowicz, M. 2017a. Unveiling exceptional Baltic bog ecohydrology, autogenic succession and climate change during the last 2000 years in CE Europe using replicate cores, multi-proxy data and functional traits of testate amoebae. *Quaternary Science Reviews*. **156**, pp.90–106.
<https://www.sciencedirect.com/science/article/pii/S0277379116306072>.
- Gallego-Sala, A. V., Charman, D.J., Brewer, S., Page, S.E., Prentice, I.C., Friedlingstein, P., Moreton, S., Amesbury, M.J., Beilman, D.W., Björck, S., Blyakharchuk, T., Bochicchio, C., Booth, R.K., Bunbury, J., Camill, P., Carless, D., Chimner, R.A., Clifford, M., Cressey, E., Courtney-Mustaphi, C., De Vleeschouwer, F., de Jong, R., Fialkiewicz-Koziel, B., Finkelstein, S.A., Garneau, M., Githumbi, E., Hribljan, J., Holmquist, J., Hughes, P.D.M., Jones, C., Jones, M.C., Karofeld, E., Klein, E.S., Kokfelt, U., Korhola, A., Lacourse, T., Le Roux, G., Lamentowicz, M., Large, D., Lavoie, M., Loisel, J., Mackay, H., MacDonald, G.M., Makila, M., Magnan, G., Marchant, R., Marcisz, K., Martínez Cortizas, A., Massa, C., Mathijssen, P., Mauquoy, D., Mighall, T., Mitchell, F.J.G., Moss, P., Nichols, J., Oksanen, P.O., Orme, L., Packalen, M.S., Robinson, S., Roland, T.P., Sanderson, N.K., Sannel, A.B.K., Silva-Sánchez, N., Steinberg, N., Swindles, G.T., Turner, T.E., Uglow, J., Väliranta, M., van Bellen, S., van der Linden, M., van Geel, B., Wang, G., Yu, Z., Zaragoza-Castells, J. and Zhao, Y. 2018. Latitudinal limits to the predicted increase of the peatland carbon sink with warming. *Nature Climate Change*. p.1. <http://www.nature.com/articles/s41558-018-0271-1>.
- Garneau, M. 2000. Peat accumulation and climate change in the High Arctic *In*: M. Garneau and B. T. Alt, eds. *Geological Survey of Canada Bulletin 529*, pp.283–293.
- Garneau, M. and Alt, B.T. 2000. *Environmental Response to Climate Change in the Canadian Arctic* [Accessed 10 July 2018]. Available from:
http://publications.gc.ca/collections/collection_2017/rncan-nrcan/M42-529-eng.pdf.
- Geruo, A., Wahr, J. and Zhong, S. 2013. Computations of the viscoelastic response of a 3-D

- compressible Earth to surface loading: an application to Glacial Isostatic Adjustment in Antarctica and Canada. *Geophysical Journal International*. **192**(2), pp.557–572.
- Gignac, L.D., Vitt, D.H., Zoltai, S.C. and Bayley, S.E. 1991. Bryophyte response surfaces along climatic, chemical, and physical gradients in peatlands of western Canada. *Nova Hedwigia*. **53**, pp.27–71.
- Glenn, M.S. and Woo, M. 1997. Spring and summer hydrology of a valley-bottom wetland, Ellesmere Island, Northwest Territories, Canada. *Wetlands*. **17**(2), pp.321–329. [<http://link.springer.com/10.1007/BF03161420>].
- Gorham, E. 1991. Northern Peatlands: Role in the Carbon Cycle and Probable Responses to Climatic Warming. *Ecological Applications*. **1**(2), pp.182–195. <http://doi.wiley.com/10.2307/1941811>.
- Grimm, E.C. 1987. CONISS: a FORTRAN 77 program for stratigraphically constrained cluster analysis by the method of incremental sum of squares. *Computers & Geosciences*. **13**(1), pp.13–35. <https://www.sciencedirect.com/science/article/pii/0098300487900227>.
- Hadenäs, L. 2003. The European species of the Calliergon–Scorpidium–Drepanocladus complex, including some related or similar species. *Meylania*. (28), pp.1–116.
- Hammer, Ø., Harper, D.A. and Ryan, P.D. 2001. PAST: Paleontological Statistics Software Package for Education and Data Analysis. *Palaeontologia Electronica*. **4**(1), p.9.
- Hammond, R.F. 1981. *The Peatlands of Ireland: Soil Survey Bulletin No. 35* [Online] 2nd ed. Dublin, Ireland: An Foras Taluntais.
- Hånnell, U. 1991. *Forest classification of peatlands in Sweden - a field guide*. Umeå, Sweden: Swedish University of Agricultural Sciences, Department of Silviculture, 16 pp.
- Hansen, J., Ruedy, R., Sato, M. and Lo, K. 2010. Global surface temperature change. *Reviews of Geophysics*. **48**(4), p.RG4004. <http://doi.wiley.com/10.1029/2010RG000345>.
- Hassol, S., Arctic Climate Impact Assessment., Arctic Monitoring and Assessment Programme., Program for the Conservation of Arctic Flora and Fauna. and International Arctic Science Committee. 2004. *Impacts of a warming Arctic : Arctic Climate Impact Assessment* Cambridge University Press.
- Heginbottom, J.A., Dubreuil, M.A. and Harker, P.A. 1995. Canada - Permafrost *In: National Atlas Information Service*, ed. *National Atlas of Canada*. Natural Resources Canada, MCR 4177.
- Helbig, M., Chasmer, L.E., Desai, A.R., Kljun, N., Quinton, W.L. and Sonnentag, O. 2017. Direct and indirect climate change effects on carbon dioxide fluxes in a thawing boreal forest-wetland landscape. *Global Change Biology*. **23**(8), pp.3231–3248. <http://doi.wiley.com/10.1111/gcb.13638>.
- Higuera, P.E., Brubaker, L.B., Anderson, P.M., Brown, T.A., Kennedy, A.T. and Hu, F.S. 2008. Frequent Fires in Ancient Shrub Tundra: Implications of Paleorecords for Arctic Environmental Change J. Chave, ed. *PLoS ONE*. **3**(3), p.e0001744.
- Hill, G.B. and Henry, G.H.R. 2011. Responses of High Arctic wet sedge tundra to climate warming since 1980. *Global Change Biology*. **17**(1), pp.276–287.

<http://doi.wiley.com/10.1111/j.1365-2486.2010.02244.x>.

- Hodgkins, S.B., Tfaily, M.M., McCalley, C.K., Logan, T.A., Crill, P.M., Saleska, S.R., Rich, V.I. and Chanton, J.P. 2014. Changes in peat chemistry associated with permafrost thaw increase greenhouse gas production. *Proceedings of the National Academy of Sciences of the United States of America*. **111**(16), pp.5819–24.
- Holden, J. and Burt, T.P. 2003. Hydrological studies on blanket peat: the significance of the acrotelm-catotelm model. *Journal of Ecology*. **91**(1), pp.86–102.
<http://doi.wiley.com/10.1046/j.1365-2745.2003.00748.x>.
- Houghton, R.A. 2007. Balancing the Global Carbon Budget. *Annual Review of Earth and Planetary Sciences*. **35**(1), pp.313–347.
- Hua, Q., Barbetti, M. and Rakowski, A.Z. 2013. Atmospheric Radiocarbon for the Period 1950–2010. *Radiocarbon*. **55**(04), pp.2059–2072.
- Ingram, H.A.P. 1978. Soil Layers in Mires: Function and Terminology. *Journal of Soil Science*. **29**(2), pp.224–227. <http://doi.wiley.com/10.1111/j.1365-2389.1978.tb02053.x>.
- Jefferies, R.L., Rockwell, R.F. and Abraham, K.F. 2004. The embarrassment of riches: agricultural food subsidies, high goose numbers, and loss of Arctic wetlands – a continuing saga. *Environmental Reviews*. **11**(4), pp.193–232.
- Johansson, T., Malmer, N., Crill, P.M., Friborg, T., Åkerman, J.H., Mastepanov, M. and Christensen, T.R. 2006. Decadal vegetation changes in a northern peatland, greenhouse gas fluxes and net radiative forcing. *Global Change Biology*. **12**(12), pp.2352–2369.
<http://doi.wiley.com/10.1111/j.1365-2486.2006.01267.x>.
- Jones, M.C., Grosse, G., Jones, B.M. and Walter Anthony, K. 2012. Peat accumulation in drained thermokarst lake basins in continuous, ice-rich permafrost, northern Seward Peninsula, Alaska. *Journal of Geophysical Research: Biogeosciences*. **117**(G2),
<http://doi.wiley.com/10.1029/2011JG001766>.
- Joosten, H. and Clarke, D. 2002. *Wise Use of Mires and Peatlands — Background Principles including a Framework for Decision-Making*. Saarijärvi, Finland: International Mire Conservation Group and International Peat Society.
- Jorgenson, M.T., Kanevskiy, M., Shur, Y., Moskalenko, N., Brown, D.R.N., Wickland, K., Striegl, R. and Koch, J. 2015. Role of ground ice dynamics and ecological feedbacks in recent ice wedge degradation and stabilization. *Journal of Geophysical Research: Earth Surface*. **120**(11), pp.2280–2297. <http://doi.wiley.com/10.1002/2015JF003602>.
- Jorgenson, M.T., Shur, Y.L. and Pullman, E.R. 2006. Abrupt increase in permafrost degradation in Arctic Alaska. *Geophysical Research Letters*. **33**(2), p.L02503.
<http://doi.wiley.com/10.1029/2005GL024960>.
- Juggins, S. 2007. C2 Version 1.5 User guide. Software for ecological and palaeoecological data analysis and visualisation. Newcastle upon Tyne, UK: Newcastle University, p.73.
- Juggins, S. 2018. Rioja: Analysis of Quaternary Science Data. R package version 0.9-15.1. Available from: <https://cran.r-project.org/package=rioja>.

- Kane, D.L., Hinzman, L.D. and Zarling, J.P. 1991. Thermal response of the active layer to climatic warming in a permafrost environment. *Cold Regions Science and Technology*. **19**(2), pp.111–122. <https://www.sciencedirect.com/science/article/pii/0165232X9190002X>.
- Kattsov, V.M., Walsh, J.E., Chapman, W.L., Govorkova, V.A., Pavlova, T. V., Zhang, X., Kattsov, V.M., Walsh, J.E., Chapman, W.L., Govorkova, V.A., Pavlova, T. V. and Zhang, X. 2007. Simulation and Projection of Arctic Freshwater Budget Components by the IPCC AR4 Global Climate Models. *Journal of Hydrometeorology*. **8**(3), pp.571–589. <http://journals.ametsoc.org/doi/abs/10.1175/JHM575.1>.
- Kaufman, D.S., Schneider, D.P., McKay, N.P., Ammann, C.M., Bradley, R.S., Briffa, K.R., Miller, G.H., Otto-Bliesner, B.L., Overpeck, J.T., Vinther, B.M. and Arctic Lakes 2k Project Members, A.L. 2k P. 2009. Recent warming reverses long-term arctic cooling. *Science*. **325**(5945), pp.1236–9.
- Keddy, P.A. 2010. *Wetland ecology : principles and conservation*. Cambridge, UK: Cambridge University Press.
- Kerbes, R.H., Meeres, K.M. and Alisauskas, R.T. 2014. *Surveys of nesting lesser snow geese and ross's geese in arctic canada, 2002 - 2009*. *Arctic Goose Joint Venture Special Publication*. U.S. Fish and Wildlife Service, Washington, D.C. and Canadian Wildlife Service, Ottawa, Ontario.
- Killick, R. and Eckley, I.A. 2014. **change**point : An R Package for Changepoint Analysis. *Journal of Statistical Software*. **58**(3), pp.1–19.
- Klein, E.S., Yu, Z. and Booth, R.K. 2013. Recent increase in peatland carbon accumulation in a thermokarst lake basin in southwestern Alaska. *Palaeogeography, Palaeoclimatology, Palaeoecology*. **392**, pp.186–195. <https://www.sciencedirect.com/science/article/pii/S0031018213004112>.
- Klinger, L.F. and Short, S.K. 1996. Succession in the Hudson Bay Lowland, Northern Ontario, Canada. *Arctic and Alpine Research*. **28**(2), pp.172–183.
- Kokelj, S. V., Lantz, T.C., Wolfe, S.A., Kanigan, J.C., Morse, P.D., Coutts, R., Molina-Giraldo, N. and Burn, C.R. 2014. Distribution and activity of ice wedges across the forest-tundra transition, western arctic Canada. *Journal of Geophysical Research: Earth Surface*. **119**(9), pp.2032–2047. <https://agupubs.onlinelibrary.wiley.com/doi/pdf/10.1002/2014JF003085>.
- Kopec, B.G., Feng, X., Michel, F.A. and Posmentier, E.S. 2016. Influence of sea ice on Arctic precipitation. *Proceedings of the National Academy of Sciences of the United States of America*. **113**(1), pp.46–51.
- Kralik, U. 1961. Ein Beitrag zur Biologie von loricate peritrichen Ziliaten, insbesondere von *Platycola truncata* Fromentel 1874. *Arch. Protistenk.* **105**, pp.201–258.
- Kuhry, P. and Turunen, J. 2006. The Postglacial Development of Boreal and Subarctic Peatlands *In: R. K. Wieder and D. H. Vitt, eds. Boreal Peatland Ecosystems* Berlin, Germany: Springer Berlin Heidelberg, pp.25–46.
- Lachenbruch, A.H. 1962. Mechanics of thermal contraction cracks and ice-wedge polygons in permafrost. *Geological Society of America Special Papers*. **70**.

- Lagarec, D. 1982. Cryogenetic mounds as indicators of permafrost conditions, northern Québec. In: *Proceedings of the Fourth Canadian Permafrost Conference*. Ottawa, Ontario, Canada: National Research Council of Canada, pp.43–48.
- Lamarre, A., Garneau, M. and Asnong, H. 2012. Holocene paleohydrological reconstruction and carbon accumulation of a permafrost peatland using testate amoeba and macrofossil analyses, Kuujuarapik, subarctic Québec, Canada. *Review of Palaeobotany and Palynology*. **186**, pp.131–141.
<https://www.sciencedirect.com/science/article/pii/S0034666712001091>.
- Lamarre, A., Magnan, G., Garneau, M. and Boucher, É. 2013. A testate amoeba-based transfer function for paleohydrological reconstruction from boreal and subarctic peatlands in northeastern Canada. *Quaternary International*. **306**, pp.88–96.
<https://www.sciencedirect.com/science/article/pii/S1040618213003194>.
- Lamentowicz, Ł., Lamentowicz, M. and Gąbka, M. 2008. Testate amoebae ecology and a local transfer function from a peatland in western Poland. *Wetlands*. **28**(1), pp.164–175.
<http://link.springer.com/10.1672/07-92.1>.
- Lavoie, M., Paré, D., Fenton, N., Groot, A. and Taylor, K. 2005. Paludification and management of forested peatlands in Canada: a literature review. *Environmental Reviews*. **13**(2), pp.21–50. <http://www.nrcresearchpress.com/doi/10.1139/a05-006>.
- Lawrence, D.M., Koven, C.D., Swenson, S.C., Riley, W.J. and Slater, A.G. 2015. Permafrost thaw and resulting soil moisture changes regulate projected high-latitude CO₂ and CH₄ emissions. *Environmental Research Letters*. **10**(9), p.094011.
- Lawrence, D.M., Slater, A.G., Romanovsky, V.E. and Nicolsky, D.J. 2008. Sensitivity of a model projection of near-surface permafrost degradation to soil column depth and representation of soil organic matter. *Journal of Geophysical Research: Earth Surface*. **113**(F2), p.F02011. <http://doi.wiley.com/10.1029/2007JF000883>.
- Liblik, L.K., Moore, T.R., Bubier, J.L. and Robinson, S.D. 1997. Methane emissions from wetlands in the zone of discontinuous permafrost: Fort Simpson, Northwest Territories, Canada. *Global Biogeochemical Cycles*. **11**(4), pp.485–494.
<http://doi.wiley.com/10.1029/97GB01935>.
- Liljedahl, A.K., Boike, J., Daanen, R.P., Fedorov, A.N., Frost, G. V., Grosse, G., Hinzman, L.D., Iijima, Y., Jorgenson, J.C., Matveyeva, N., Necsoiu, M., Reynolds, M.K., Romanovsky, V.E., Schulla, J., Tape, K.D., Walker, D.A., Wilson, C.J., Yabuki, H. and Zona, D. 2016. Pan-Arctic ice-wedge degradation in warming permafrost and its influence on tundra hydrology. *Nature Geoscience*. **9**(4), pp.312–318. <http://www.nature.com/articles/ngeo2674>.
- Limpens, J., Berendse, F., Blodau, C., Canadell, J.G., Freeman, C., Holden, J., Roulet, N., Rydin, H. and Schaeppman-Strub, G. 2008. Peatlands and the carbon cycle: from local processes to global implications- a synthesis. *Biogeosciences*. **5**, pp.1475–1491.
www.biogeosciences.net/5/1475/2008/.
- Loisel, J., Yu, Z., Beilman, D.W., Camill, P., Alm, J., Amesbury, M.J., Anderson, D., Andersson, S., Bochicchio, C., Barber, K., Belyea, L.R., Bunbury, J., Chambers, F.M., Charman, D.J., De Vleeschouwer, F., Fiałkiewicz-Kozieł, B., Finkelstein, S.A., Gałka, M., Garneau, M., Hammarlund, D., Hinchcliffe, W., Holmquist, J., Hughes, P., Jones, M.C., Klein, E.S.,

- Kokfelt, U., Korhola, A., Kuhry, P., Lamarre, A., Lamentowicz, M., Large, D., Lavoie, M., MacDonald, G., Magnan, G., Mäkilä, M., Mallon, G., Mathijssen, P., Mauquoy, D., McCarroll, J., Moore, T.R., Nichols, J., O'Reilly, B., Oksanen, P., Packalen, M., Peteet, D., Richard, P.J., Robinson, S., Ronkainen, T., Rundgren, M., Sannel, A.B.K., Tarnocai, C., Thom, T., Tuittila, E.-S., Turetsky, M., Väiliranta, M., van der Linden, M., van Geel, B., van Bellen, S., Vitt, D., Zhao, Y. and Zhou, W. 2014. A database and synthesis of northern peatland soil properties and Holocene carbon and nitrogen accumulation. *The Holocene*. **24**(9), pp.1028–1042. <http://journals.sagepub.com/doi/10.1177/0959683614538073>.
- Loisel, J., Yu, Z., Beilman, D.W., Kaiser, K. and Parnikoza, I. 2017. Peatland ecosystem processes in the maritime antarctic during warm climates. *Scientific Reports*. **7**(1), p.12344. <http://www.nature.com/articles/s41598-017-12479-0>.
- MacDonald, G.M., Beilman, D.W., Kremenetski, K. V, Sheng, Y., Smith, L.C. and Velichko, A.A. 2006. Rapid early development of circumarctic peatlands and atmospheric CH₄ and CO₂ variations. *Science*. **314**(5797), pp.285–288.
- Mack, M.C., Bret-Harte, M.S., Hollingsworth, T.N., Jandt, R.R., Schuur, E.A.G., Shaver, G.R. and Verbyla, D.L. 2011. Carbon loss from an unprecedented Arctic tundra wildfire. *Nature*. **475**(7357), pp.489–492. <http://www.nature.com/articles/nature10283>.
- Mackay, J.R. 1974. Ice-Wedge Cracks, Garry Island, Northwest Territories. *Canadian Journal of Earth Sciences*. **11**(10), pp.1366–1383. <http://www.nrcresearchpress.com/doi/10.1139/e74-133>.
- Mauquoy, D. and van Geel, B. 2007. Mire and peat macros *In*: S. A. Elias, ed. *Encyclopedia of Quaternary Science*. Amsterdam, Netherlands: Elsevier, pp.2315–2336.
- McLaughlin, J. and Webster, K. 2013. *Effects of a Changing Climate on Peatlands in Permafrost Zones : A Literature Review and Application to Ontario's Far North*. Sault Ste Marie, Ontario, Canada: Ontario Forest Research Institute, Ontario Ministry of Natural Resources.
- Microworld 2018. Microworld: world of amoeboid organisms. Available from: <https://www.arcella.nl/>.
- Mieczan, T. 2010. Vertical Micro-Zonation of Testate Amoebae and Ciliates in Peatland Waters in Relation to Potential Food Resources and Grazing Pressure. *International Review of Hydrobiology*. **95**(1), pp.86–102. <http://doi.wiley.com/10.1002/iroh.200911188>.
- Minke, M., Donner, N., Karpov, N., de Klerk, P. and Joosten, H. 2009. Patterns in vegetation composition, surface height and thaw depth in polygon mires in the Yakutian Arctic (NE Siberia): a microtopographical characterisation of the active layer. *Permafrost and Periglacial Processes*. **20**(4), pp.357–368. <http://doi.wiley.com/10.1002/ppp.663>.
- Mitchell, E.A.D., Buttler, A.J., Warner, B.G. and Gobat, J.-M. 1999. Ecology of testate amoebae (Protozoa: Rhizopoda) in *Sphagnum* peatlands in the Jura mountains, Switzerland and France. *Écoscience*. **6**(4), pp.565–576. <https://www.tandfonline.com/doi/full/10.1080/11956860.1999.11682555>.
- Moore, T.R. and Roulet, N.T. 1993. Methane flux: Water table relations in northern wetlands. *Geophysical Research Letters*. **20**(7), pp.587–590.

<https://agupubs.onlinelibrary.wiley.com/doi/abs/10.1029/93GL00208%4010.1002/%28IS SN%291944-8007.GRL40>.

- Morris, P.J., Baird, A.J., Young, D.M. and Swindles, G.T. 2015. Untangling climate signals from autogenic changes in long-term peatland development. *Geophysical Research Letters*. **42**(24), 10,788-10,797. <http://doi.wiley.com/10.1002/2015GL066824>.
- Morris, P.J., Swindles, G.T., Valdes, P.J., Ivanovic, R.F., Gregoire, L.J., Smith, M.W., Tarasov, L., Haywood, A.M. and Bacon, K.L. 2018. Global peatland initiation driven by regionally asynchronous warming. *Proceedings of the National Academy of Sciences of the United States of America*. **115**(19), pp.4851–4856.
- Morris, P.J., Waddington, J.M., Benschoter, B.W. and Turetsky, M.R. 2011. Conceptual frameworks in peatland ecohydrology: looking beyond the two-layered (acrotelm-catotelm) model. *Ecohydrology*. **4**(1), pp.1–11. <http://doi.wiley.com/10.1002/eco.191>.
- Myers-Smith, I.H., Forbes, B.C., Wilmsking, M., Hallinger, M., Lantz, T., Blok, D., Tape, K.D., Macias-Fauria, M., Sass-Klaassen, U., Lévesque, E., Boudreau, S., Ropars, P., Hermanutz, L., Trant, A., Collier, L.S., Weijers, S., Rozema, J., Rayback, S.A., Schmidt, N.M., Schaeppman-Strub, G., Wipf, S., Rixen, C., Ménard, C.B., Venn, S., Goetz, S., Andreu-Hayles, L., Elmendorf, S., Ravolainen, V., Welker, J., Grogan, P., Epstein, H.E. and Hik, D.S. 2011. Shrub expansion in tundra ecosystems: dynamics, impacts and research priorities. *Environmental Research Letters*. **6**(4), p.045509.
- National Wetlands Working Group. 1997. *Wetlands of Canada, Ecological land classification series, no. 24*. Waterloo, Ontario, Canada: Wetlands Research Centre, University of Waterloo.
- Nicholson, B.J. and Gignac, L.D. 1995. Ecotope Dimensions of Peatland Bryophyte Indicator Species along Gradients in the Mackenzie River Basin, Canada. *The Bryologist*. **98**(4), p.437. <https://www.jstor.org/stable/3243583?origin=crossref>.
- Oechel, W.C., Vourlitis, G.L., Hastings, S.J., Ault, R.P. and Bryant, P. 1998. The effects of water table manipulation and elevated temperature on the net CO₂ flux of wet sedge tundra ecosystems. *Global Change Biology*. **4**(1), pp.77–90. <http://doi.wiley.com/10.1046/j.1365-2486.1998.00110.x>.
- Oksanen, J., Blanchet, F.G., Friendly, M., Kindt, R., Legendre, P., McGlenn, D., Minchin, P.R., O’Hara, R.B., Simpson, G.L., Solymos, P., Stevens, M.H.H., Szoecs, E. and Wagner, H. 2017. *vegan: Community Ecology Package*. Available from: <https://cran.r-project.org/package=vegan>.
- Olefeldt, D. and Roulet, N.T. 2012. Effects of permafrost and hydrology on the composition and transport of dissolved organic carbon in a subarctic peatland complex. *Journal of Geophysical Research: Biogeosciences*. **117**(G1). <http://doi.wiley.com/10.1029/2011JG001819>.
- Olefeldt, D., Turetsky, M.R., Crill, P.M. and McGuire, A.D. 2013. Environmental and physical controls on northern terrestrial methane emissions across permafrost zones. *Global Change Biology*. **19**(2), pp.589–603. <http://doi.wiley.com/10.1111/gcb.12071>.
- Ott, C.A. and Chimner, R.A. 2016. Long-term peat accumulation in temperate forested

- peatlands (*Thuja occidentalis* swamps) in the Great Lakes region of North America. *Mires and Peat*. **18**, pp.1–9.
- Ovenden, L. 1988. *Holocene proxy-climate data from the Canadian Arctic*. Ottawa, Ontario, Canada: Department of Energy, Mines and Resources.
- Ovenden, L. 1990. Peat Accumulation in Northern Wetlands. *Quaternary Research*. **33**(03), pp.377–386.
- Paavilainen, E. and Päivänen, J. 1995. *Peatland forestry : ecology and principles*. Berlin, Germany: Springer-Verlag.
- Payne, R.J. 2011. Can testate amoeba-based palaeohydrology be extended to fens? *Journal of Quaternary Science*. **26**(1), pp.15–27. <http://doi.wiley.com/10.1002/jqs.1412>.
- Pelletier, N., Talbot, J., Olefeldt, D., Turetsky, M., Blodau, C., Sonnentag, O. and Quinton, W.L. 2017. Influence of Holocene permafrost aggradation and thaw on the paleoecology and carbon storage of a peatland complex in northwestern Canada. *The Holocene*. **27**(9), pp.1391–1405. <http://journals.sagepub.com/doi/10.1177/0959683617693899>.
- Peltier, W.R. 2004. Global glacial isostasy and the surface of the ice-age Earth: the ICE-5G (VM2) model and GRACE. *Annual Review of Earth and Planetary Sciences*. **32**(1), pp.111–149.
- Qin, Y., Mitchell, E.A.D., Lamentowicz, M., Payne, R.J., Lara, E., Gu, Y., Huang, X. and Wang, H. 2013. Ecology of testate amoebae in peatlands of central China and development of a transfer function for paleohydrological reconstruction. *Journal of Paleolimnology*. **50**(3), pp.319–330. <http://link.springer.com/10.1007/s10933-013-9726-6>.
- R Core Team 2018. R: a language and environment for statistical computing. Available from: <https://www.r-project.org>.
- Reimer, P.J., Bard, E., Bayliss, A., Beck, J.W., Blackwell, P.G., Ramsey, C.B., Buck, C.E., Cheng, H., Edwards, R.L., Friedrich, M., Grootes, P.M., Guilderson, T.P., Hafliðason, H., Hajdas, I., Hatté, C., Heaton, T.J., Hoffmann, D.L., Hogg, A.G., Hughen, K.A., Kaiser, K.F., Kromer, B., Manning, S.W., Niu, M., Reimer, R.W., Richards, D.A., Scott, E.M., Southon, J.R., Staff, R.A., Turney, C.S.M. and van der Plicht, J. 2013. IntCal13 and Marine13 Radiocarbon Age Calibration Curves 0–50,000 Years cal BP. *Radiocarbon*. **55**(04), pp.1869–1887.
- Reimer, P.J., Brown, T.A. and Reimer, R.W. 2004. Discussion: Reporting and Calibration of Post-Bomb ¹⁴C Data. *Radiocarbon*. **46**(03), pp.1299–1304.
- Riordan, B., Verbyla, D. and McGuire, A.D. 2006. Shrinking ponds in subarctic Alaska based on 1950–2002 remotely sensed images. *Journal of Geophysical Research: Biogeosciences*. **111**(G4). <http://doi.wiley.com/10.1029/2005JG000150>.
- Robinson, S.D., Turetsky, M.R., Kettles, I.M. and Wieder, R.K. 2003. Permafrost and peatland carbon sink capacity with increasing latitude *In: Proceedings of the 8th International Conference on Permafrost.*, pp.965–970.
- Roe, H.M., Elliott, S.M. and Patterson, R.T. 2017. Re-assessing the vertical distribution of testate amoeba communities in surface peats: Implications for palaeohydrological studies. *European Journal of Protistology*. **60**, pp.13–27.

- <https://www.sciencedirect.com/science/article/pii/S0932473917300767>.
- Rydin, H. and Jeglum, J.K. 2006. *The Biology of Peatlands* Oxford, UK: Oxford University Press.
- Sannel, A.B.K. and Kuhry, P. 2008. Long-term stability of permafrost in subarctic peat plateaus, west-central Canada. *The Holocene*. **18**(4), pp.589–601.
<http://journals.sagepub.com/doi/10.1177/0959683608089658>.
- Schädel, C., Bader, M.K.-F., Schuur, E.A.G., Biasi, C., Bracho, R., Čapek, P., De Baets, S., Diáková, K., Ernakovich, J., Estop-Aragones, C., Graham, D.E., Hartley, I.P., Iversen, C.M., Kane, E., Knoblauch, C., Lupascu, M., Martikainen, P.J., Natali, S.M., Norby, R.J., O'Donnell, J.A., Chowdhury, T.R., Šantrůčková, H., Shaver, G., Sloan, V.L., Treat, C.C., Turetsky, M.R., Waldrop, M.P. and Wickland, K.P. 2016. Potential carbon emissions dominated by carbon dioxide from thawed permafrost soils. *Nature Climate Change*. **6**(10), pp.950–953.
<http://www.nature.com/articles/nclimate3054>.
- Schuur, E.A.G., McGuire, A.D., Schädel, C., Grosse, G., Harden, J.W., Hayes, D.J., Hugelius, G., Koven, C.D., Kuhry, P., Lawrence, D.M., Natali, S.M., Olefeldt, D., Romanovsky, V.E., Schaefer, K., Turetsky, M.R., Treat, C.C. and Vonk, J.E. 2015. Climate change and the permafrost carbon feedback. *Nature*. **520**(7546), pp.171–179.
<http://www.nature.com/articles/nature14338>.
- Screen, J.A. and Simmonds, I. 2010. The central role of diminishing sea ice in recent Arctic temperature amplification. *Nature*. **464**(7293), pp.1334–1337.
<http://www.nature.com/articles/nature09051>.
- Seppälä, M. 1982. An experimental study of the formation of palsas *In: Proceedings of the Fourth Canadian Permafrost Conference*. Ottawa, Ontario: National Research Council of Canada, pp.36–42.
- Serreze, M.C., Barrett, A.P., Stroeve, J.C., Kindig, D.N. and Holland, M.M. 2009. The emergence of surface-based Arctic amplification. *The Cryosphere*. **3**(1), pp.11–19.
- Serreze, M.C. and Barry, R.G. 2011. Processes and impacts of Arctic amplification: A research synthesis. *Global and Planetary Change*. **77**(1–2), pp.85–96.
<https://www.sciencedirect.com/science/article/pii/S0921818111000397>.
- Smith, A.J.E. 2004. *The Moss Flora of Britain and Ireland* 2nd ed. Cambridge, United Kingdom: Cambridge University Press.
- Smith, H.G. 1992. Distribution and ecology of the testate rhizopod fauna of the continental Antarctic zone. *Polar Biology*. **12**(6–7), pp.629–634.
<http://link.springer.com/10.1007/BF00236985>.
- Smith, L.C., MacDonald, G.M., Velichko, A.A., Beilman, D.W., Borisova, O.K., Frey, K.E., Kremenetski, K. V and Sheng, Y. 2004. Siberian Peatlands a Net Carbon Sink and Global Methane Source Since the Early Holocene. *Science*. **303**(5656), pp.353–356.
- Smith, L.C., Sheng, Y. and MacDonald, G.M. 2007. A first pan-Arctic assessment of the influence of glaciation, permafrost, topography and peatlands on northern hemisphere lake distribution. *Permafrost and Periglacial Processes*. **18**(2), pp.201–208.
<http://doi.wiley.com/10.1002/ppp.581>.

- Smith, L.C., Sheng, Y., MacDonald, G.M. and Hinzman, L.D. 2005. Disappearing Arctic Lakes. *Science* . **308**(5727), p.1429.
- Speed, J.D.M., Cooper, E.J., Jónsdóttir, I.S., Van Der Wal, R. and Woodin, S.J. 2010. Plant community properties predict vegetation resilience to herbivore disturbance in the Arctic. *Journal of Ecology*. **98**(5), pp.1002–1013. <http://doi.wiley.com/10.1111/j.1365-2745.2010.01685.x>.
- Steere, W.C. and Scotter, G.W. 1979. Bryophytes of Banks Island, Northwest Territories, Canada. *Canadian Journal of Botany*. **57**(10), pp.1136–1149. <http://www.nrcresearchpress.com/doi/10.1139/b79-137>.
- Swindles, G.T., Amesbury, M.J., Turner, T.E., Carrivick, J.L., Woulds, C., Raby, C., Mullan, D., Roland, T.P., Galloway, J.M., Parry, L., Kokfelt, U., Garneau, M., Charman, D.J. and Holden, J. 2015. Evaluating the use of testate amoebae for palaeohydrological reconstruction in permafrost peatlands. *Palaeogeography, Palaeoclimatology, Palaeoecology*. **424**, pp.111–122. <https://www.sciencedirect.com/science/article/pii/S003101821500053X>.
- Swindles, G.T., Morris, P.J., Baird, A.J., Blaauw, M. and Plunkett, G. 2012. Ecohydrological feedbacks confound peat-based climate reconstructions. *Geophysical Research Letters*. **39**(11). <http://doi.wiley.com/10.1029/2012GL051500>.
- Swindles, G.T., Morris, P.J., Mullan, D., Watson, E.J., Turner, T.E., Roland, T.P., Amesbury, M.J., Kokfelt, U., Schoning, K., Pratte, S., Gallego-Sala, A., Charman, D.J., Sanderson, N., Garneau, M., Carrivick, J.L., Woulds, C., Holden, J., Parry, L. and Galloway, J.M. 2015. The long-term fate of permafrost peatlands under rapid climate warming. *Scientific Reports*. **5**(1), p.17951. <http://www.nature.com/articles/srep17951>.
- Swindles, G.T., Morris, P.J., Wheeler, J., Smith, M.W., Bacon, K.L., Edward Turner, T., Headley, A. and Galloway, J.M. 2016. Resilience of peatland ecosystem services over millennial timescales: evidence from a degraded British bog. *Journal of Ecology*. **104**(3), pp.621–636. <http://doi.wiley.com/10.1111/1365-2745.12565>.
- Tape, K., Sturm, M. and Racine, C. 2006. The evidence for shrub expansion in Northern Alaska and the Pan-Arctic. *Global Change Biology*. **12**(4), pp.686–702. <http://doi.wiley.com/10.1111/j.1365-2486.2006.01128.x>.
- Tarnocai, C. 2006. The effect of climate change on carbon in Canadian peatlands. *Global and Planetary Change*. **53**(4), pp.222–232. <https://www.sciencedirect.com/science/article/pii/S0921818106001202>.
- Tarnocai, C., Canadell, J.G., Schuur, E.A.G., Kuhry, P., Mazhitova, G. and Zimov, S. 2009. Soil organic carbon pools in the northern circumpolar permafrost region. *Global Biogeochemical Cycles*. **23**(2), p.GB2023. <http://doi.wiley.com/10.1029/2008GB003327>.
- Tarnocai, C., Kettles, I.M. and Lacelle, B. 2011. *Peatlands of Canada*. Geological Survey of Canada, Open File 6561 (map, scale 1:6 500 000). Available from: <http://geoscan.nrcan.gc.ca/starweb/geoscan/servlet.starweb?path=geoscan/fulle.web&search1=R=288786>.
- Taylor, L.S., Swindles, G.T., Morris, P.J. and Gařka, M. 2019. Ecology of peatland testate amoebae in the Alaskan continuous permafrost zone. *Ecological Indicators*. **96**, pp.153–

162. <https://www.sciencedirect.com/science/article/pii/S1470160X18306502>.
- Tolonen, K. and Turunen, J. 1996. Accumulation rates of carbon in mires in Finland and implications for climate change. *The Holocene*. **6**(2), pp.171–178.
<http://journals.sagepub.com/doi/10.1177/095968369600600204>.
- Turetsky, M.R., Benscoter, B., Page, S., Rein, G., van der Werf, G.R. and Watts, A. 2015. Global vulnerability of peatlands to fire and carbon loss. *Nature Geoscience*. **8**(1), pp.11–14.
<http://www.nature.com/articles/ngeo2325>.
- Turetsky, M.R., Wieder, R.K., Vitt, D.H., Evans, R.J. and Scott, K.D. 2007. The disappearance of relict permafrost in boreal north America: Effects on peatland carbon storage and fluxes. *Global Change Biology*. **13**(9), pp.1922–1934. <http://doi.wiley.com/10.1111/j.1365-2486.2007.01381.x>.
- Vardy, S.R., Warner, B.G. and Asada, T. 2005. Holocene environmental change in two polygonal peatlands, south-central Nunavut, Canada. *Boreas*. **34**(3), pp.324–334.
<http://doi.wiley.com/10.1111/j.1502-3885.2005.tb01104.x>.
- Vardy, S.R., Warner, B.G., Turunen, J. and Aravena, R. 2000. Carbon accumulation in permafrost peatlands in the Northwest Territories and Nunavut, Canada. *The Holocene*. **10**(2), pp.273–280. <http://journals.sagepub.com/doi/10.1191/095968300671749538>.
- Vincent, J.-S., Occhietti, S., Rutter, N., Lortie, G., Guilbault, J.-P. and De Boutray, B. 1983. The late Tertiary-Quaternary stratigraphic record of the Duck Hawk Bluffs, Banks Island, Canadian Arctic Archipelago. *Canadian Journal of Earth Science*. **20**, pp.1694–1712.
- Vitt, D.H. and Chee, W.-L. 1990. The relationships of vegetation to surface water chemistry and peat chemistry in fens of Alberta, Canada. *Vegetatio*. **89**(2), pp.87–106.
<http://link.springer.com/10.1007/BF00032163>.
- Vitt, D.H., Halsey, L.A. and Zoltai, S.C. 1994. The Bog Landforms of Continental Western Canada in Relation to Climate and Permafrost Patterns The Bog Landforms of Continental Western Canada in Relation to Climate and Permafrost Patterns. *Arctic and Alpine Research*. **26**(1), pp.1–13.
- Vitt, D.H., Li, Y., Belland, R.J. and Belland, R.J. 1995. Patterns of Bryophyte Diversity in Peatlands of Continental Western Canada. *The Bryologist*. **98**(2), p.218.
<https://www.jstor.org/stable/3243306?origin=crossref>.
- De Vleeschouwer, F., Chambers, F.M. and Swindles, G.T. 2010. Coring and sub-sampling of peatlands for palaeoenvironmental research. *Mires and Peat*. **7**, pp.1–10.
- Waddington, J.M., Morris, P.J., Kettridge, N., Granath, G., Thompson, D.K. and Moore, P.A. 2015. Hydrological feedbacks in northern peatlands. *Ecohydrology*. **8**(1), pp.113–127.
<http://doi.wiley.com/10.1002/eco.1493>.
- Walker, D.A., Raynolds, M.K., Daniëls, F.J.A., Einarsson, E., Elvebakk, A., Gould, W.A., Katenin, A.E., Kholod, S.S., Markon, C.J., Melnikov, E.S., Moskalenko, N.G., Talbot, S.S., Yurtsev, B.A. and The other members of the CAVM Team, T. other members of the C. 2005. The Circumpolar Arctic vegetation map. *Journal of Vegetation Science*. **16**(3), pp.267–282.
<http://doi.wiley.com/10.1111/j.1654-1103.2005.tb02365.x>.

- Warner, B.G. and Charman, D.J. 1994. Holocene changes on a peatland in northwestern Ontario interpreted from testate amoebae (Protozoa) analysis. *Boreas*. **23**(3), pp.270–279. <http://doi.wiley.com/10.1111/j.1502-3885.1994.tb00949.x>.
- Warner, B.G. and Chengalath, R. 1991. *Habrotrocha angusticollis* (Bdelloidea, Rotifera): A new paleoecological indicator in Holocene peat deposits in Canada. *SIL Proceedings, 1922-2010*. **24**(5), pp.2738–2740.
- Wieder, R.K., Vitt, D.H. and Benschoter, B.W. 2006. Peatlands and the Boreal Forest *In*: R. K. Wieder and D. H. Vitt, eds. *Boreal Peatland Ecosystems* Berlin: Springer Berlin Heidelberg, pp.1–8. http://link.springer.com/10.1007/978-3-540-31913-9_1.
- Woo, M.-K. and Winter, T.C. 1993. The role of permafrost and seasonal frost in the hydrology of northern wetlands in North America. *Journal of Hydrology*. **141**(1–4), pp.5–31. <https://www.sciencedirect.com/science/article/pii/0022169493900439>.
- Woo, M. and Young, K.L. 2014. Disappearing semi-permanent snow in the High Arctic and its consequences. *Journal of Glaciology*. **60**(219), pp.192–200.
- Woo, M. and Young, K.L. 2006. High Arctic wetlands: Their occurrence, hydrological characteristics and sustainability. *Journal of Hydrology*. **320**(3–4), pp.432–450. <https://www.sciencedirect.com/science/article/pii/S0022169405003604>.
- Woo, M. and Young, K.L. 2003. Hydrogeomorphology of patchy wetlands in the High Arctic, polar desert environment. *Wetlands*. **23**(2), pp.291–309. <http://link.springer.com/10.1672/8-20>.
- Yi, S., Woo, M. and Arain, M.A. 2007. Impacts of peat and vegetation on permafrost degradation under climate warming. *Geophysical Research Letters*. **34**(16). <http://doi.wiley.com/10.1029/2007GL030550>.
- Yu, Z., Beilman, D.W. and Jones, M.C. 2009. Sensitivity of Northern Peatland Carbon Dynamics to Holocene Climate Change. Carbon Cycling in Northern Peatlands. *Carbon Cycling in Northern Peatlands*. **184**, pp.55–69.
- Yu, Z., Loisel, J., Brosseau, D.P., Beilman, D.W. and Hunt, S.J. 2010. Global peatland dynamics since the Last Glacial Maximum. *Geophysical Research Letters*. **37**(13), p.L13402. <http://doi.wiley.com/10.1029/2010GL043584>.
- Yu, Z.C. 2012. Northern peatland carbon stocks and dynamics: a review. *Biogeosciences*. **9**(10), pp.4071–4085. <https://www.biogeosciences.net/9/4071/2012/>.
- Zoltai, S.C. 1993. Cyclic Development of Permafrost in the Peatlands of Northwestern Alberta. *Arctic and Alpine Research*. **25**(3), pp.240–246.
- Zoltai, S.C. and Martikainen, P.J. 1996. Estimated extent of forested peatlands and their role in the global carbon cycle *In*: *Forest Ecosystems, Forest Management and the Global Carbon Cycle* Berlin, Heidelberg: Springer , pp.47–58. http://link.springer.com/10.1007/978-3-642-61111-7_5.
- Zoltai, S.C. and Pollett, F.C. 1983. Wetlands in Canada: Their Classification, Distribution, and Use *In*: A. J. P. Gore, ed. *Mires: Swamp, Bog, Fen and Moor*. Amsterdam: Elsevier, pp.245–268.

Zoltai, S.C. and Tarnocai, C. 1975. Perennially Frozen Peatlands in the Western Arctic and Subarctic of Canada. *Canadian Journal of Earth Sciences*. **12**(1), pp.28–43.
<http://www.nrcresearchpress.com/doi/10.1139/e75-004>.

APPENDIX

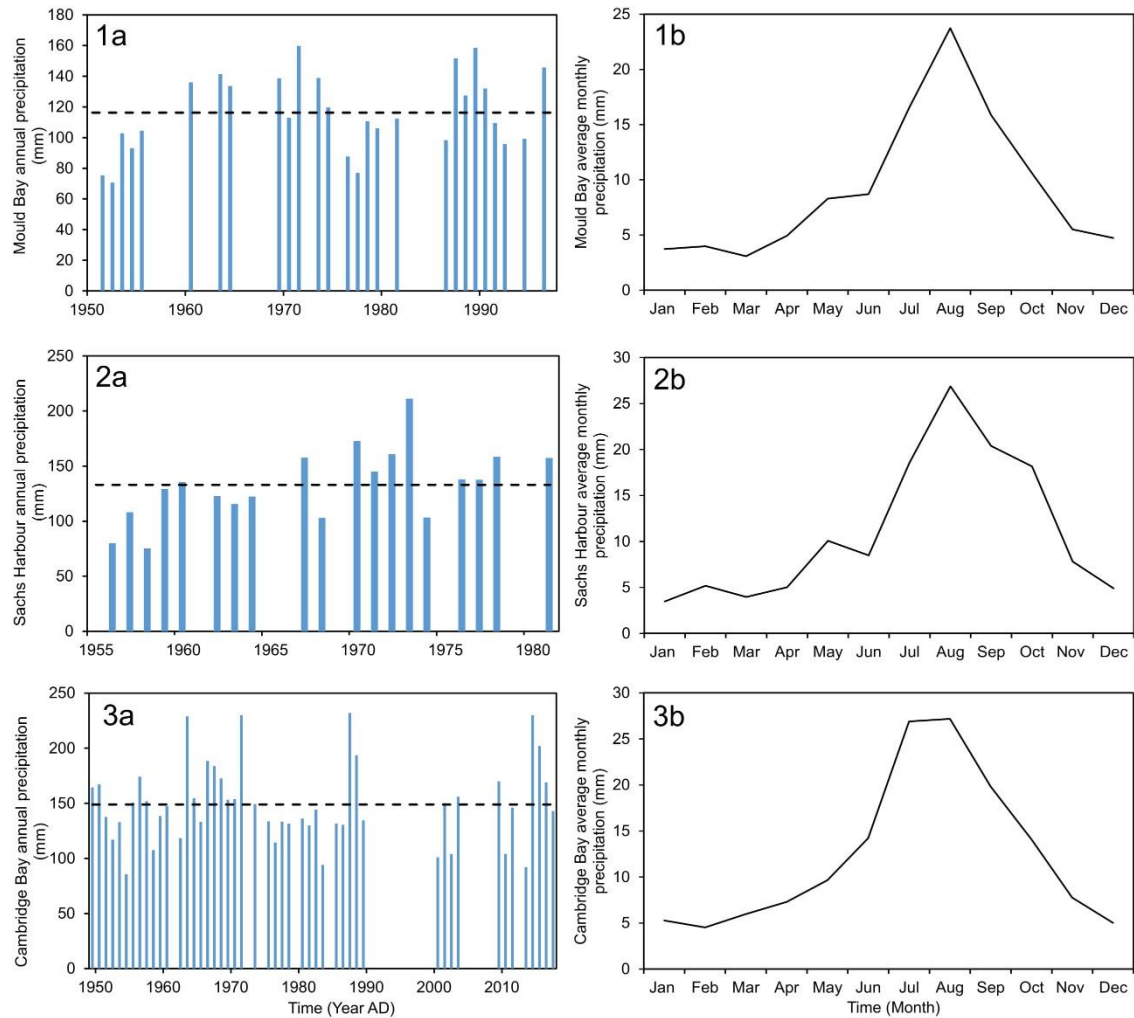


Figure A1. Available precipitation data for my study sites in the western Canadian Arctic study region: 1) Mould Bay, 2) Sachs Harbour and 3) Cambridge Bay. A) Annual precipitation trends. B) Average monthly precipitation. Source: Climate explorer site and Environment Canada.